TFY4225 Nuclear and Radiation physics

1.)
Basic concepts (Lilley Chap.1)

The Nuclei

Notation

The composition of a nucleus is often described using the notation:

$${}^{A}_{Z}\mathrm{X}_{N}$$

X represents the atoms name. A is defined to be the mass number, Z is the atomic number and N is the neutron number.
It is of course sufficient to describe the nuclei by^{A}X, since X automatically determines the letter Z, which was defined above to be the atom number.

Particle masses

Particle	Index	Mass
Neutron	m_n	$m_n = 1.008665u$
Proton	m_p	$m_p = 1.007276u$
Electron	m_e	$m_e = 0.000549u$

Where u is the atomic mass unit, and 1u$\equiv \frac{1}{12}m({}^{12}C)$

Particle data

All of the three particles above are spin- $\frac{1}{2}$ fermions with non-zero magnetic moments μ_b. The neutron and the proton belong to the Baryon (composition of three quarks) family and the electron is a lepton.

Atomic mass of nucleus ${}^{A}_{Z}$X

$$m(A,Z) = Zm_H + (A-Z)m_n - \frac{B}{c^2} \tag{1}$$

Where B represents the total binding energy of ${}^{A}_{Z}X$. For this to be valid, one has assumed that the mean binding energy of the electrons in ${}^{A}_{Z}X$ is the same as in ${}^{1}_{1}H$. Mass excess of ${}^{A}_{Z}X$ is defined in atomic mass units(u) to be:

$$\Delta = m(A,Z) - A \tag{2}$$

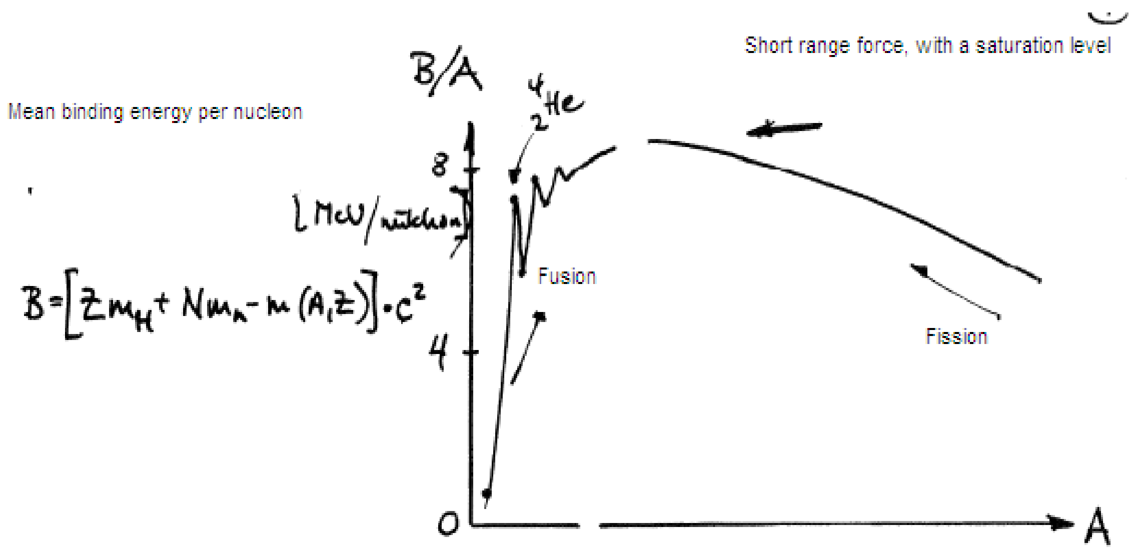

$$B = \left[Z m_H + N m_n - m(A,Z) \right] \cdot c^2$$

The nuclear potential (Strong force)

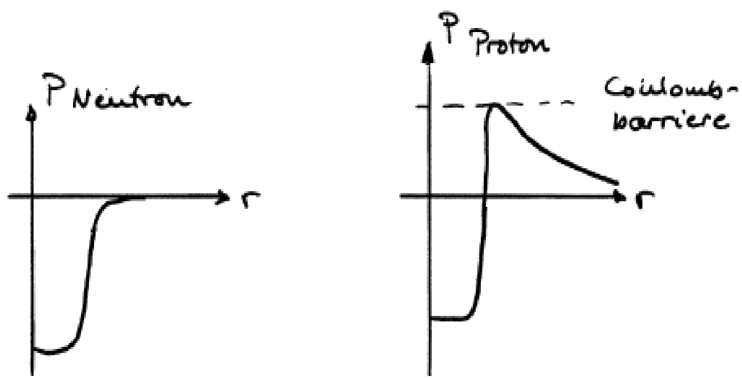

The potential within a nucleus can be approximately modelled as an infinite spherical potential well where the potential is zero inside a given radius, and infinity outside it. This can be expressed as:

$$V = \begin{cases} 0, & \text{if r} \leq \text{a} \\ \infty, & \text{if r} > \text{a} \end{cases} \tag{3}$$

Inserting 3 into the Schrødinger equation:

$$H\psi = E\psi \tag{4}$$

Assuming a separable wave function solution of the form $\psi = R(r) \cdot Y_l^m(\phi, \theta)$ where Y_l^m represents the spherical harmonics.

The radial part of the wave function $R(r) = j_l(kr)$, is a spherical Bessel function.

Boundary condition: $j_l(kr) = 0$ for $kr = ka$

$l = 0 : j_0(kr) = \frac{\sin kr}{kr} \rightarrow j_0(ka) = 0$ for $ka = n \cdot \pi$. The wave function has its n'th zero at $r = a$.
$l = 1 : j_1(kr) = \frac{\sin kr}{(kr)^2} - \frac{coskr}{kr}$

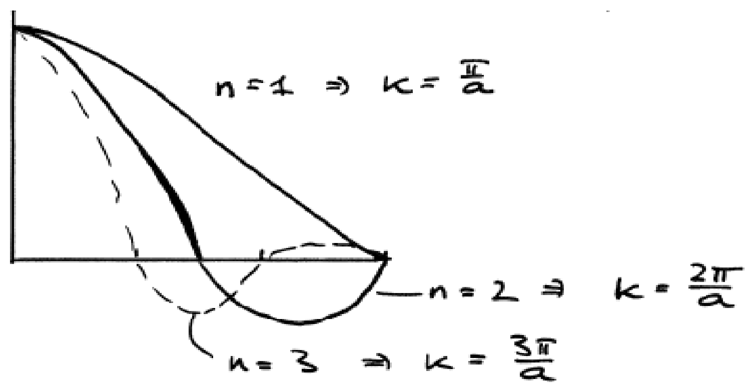

A centrifugal potential arises from the angular motion for $l \neq 0$.$\Rightarrow$ Energy levels $E = E_{nl}$. l is substituted with s,p,d,f for l=0,1,2,3....
For each value of l we have $2l + 1$ values for the quantum number $m_l = 0, \pm1, \pm2.... \pm l$

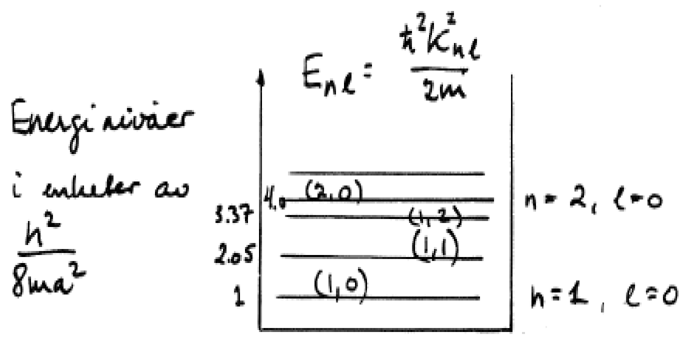

This simple model arranges the energy levels, E_{nl},in the right order up to a nucleus size of A=40.

Stability and existence of nuclei

Chart of nuclides

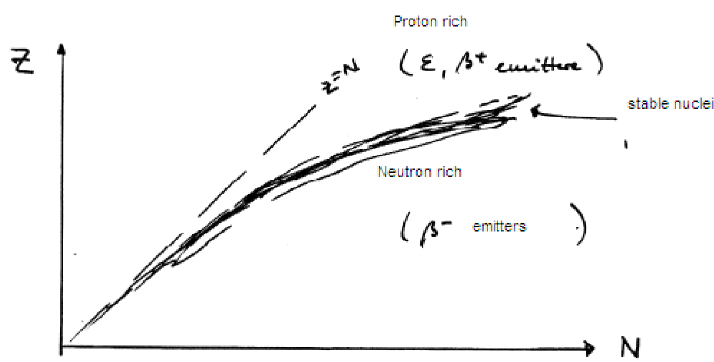

Radioactivity

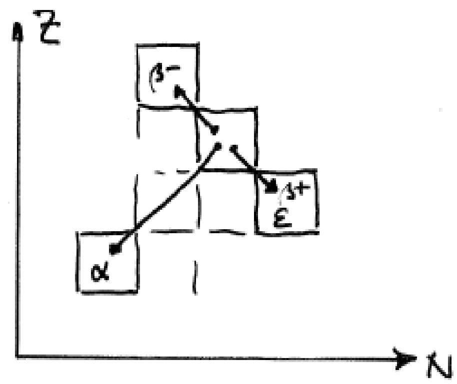

Spontaneous radioactive processes:

With or without a secondary gamma ray emission. $\begin{cases} \alpha \\ \beta^- \\ \beta^+ \\ electroncapture \end{cases}$

$\underline{\alpha}$: Induced by strong interactions ${}^A_Z X \rightarrow^{A-4}_{Z-2} X' +^4_2 \alpha,$ $Q_\alpha = c^2(m_P - m_D - m_{He}) = T_{x'} + T_\alpha$

$T_\alpha = \frac{Q_\alpha}{1+\frac{m_\alpha}{m_{x'}}}$

$\underline{\beta^-}$: Induced by weak interactions ${}^A_Z X \rightarrow^A_{Z+1} X' + \beta^- + \overline{\nu}$ $Q_{\beta_-} = c^2(m_P - m_D) = T_{x'} + T_{\beta^-} + T_{\overline{\nu}}$

$Q_{\beta^-} = (\Delta_P - \Delta_D), T_{x'} \simeq 0$

$\underline{\beta^+}$: Induced by weak interactions ${}^A_Z X \rightarrow^A_{Z-1} X' + \beta^+ + \nu$ $Q_{\beta^+} = c^2(m_P - m_D - 2m_e) = T_{x'} + T_{\beta^+} + T_\nu$

$Q_{\beta^+} = (\Delta_P - \Delta_D - 2m_e)c^2,\ T_{x'} \simeq 0$

$\underline{\varepsilon}$: Induced by weak interactions ${}^A_Z X + e^- \rightarrow^A_{Z-1} X' + \nu$ $Q_{EC} = (m_P - m_D)c^2 - E_B = T_\nu$

Electron capture, where an electron is absorbed by the nucleus, is an energetically favorable process which is competing with the β^+ disintegration process. ε is followed by characteristic X-ray radiation.

$\underline{\gamma}$: Induced by E.M interactions ${}^A_Z X^* \rightarrow^A_Z X + \gamma$ $Q_\gamma = (m_P - m_D)c^2 = T'_x + h\nu$

$T_{x'} \simeq 0$

γ- and X-ray radiation are both secondary processes, which are characteristic of the final daughter nucleus after a disintegration.

The disintegration constant λ

$$\frac{dN}{dt} = -\lambda \cdot N \Rightarrow N(t) = N(0)e^{-\lambda t} \tag{5}$$

In the equation above, one can see that λ represents a constant transition probability per unit time.
$[\lambda] = s^{-1} = Bq$
A good argument supporting the assumed disintegration model in 5 is based on elementary time-dependent perturbation theory.

Radioactivity. Disintegration kinetics

Statistically defined variables:

Half-life	$T_{\frac{1}{2}}$,	$T_{\frac{1}{2}} = \frac{\ln 2}{\lambda} \simeq \frac{0.693}{\lambda}$
Mean life-time	τ,	$\tau = \frac{1}{N_0}\int_0^\infty t\lambda N(t)dt = \frac{1}{\lambda}$
Activity	A,	$A = \lambda \cdot N$
Specific activity	SA	$SA = \lambda \cdot n$ (n is the number of atoms per mass unit)
		$n = \frac{N_A}{A}$ where N_A is Avogadro's number,and A is the molar mass of the atom.

1Bq is defined to be the amount of radio-nuclei you need of a specific isotope, to get one disintegration per second.

Disintegration chains

A disintegration chain appears when the daughter nucleus of the previous disintegration is unstable.

$$\mathrm{A} \xrightarrow{\lambda_A} \mathrm{B} \xrightarrow{\lambda_B} \mathrm{C}$$

Using equation 5 in several steps, assuming that nucleus C is stable, this reaction becomes:

$$\frac{dN_A}{dt} = -\lambda_A \cdot N_A; \qquad \frac{dN_B}{dt} = \lambda_A \cdot N_A - \lambda_B \cdot N_B; \qquad \frac{dN_C}{dt} = \lambda_B \cdot N_B \tag{6}$$

Example:

C stable $\Rightarrow N_A + N_B + N_C = N_0$, initial values: $N_A(0) = N_0$; $N_B(0) = N_C = 0$
$\Rightarrow$

$N_B = \frac{\lambda_A N_A}{\lambda_B - \lambda_A}(e^{-\lambda_A t} - e^{-\lambda_B t})$ (Correction:In this equation NA=NA(0)=N0)

$N_A = N_0 e^{-\lambda_A t}$
$\Rightarrow$
$N_B = \frac{\lambda_A}{\lambda_B} N_0 (1 - e^{-\lambda_B t})$ if $\lambda_A << \lambda_B$

<u>Permanent equilibrium for $t >> 1/\lambda_B$ ($T_A \gg T_B$)</u>:

$Q_B = \lambda_B N_B \rightarrow \lambda_A N_A = Q_A$

<u>Transient equilibrium($T_A > T_B$)</u>:

$Q_B = \lambda_B N_B \rightarrow \frac{\lambda_A \lambda_B N_0}{\lambda_B - \lambda_A} e^{-\lambda_A t} = Q_A$

$Q_B \rightarrow \frac{\lambda_B}{\lambda_B - \lambda_A} Q_A$ When t $\rightarrow \infty$

<u>No equilibrium ($T_A < T_B$)</u>

Nuclear reactions

$$\overbrace{a + \underbrace{A}_{Target\quad nucleus}}^{Entrance\quad channel} \rightarrow \overbrace{B + b}^{Exit\quad channel}$$

<u>Energy released</u>: $Q = (m_a + m_A - m_b - m_B)c^2$ $\quad$ Q $\begin{cases} > 0, \text{exoterm, releases energy} \\ < 0, \text{endoterm, absorbs energy} \end{cases}$

Scattering cross-section

Cross-section

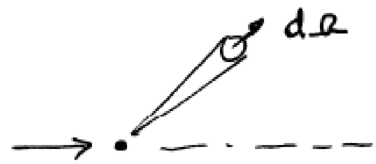

Number of particles per second within $d\vec{\Omega}$:	$dR = d\sigma \cdot \dot{\Phi}$ per target atom.
Total cross-section:	$\sigma = \int_\Omega \frac{d\sigma}{d\Omega} d\Omega$ per target atom
Total rate of particles for a target consisting of N particles:	$R = \sigma N \cdot \dot{\Phi}$

Where σ is commonly given in barns(b). 1b=$10^{-28}m^2$

Examples:

Example: Production of isotopes by neutron capture

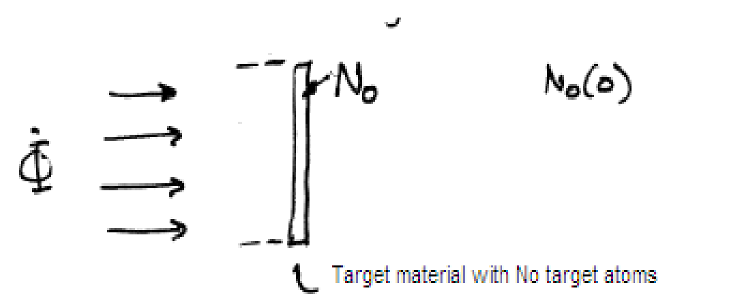

Production rate: $\frac{dN_0(t)}{dt} = -\sigma\dot{\Phi}N_0$

The radioactive nuclei produced have a disintegration constant λ

Rate of change of produced nuclei: $\frac{dN_1(t)}{dt} = \sigma\dot{\Phi}N_0(t) - \lambda N_1(t)$

Instantaneous radioactivity due to the produced nuclei: $A_1 = \lambda \cdot N_1$

Example: Rutherford scattering

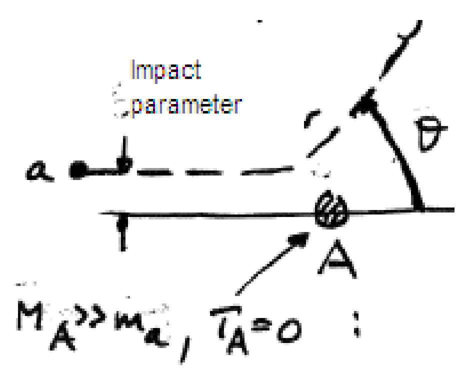

Elastic scattering; Central-symmetric Coulomb potential.

Differential cross-section: $\frac{d\sigma}{d\Omega} = \left[\frac{Z_1 Z_2 e^2}{16\pi\varepsilon_0 T_a}\right]^2 \frac{1}{\sin^4\frac{\theta}{2}}$

2.)
Radiation-matter interaction (Lilley Chap.5)

Interaction of charged particles with matter

Coulomb interactions

What characterizes these interactions, is that their origin of existence is due to the long range Coulomb-force.

Type of interaction / Interacts with	Elastic	Inelastic
Electrons		Ionisation
Nuclei	Rutherford Scattering	Brems strahlung

These interaction processes result in a continuous retardation of charged particles, because of the long range Coulomb force.

Heavy charged particles

Energy transfer

Heavy charged particle of mass M, velocity $\vec{V}$, and charge ze interacts with atomic electron of the material.

Assuming the binding energy of the electron, $E_B = 0$ and that initially the electron is found at rest.

Conservation of energy and momentum: $T_M = T'_M + T'_e$

$$\vec{p_M} = \vec{p_M}' + \vec{p_e}'$$

Maximum energy transfer happens when the particles collide head-on. An approximate non relativistic calculation of the maximum energy transfer from the heavy ion to the electron follows below.

Non relativistic calculation: $pc = \sqrt{T(T + 2mc^2)} \simeq c\sqrt{2mT}$

Maximum energy transfer: $T'_{emax} = \frac{4mM}{(m+M)^2} T_M$

For a heavy charged particle $m \ll M \Rightarrow$ $T'_{emax} = 2mV^2$

Where V is the initial velocity of the heavy particle, and m is the electron mass. The relativistic expression is a bit more complicated.

Relativistic expression for maximum energy transfer: $T'_{emax} = \frac{2\gamma^2 mV^2}{1+\frac{2\gamma m}{M}+\frac{m^2}{M^2}}$

Where γ represents the Lorenz factor:

$$\gamma = \frac{1}{\sqrt{1 - (\frac{V}{c})^2}} \tag{1}$$

Stopping power for heavy charged particles interacting with electrons.

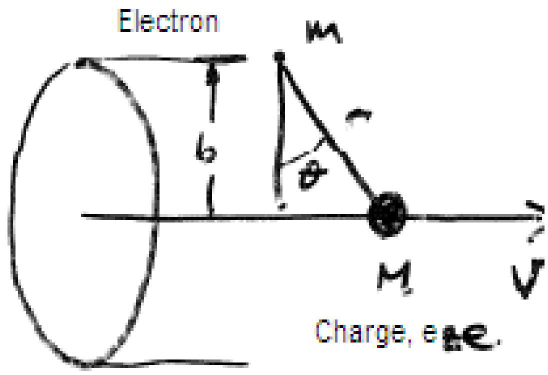

<u>Collision stopping power:</u> $S_c = -\frac{dT}{dx}$

Force acting on the heavy particle: $\vec{F} = \frac{1}{4\pi\varepsilon}\frac{ze^2}{r^2}\hat{e_r}$

S_c is loss of kinetic energy per unit path length in the scattering medium, due to interactions between the heavy charged particle and the electrons.
All the electrons in a cylinder shell with a collision parameter b contribute equally to the stopping power, since the Coulomb force is spherically symmetric.

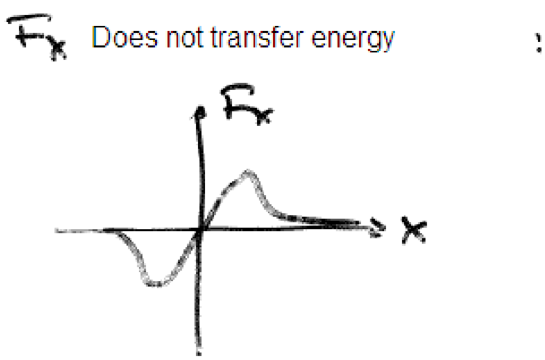

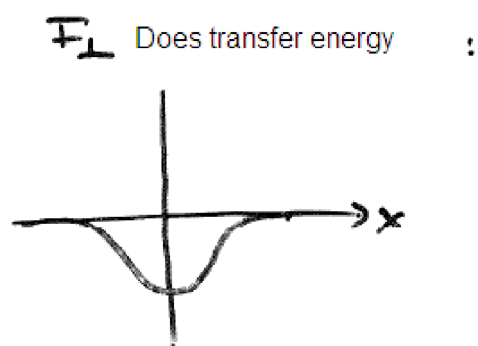

If the x direction is defined to be along the charged particle's direction as earlier implied, F_x does not transfer energy. However, $F_\perp$ does:

Momentum transfer: $\Delta p_{\perp} = \int |F| \cos\theta dt = \frac{ze^2}{4\pi\varepsilon_0} \int_{-\frac{\pi}{2}}^{\frac{\pi}{2}} \frac{\cos^3\theta}{b^2} \frac{b}{V} \frac{d\theta}{\cos^2\theta}$

This is found assuming that: V$\simeq$ constant

Energy transferred to the electron: $E = \frac{(\Delta p \perp)^2}{2m_e} = \frac{1}{(4\pi\varepsilon_0)^2} \frac{2z^2e^4}{m_e V^2 b^2}$

The differential cross section for energy transfer between E and $E + dE$, per electron in the stopping medium:

$$d\sigma(E) = \frac{d\sigma(E)}{dE} dE = |2\pi b db| = \frac{2\pi z^2 e^4}{(4\pi\varepsilon_0)^2 m_e V^2} \frac{dE}{E^2} \tag{2}$$

Again returning to the stopping power: $S_c = -\frac{dT}{dx} = -\frac{dE}{dx} = n_v Z \int_{E_{min}}^{E_{max}} \frac{d\sigma}{dE} E dE$

The total contribution to the interaction probability from all of the electrons inside the cylinder shell(d^3V) is worked out below. n_v is the number of atoms per unit volume.

Further on: $n_v Z d^3 V = n_v Z \frac{d\sigma(E)}{dE} dE dx$; $n_v = \frac{N_A}{A} \cdot \rho$

The Stopping power: $S_c = \int_{E_{min}}^{E_{max}} n_v Z \frac{2\pi z^2 e^4}{(4\pi\epsilon_0)^2 m_e V^2} \frac{dE}{E^2} E$

The total stopping power then comes out to be:

$$S_c = \frac{2\pi z^2 r_0^2 m_e c^2}{\beta^2} n_v Z \Big[\ln \frac{E_{max}}{E_{min}} \Big]; \quad r_0 = \frac{e^2}{4\pi\epsilon_0 m_e c^2} \tag{3}$$

Going back to the non relativistic case: $E_{max} = \frac{4mM}{(m+M)^2} T_M$

For heavy particles($M \gg m$) $\Rightarrow$ $E_{max} = 2m_e V^2$

$E_{min} = \frac{I^2}{2m_e V^2}$ (I=mean exitation energy)

Mass stopping-power (non relatisvistic): $\frac{S_e}{\rho} = \frac{2\pi z^2 r_0^2}{\beta^2} m_e c^2 N_a \Big[\frac{Z}{A}\Big] 2 \ln \Big[\frac{Q_{max}}{I}\Big]$,

$(M \gg m), Q_{max} \equiv E_{max}$

Relativistic expression with corrections:

$$\frac{S_c}{\rho} = N_A \frac{Z}{A} \cdot \frac{z^2 e^4}{4\pi\epsilon_0^2 m_e V^2} \Big[\ln \frac{Q_{max}}{I} - \ln(l - \beta^2) - \beta^2 - \frac{c(\beta^2)}{Z} - \frac{1}{2}\delta \Big] \tag{4}$$

Where A represents the molar mass of the stopping material, V is the particle velocity.

The two last terms in the expression are added as a shell correction and a density effect, respectively.

The last term is a correction which appears because there is also a field set up from other atoms in the stopping material.
Note that this expression is independent of the mass of the incoming particle.

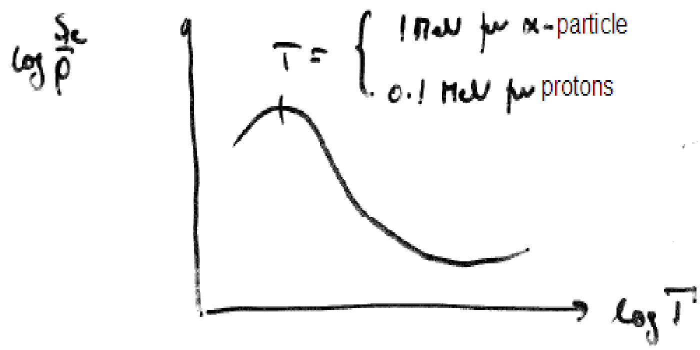

Stopping-power for composite materials: $n_v Z \ln I \Rightarrow \sum_i n_{vi} Z_i \ln I_i$

Range

Range for heavy charged particles

Mono energetic particles, for example α particles:

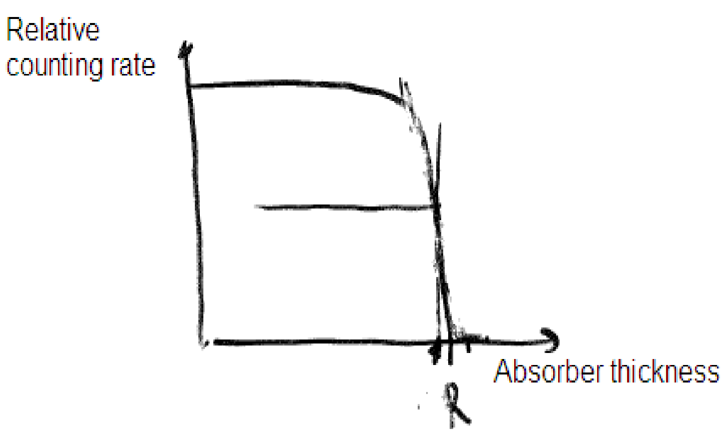

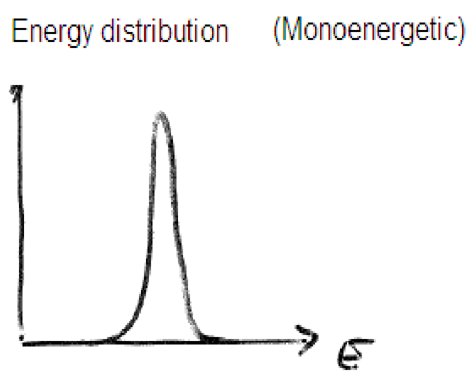

Particle range in a stopping-material: $R(T) = \int_T^0 \frac{dT}{-\frac{dT}{dx}}$

$-\frac{dT}{dx} = z^2 G(\beta)$

$dT = g(\beta) \cdot M d\beta$

Particle range in a stopping-material: $R(\beta) = \frac{M}{z^2} \int_\beta^0 h(\beta) d\beta = \frac{M}{z^2} f(\beta)$

This is a useful formula for comparing range of particles having identical initial velocity.

Linear energy transfer(LET): $LET = \left[-\frac{dT}{dx} \right]_c$

NOTE! The range is defined to be the distance along the particle track, not the penetration depth. Generally, we have $R > x_0$ where x_0 is the penetration depth. Nevertheless, for heavy charged particles: $R \simeq x_0$. This means that a heavy charged particle, fired at a target medium, will travel along a path that hardly deviates from it's original direction, until it is retarded down to zero velocity.

β-particles

Stopping-power for β-particles (z=1)

$$\frac{S_c}{\rho} = N_A \frac{Z}{A} \frac{e^4}{4\pi\varepsilon_0 m_e c^2 \beta^2} \left[\ln \frac{m_e c^2 \tau \sqrt{\tau + 2}}{\sqrt{2} I} + F^{\pm}(\beta) \right] \tag{5}$$

τ represents the β-particle's kinetic energy: $\tau = \frac{T}{m_e c^2}$

For electrons: $F^-(\beta) = \frac{1-\beta^2}{2} \left[1 + \frac{\tau^2}{8} - (2\tau + 1) \ln 2 \right]$

For positrons: $F^+(\beta) = \ln 2 - \frac{\beta^2}{24} \left[23 + \frac{14}{\tau+2} + \frac{10}{(\tau+2)^2} + \frac{4}{(\tau+2)^3} \right]$

Differences between β, and heavy charged particles' interactions with matter:

1 β-particles can loose all their energy in one collision with an atomic electron.

2 β^--particles are identical with the object they interact with (electrons).

(We assume that the electron with the lowest energy is the one that belonged to the material.)

3 Relativistic formulas are required (for $T_e > 10keV$).

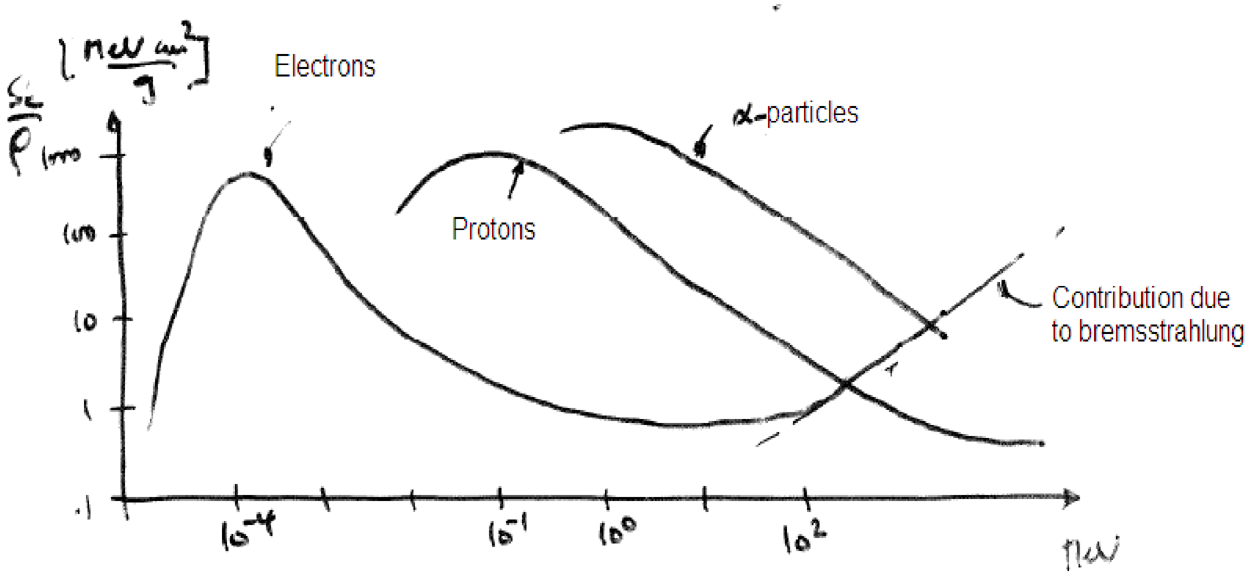

Bremsstrahlung contribution to the stopping power

$$\frac{-\left[\frac{dE}{dx}\right]_{rad}}{-\left[\frac{dE}{dx}\right]_{col}} \simeq \frac{ZE}{800} = \underbrace{2.5 \cdot 10^{-4} ZE}_{E\ is\ total\ energy\ in\ MeV} \tag{6}$$

Effective bremsstrahlung contribution:

$$Y(T_0) = \frac{1}{T_0}\int_0^{T_0} y(T)dT \simeq \frac{6 \cdot 10^{-4} Z \overbrace{T}^{MeV}}{1 + 6 \cdot 10^{-4} ZT}; \quad y(T) \equiv \frac{-\left[\frac{dT}{dx}\right]_{rad}}{-\left[\frac{dT}{dx}\right]_{tot}} \tag{7}$$

This is the fraction of the incoming particle's kinetic energy, which is converted into bremsstrahlung during the entire retardation process.

Range for β-particles

Usually, electrons have a continuous energy spectrum up to E_{max}, and the range is defined relative to this energy E_{max}. The electron range is always greater than the penetration depth. NOTE that in this case it is very important to use the total stopping power in the calculations, since the bremsstrahlung contribution is highly significant.

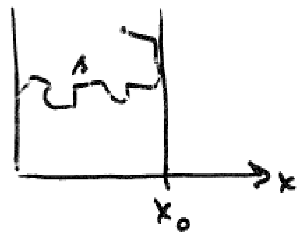

$$R(T) = \int_s ds = \int_T^0 \frac{dT}{\left(-\frac{dT}{dx}\right)_{tot}}$$

$$R(T) = \int_s ds = \int_T^0 \frac{dT}{-\left[\frac{dT}{dx}\right]_{tot}} \tag{8}$$

Photons

Photon interactions

Type of interaction: / Interacts with:	Elastic scattering (Coherent)	Inelastic scattering (Incoherent)	Absorption
Atomic electrons	$\sigma_{Coh.sc} \equiv \sigma_R$ Rayleigh	$\sigma_{Incoh.sc} \equiv \sigma_{CT}$ Compton	σ_{pe} Photo-electric effect
Nuclei/Nucleons	Elastic nuclear scattering	Nuclear resonance scattering	Photo-nuclear reactions
Electric field from charged particles			σ_{pp} Pair production

Attenuation coefficients

When measuring attenuation coefficients, one always measure in a "good(proper) geometry" setup.

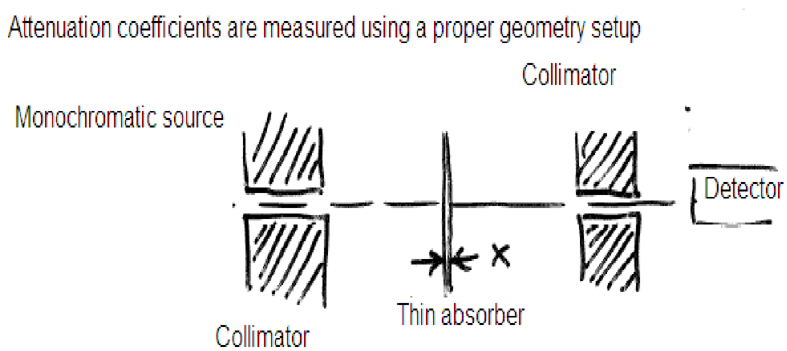

Detected intensity with/without absorber $\frac{I}{I_0} = e^{-\mu_l \cdot x}$

Linear attenuation coeff: $\mu_l =_{x \to 0}^{lim} \frac{1}{x} \ln \frac{I_0}{I} = -\frac{1}{I} \frac{dI}{dx}$

Atomic attenuation coeff: $\sigma^a = \frac{\mu_l}{n_V}$

Mass attenuation coeff: $\frac{\mu_l}{\rho} = \sigma^a \frac{N_A}{A}$

The atomic attenuation coefficient is often called the atomic scattering cross-section. This is measured in barn. n_v is the number of atoms per unit volume.
The atomic cross-sections for the different atoms in composite materials are additive.

Photon - atomic electron interaction

Compton scattering:

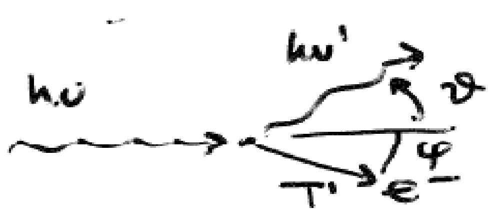

Assuming that the electron is free and initially at rest:

Conservation of energy: $h\nu + m_e c^2 = h\nu' + \gamma m_e c^2$

Conservation of momentum: $\frac{h\nu}{c} = \frac{h\nu'}{c}\cos\theta + p_e' \cos\phi$

Relativistic electron after interaction: $(p_e' c)^2 = T'(T' + 2m_e c^2)$

Neglecting the electronic binding energy(as earlier implied): $T' = h(\nu - \nu')$

Change in wavelength: $\Delta\lambda = \lambda' - \lambda = \lambda_c(1 - cos\theta)$

Compton wavelength: $\lambda_c = \frac{h}{m_e c}$

Scattered photon's energy:$h\nu' = \frac{h\nu}{1+\alpha(1-\cos\theta)}$,$\alpha = \frac{h\nu}{m_e c^2}$

Scattering angles: $\cot\phi = (1+\alpha)\tan\frac{\theta}{2}$

Minimum scattering: $\theta \simeq 0 \Rightarrow \phi = \frac{\pi}{2}$; $h\nu' \simeq h\nu$; $T_e' \simeq 0$

Maximum scattering: $\theta = \pi \Rightarrow \phi = 0$; $h\nu' \to \frac{h\nu}{1+2\alpha}$; $T_e' = h\nu\frac{2\alpha}{1+2\alpha}$

Fraction of energy scattered: $\frac{h\nu'}{h\nu}$

Fraction of energy transferred to the Compton electron: $(1 - \frac{h\nu'}{h\nu})$

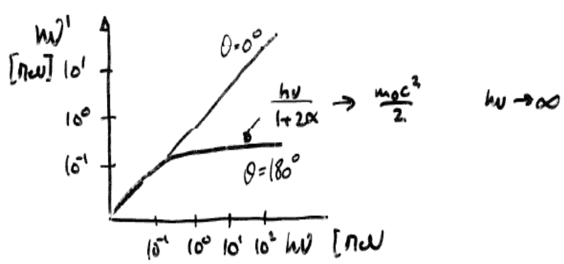

Klein-Nishina cross-section (per electron)

$$\frac{\sigma_{e,KN}}{d\Omega} = \frac{r_0^2}{2}\Big[\frac{1+\cos^2\theta}{[1+\alpha(1-\cos\theta)]^2} + \frac{\alpha^2(1-cos\theta)^2}{[1+\alpha(1-\cos\theta)]^3}\Big] \tag{9}$$

Where r_0 is the classical electron radius as defined before.

Alternatively:

$$\frac{d\sigma_{e,KN}}{d\Omega} = \frac{r_0^2}{2}\Big[\frac{\nu'}{\nu}\Big]^2\Big[\frac{\nu}{\nu'} + \frac{\nu'}{\nu} - \sin^2(\theta)\Big] \tag{10}$$

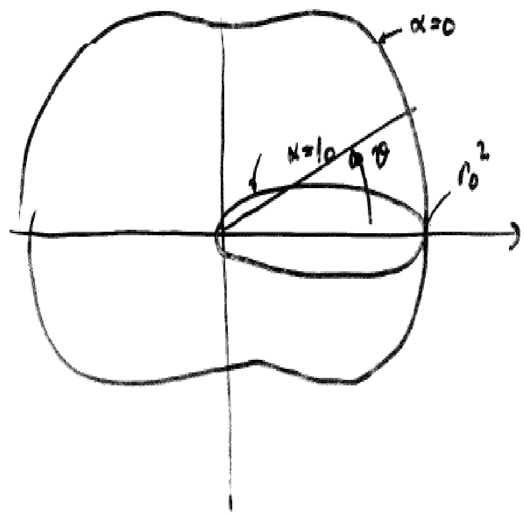

For low energies, $\alpha \to 0$:

$$\frac{d\sigma_{KN}}{d\Omega} \to \frac{r_0^2}{2}[1 + \cos^2\theta]$$

This cross-section describes scattering of photons by a free electron target, consistent with classical electro-magnetic theory. This is also called the Thomson cross section. This scattering process results in coherent scattering($h\nu' = h\nu$). In reality one has to introduce a scattering form-factor $\mathcal{F}$, for this formula to agree with experimental data.

Cross section for coherent scattering (Low energy description)

$$\frac{d\sigma_{koh.sc}}{d\Omega} = \frac{r_0^2}{2}(1 + \cos^2\theta)\Big[F(h\nu, \theta, Z)\Big]^2 \tag{11}$$

Cross section for incoherent scattering

$$\frac{d\sigma_{is}}{d\Omega} = \frac{d\sigma_{KN}}{d\Omega} S(h\nu, \theta, Z) \tag{12}$$

S is here a structure-factor (fraction of incoherent scattering). This factor describes the probability for the target atom to get excited, or ionized after interacting with the incoming photon.
Incoherent scattering $\equiv$ compton scattering:

Total compton scattering cross-section $\sigma_{CT} = \sigma_{CA} + \sigma_{CS}$

Cross-section describing energy transfer to scattered photon: $\sigma_{CS} = \frac{h\nu'}{h\nu}\sigma_{CT}$

Cross-section describing energy transfer to compton electron: $\sigma_{CA} = \left[1 - \frac{h\nu'}{h\nu}\right]\sigma_{CT}$

Photo-electric effect

This is not possible for a free electron (There is no solution to the compton equations for $h\nu' = 0$).

Kinetic energy for the electron: $T_e' = h\nu - E_B$

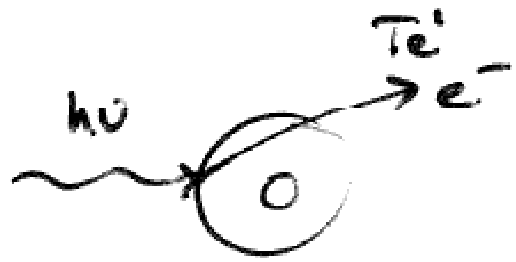

Photon - Coulomb field interaction

Pair production

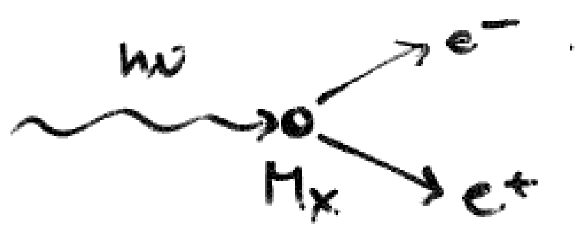

Threshold energy: $h\nu \geq 2m_oc^2\left[1 + \frac{m_0c^2}{M_xc^2}\right]$

Photon - nuclear Coulomb field interaction($M_x \gg m_0$): $h\nu \geq 2m_0c^2$

Triplet production

Photon-electronic Coulomb field interaction:($M_x = m_0$): $\quad h\nu \geq 4m_0c^2$

In this case, there is no way telling which two of the electrons are the produced ones, and which one is the original target. That is why the process is called :"triplet production".

β^+ annihilation

β^+ annihilation is usually a result of positronium($\beta^+ \& e^-$) being formed after the β^+ particle has lost its kinetic energy. Positronium has lifetime, $\tau \simeq 10^{-10}s$. Alternatively, the β^+ annihilation can occur "in flight".

Total interaction cross-section for photons

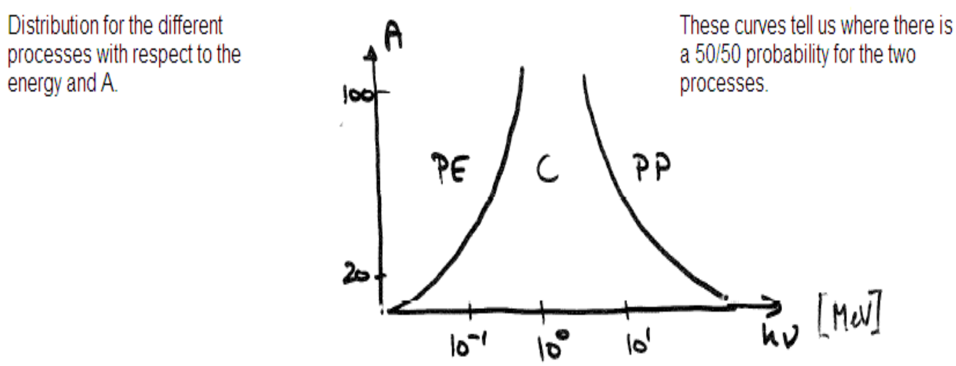

Total attenuation coeff: $\quad \mu = \mu_R + \mu_{PE} + \mu_{CT} + \mu_{PP}$

Mass-energy transfer coefficient, ($\frac{\mu_{tr}}{\rho}$) represents the fraction of the incoming photon's energy, which is transferred to charged particles (secondary electrons), thus increasing their kinetic energy.

$$\frac{\mu_{tr}}{\rho} = \frac{\mu_{PE}}{\rho}\Big[1 - \frac{\delta}{h\nu}\Big] + \frac{\mu_{CT}}{\rho}\Big[1 - \frac{h\nu'}{h\nu}\Big] + \frac{\mu_{PP}}{\rho}\Big[1 - \frac{2m_0c^2}{h\nu}\Big] \tag{13}$$

δ represents the mean energy emitted by characteristic X-ray radiation. $\delta = E_B \cdot$Probability for a de-excitation by X-ray radiation, as opposed to Auger electron emission.

Mass-energy absorption coefficient:

$$\frac{\mu_{en}}{\rho} = \left[\frac{\mu_{tr}}{\rho}\right][1-g] \tag{14}$$

g is the fraction of the secondary electrons' energy, which is emitted as bremsstrahlung. (This energy is not locally deposited in the stopping media)

Z-dependence of the photon cross sections

Generally:	$\sigma^a = Z \cdot \sigma^e$
σ^e is one of the electron cross-sections, for example σ_{KN}	
Linear attenuation coeff:	$\frac{\mu_l}{\rho} = \sigma^a \frac{N_A}{A} = \sigma^e \frac{Z}{A} N_A$
For most materials, Z$\simeq$ 0.45A for $A > 1$:	$\frac{\mu_l}{\rho} \simeq 0.45 N_A \sigma^e$

This means that $\frac{\mu_l}{\rho} \simeq$ constant(close to Z-independency) within the Compton range.

Photo-electric effect:	$\sigma^a_{PE} \propto \frac{Z^4}{(h\nu)^3}$
Compton:	$\sigma^a_{CT} \propto Z \rightarrow \sigma^e_{CT} \simeq$ constant
Pair production:	$\sigma^a_{PP} \propto Z^2$

Neutrons

Classification of neutrons

Thermal neutrons:	$E \simeq 0.025 eV$
Epithermal neutrons:	$E \simeq 1 eV$
Slow neutrons:	$E \simeq 1 keV$
Fast neutrons:	$100 keV - 10 MeV$

Neutron sources

(α, n)-sources consist of an α-emitter and ^{9}Be:$\Rightarrow$ $\;{}^4_2He +^9_4 Be \rightarrow^{12}_6 C + n$

For example, a mixture of ^{226}Ra and ^9Be $\Rightarrow$ constant neutron emission rate (not mono-energetic, due to energy loss of the α-particles in the sample).

(γ, n)-sources give nearly mono-energetic neutrons.: $\gamma +^9_4 Be \rightarrow^8_4 Be + n$

The γ-photon's threshold energy for this process to work: $h\nu \geq E_b$

Where E_b is the binding energy of the neutron.

Spontaneous fission, for instance: ^{252}Cf

Nuclear reactions: Choosing a specific T_a and exit angle θ $\Rightarrow$ Selective mono-energetic neutron flux.

Example:

$^3H + d \rightarrow^4 He + n$ Q=17.6MeV

$^9Be +^4 He \rightarrow^{12} C + n$ Q=5.7MeV

Reactor as a source: Large flux of neutrons for activation analysis.

Absorption and moderation of neutrons

There are several possible reactions for fast neutrons: (n,p), (n,α), (n, 2n) Usually, these reactions have very strong resonances.

Without the resonances: $\sigma \propto \frac{1}{v}$

Attenuation of mono-energetic neutrons: $I = I_0 e^{-\sigma_t n x} = I_0 e^{-\Sigma x}$

Where Σ represents the "macroscopic cross-section".(But really is a linear attenuation coefficient)

Energy distribution after scattering of mono-energetic neutrons

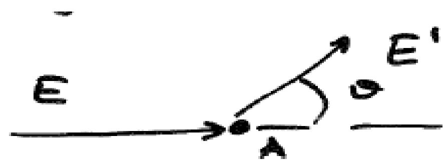

Scattering is isotropic in the CM frame.

$$\frac{E'}{E} = \frac{A^2 + 2A\cos\theta + 1}{(A+1)^2}$$

$$\left(\frac{E'}{E}\right)_{min} = \left[\frac{A-1}{A+1}\right]^2, \quad for \quad \theta = \pi \tag{15}$$

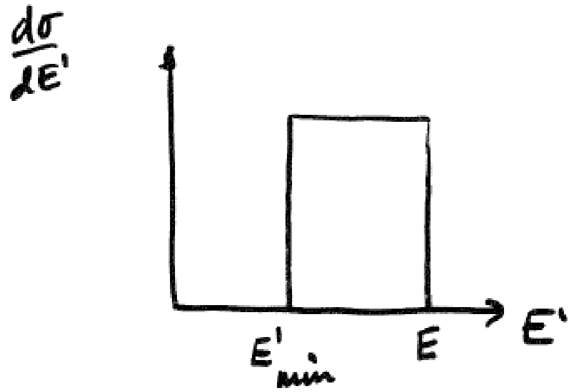

Logarithmic decrement:	$\xi = \frac{1}{4\pi}\int \ln\frac{E}{E'} \cdot d\Omega = 1 + \frac{(A-1)^2}{2A}\ln\frac{A-1}{A+1}$
Median energy after n interactions:	E'_n
This energy is defined as:	$\ln E'_n \equiv \overline{\ln E_n} = \ln E_0 - n\xi$

Example:Thermal moderation of neutrons

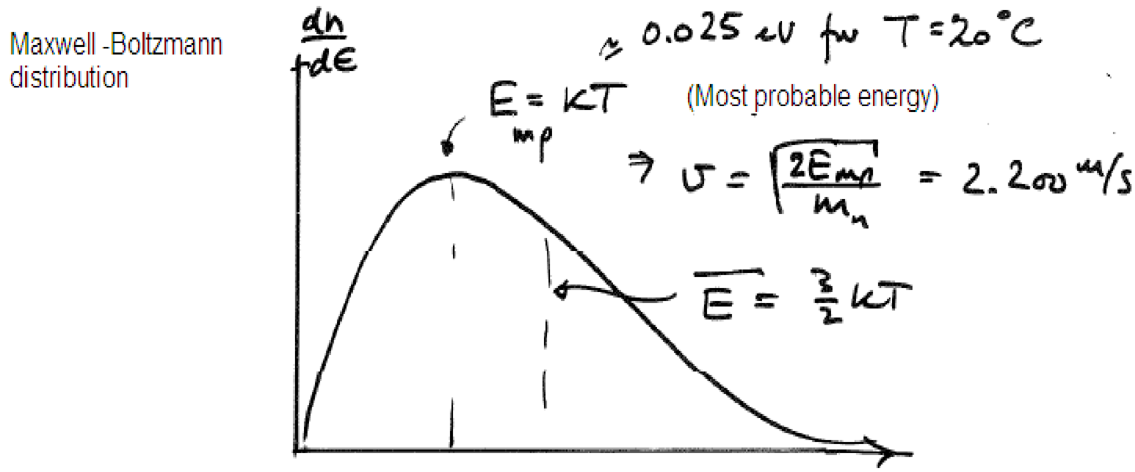

Thermalizing 2 MeV neutrons in different moderators:

Moderator	ξ	n
1^H	1.0	18
2^H	0.725	25
^{12}C	0.158	115
^{238}U	0.008	2200

3.)

Particle detectors and accelerators (Lilley Chap. 6)

Detectors

Gas filled ionisation chamber

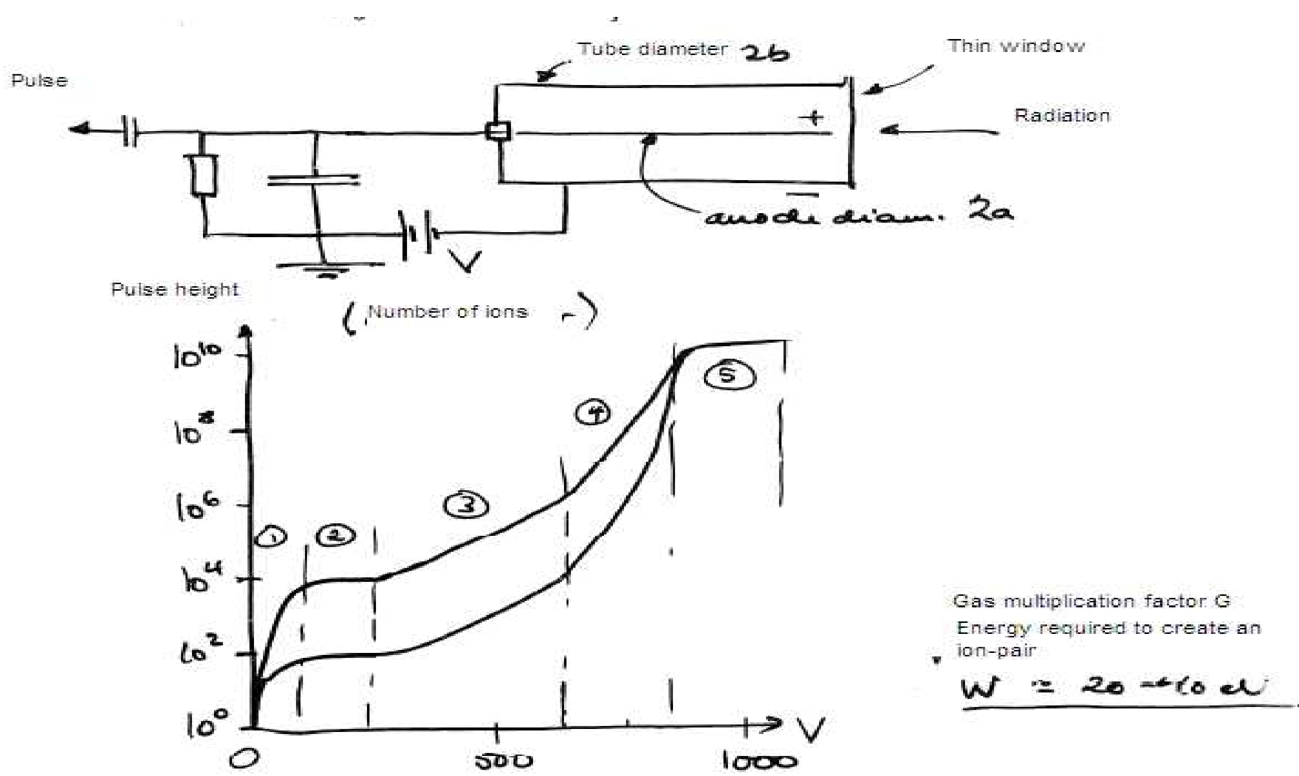

Electric field $E = \frac{V}{r \ln \frac{b}{a}}$

Gas multiplication factor: G

Required energy per ion-pair produced: $W = 20 - 40 eV$

Figure explanation

1.) Recombination ($G < 1$)

2.) Ionisation chamber. All the ion-pairs produced are collected by the electrodes, and there is no secondary ionisation.

3.) Proportional counter. Puls height $\propto$ energy ($G > 1$)

4.) Area with limited proportionality due to nonlinearity

5.) Geiger-Müller range. Full discharge cascade ($G \to \infty$)

Semiconductor detectors

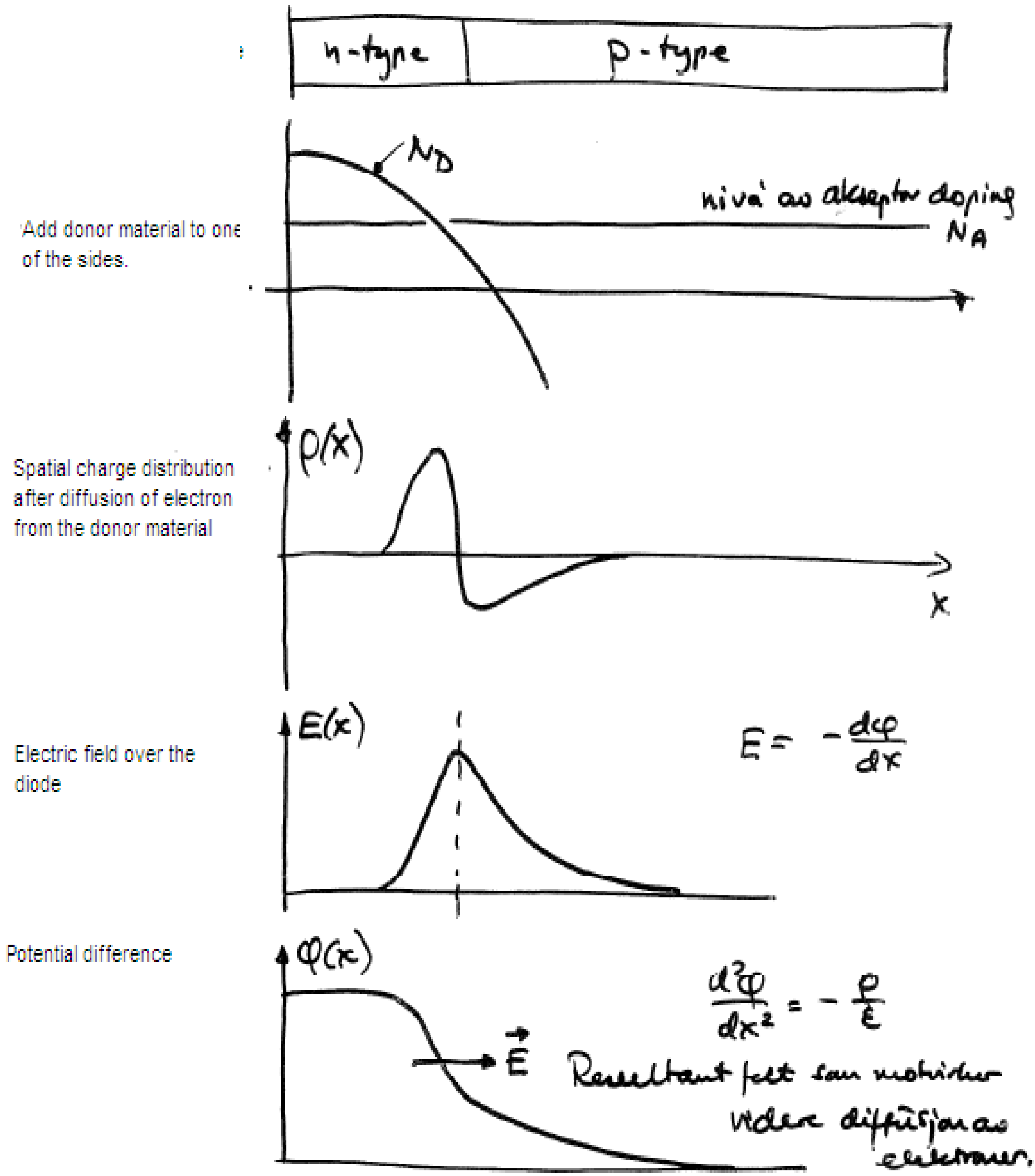

Depletion region:

There is an area containing no free charge-carriers on the border between the n and p material. This is called the active detector volume.

Reversed high voltage:

This results in a greater depletion region, as the active detector volume increases.

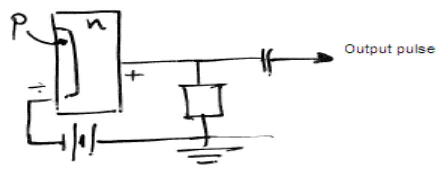

Different detectors

Surface barrier detector:

The active detection area is very close to the surface, but it is not particularly thick. This detector is well suitable for $\alpha-$ and $\beta-$ detection.

Ge(Li)-detector($\gamma-$detection):

The active detection volume is large because of neutralization of p-type material by inoculating Li. The disadvantage is that this detector always has to be kept cooled down (Liquid Nitrogen) to prevent leakage of Li.

HPGe-detector:

This is a modern detector for $\gamma-$detection. This detector has a big active detection volume, due to the ultra pure Ge "intrinsic" material inserted between the p- and n-region. The detector is cooled down during the detection sessions to reduce noise, but when not used it can be kept at room temperatures.

General advantages gained by using semi-conductor detectors:

1.) Very good energy resolution, since ion-pair production requires only a small amount of energy.($W \simeq 3eV$)

2.) Well defined linearity and good stability.

Scintillation counter

A scintillator (fluid or crystal) is excited by secondary electrons. This results in emission of visible light which can be detected by a photo-multiplier-tube.(PMT)

NaI(Tl)-crystal detector

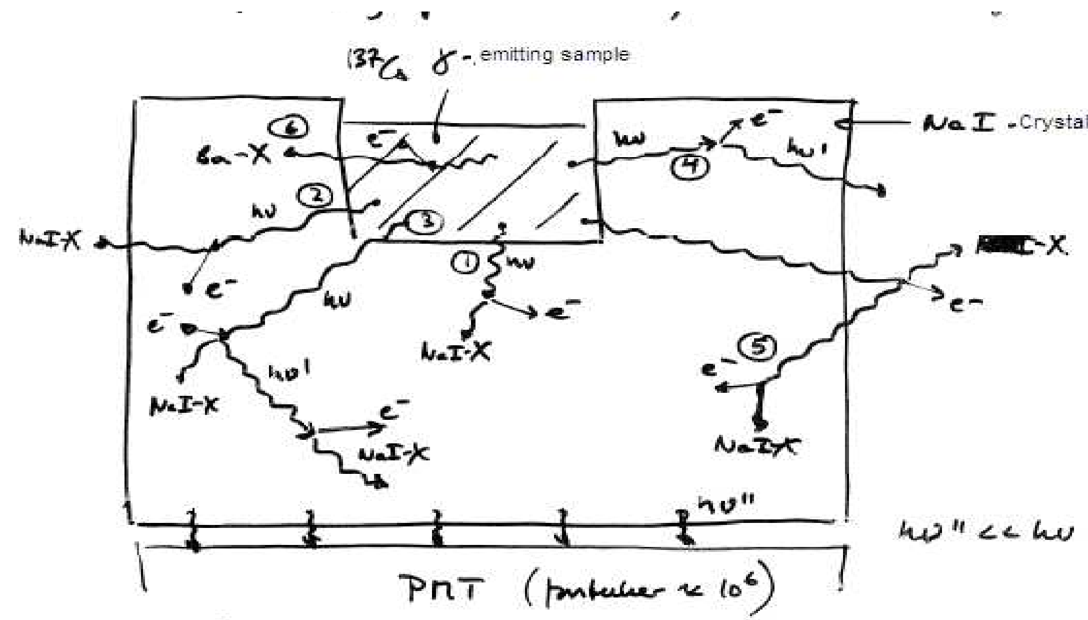

Spectrum

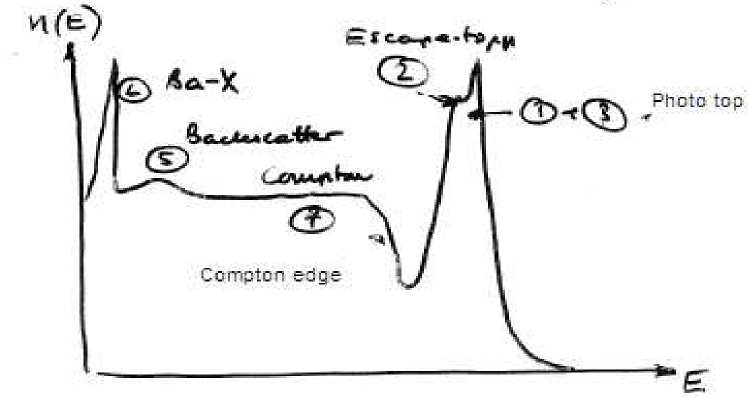

The crystal's excitation energy is converted into visible light by Tl-doping.

The Compton edge is given by the maximum energy of the Compton electron:

Maximum energy: $E_{max} = T'_{emax} = h\nu \frac{2\alpha}{1+2\alpha}; \alpha = \frac{h\nu}{m_e c^2}$

Photo-fraction: $f = \frac{\#\ \textit{Counts in full energy peak}}{\#\ \textit{Total counts}}$

Counting-efficiency ε, which is used
to find the radioactivity A in a sample
by using the counting rate r in the photo-peak: $r = \varepsilon A$

$$\varepsilon = f \cdot p_{vxv} \Omega \cdot k$$

In the last expression, f is the photo-fraction, p_{vxv} is the probability for interaction within the detector, Ω represents the solid angle seen by the detector and k is the number of photons with energy $h\nu$ emitted per disintegration.

Inside the detector, the photon energy $h\nu$ is deposited as kinetic energy for n charge-carriers (electrons from the photo-cathode of the PMT) which again results in a measurable pulse.

Measured energy E: $E \propto n$

Where n is Poisson distributed, which again means that:

Standard deviation $\sigma = \sqrt{n}$

Energy variance $(\Delta E)^2 \propto \underbrace{n}_{\textit{Poisson variance}} + \overbrace{\sigma_0^2}^{\textit{Rest variance}}$

$$(\Delta E)^2 \simeq a \cdot E + b$$

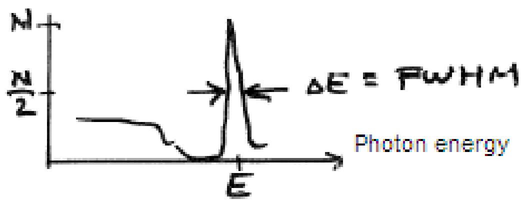

Neutron detectors

Detection of neutrons is based on detection of secondary ionizing particles.

^{10}B gas detector: BF_3 gas naturally contains 20% ^{10}B

Thermal capture cross-section: $\sigma_{thermalcap} = 3840b$ for $^{10}B \propto \frac{1}{v}$ up to 100keV

$$^{10}_{5}B +^{1}_{0} n \rightarrow \begin{cases} ^{7}_{3}Li^{*} +^{4}_{2} He: & Q_{96\%}\text{=2.31MeV} \begin{cases} T_{Li} = & 0.84\text{MeV} \\ T_{He} = & 1.47\text{MeV} \end{cases} \\ ^{7}_{3}Li +^{4}_{2} He: & Q_{4\%}\text{=2.79MeV} \begin{cases} T_{Li} = & 1.01\text{MeV} \\ T_{He} = & 1.78\text{MeV} \end{cases} \end{cases}$$

Detection pulse distribution

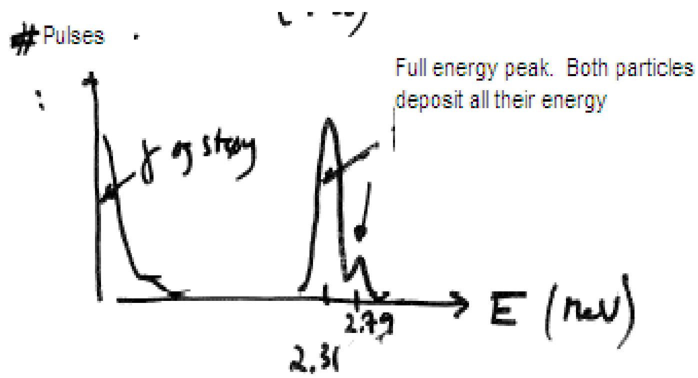

The advantage of having a $\frac{1}{v}$ dependent cross-section

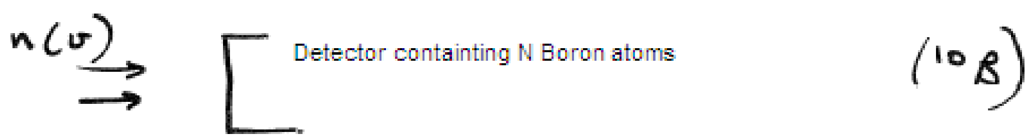

Flux of neutrons entering the detector with a velocity $v \in (v, v + dv)$: $\dot{\Phi}(v) = n(v)v \cdot dv$

Counting rate: $dR = N\sigma(v)n(v)vdv$

$$R = \int N\sigma(v)n(v)vdv = constant \int n(v)dv = const \cdot n$$

Where n is the neutron density. This means that the detector's counting rate is proportional to the neutron density and hence, independent of the neutrons' velocity.

How to find the neutron energy by diffraction

For thermal neutrons, the wavelength $\lambda \simeq 0.1nm$, which is comparable to the distance d between the atoms inside a crystal.

Constructive interference condition: $n\lambda = 2d\sin\theta$, $n = 1, 2, 3...$

Proton recoil spectroscopy:

Conservation of energy: $E_R = E - E' = E \cdot \cos^2\theta$

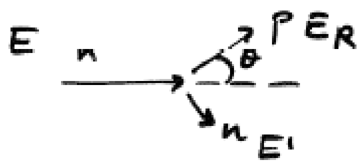

If this interaction is measured using a lioquid scintillator, there is no angular resolution:

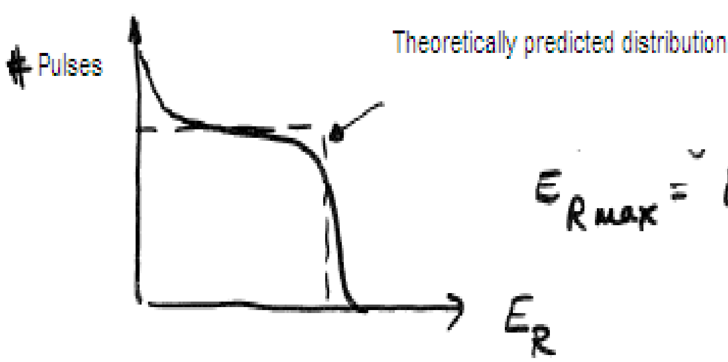

$$E_{R\,max} \simeq E - E'_{min} = E \cdot \frac{4A}{(A+1)^2}$$

Particle identification

ΔE-E telescope

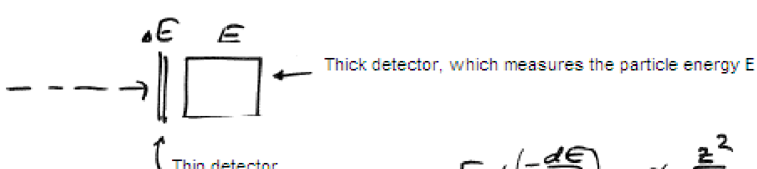

$$\Delta E \propto \left(-\frac{dE}{dx}\right)_{col} \propto \frac{z^2}{v^2} << E$$

Energy loss: $\Delta E = \left[-\frac{dE}{dx} \right]_{col} \propto \frac{z^2}{v^2} \ll E$

$\Delta E - E$ relation: $\Delta E \cdot E \propto \frac{z^2}{v^2}[\frac{1}{2}mv^2] \propto mz^2$; $\Delta E \propto \frac{mz^2}{E}$

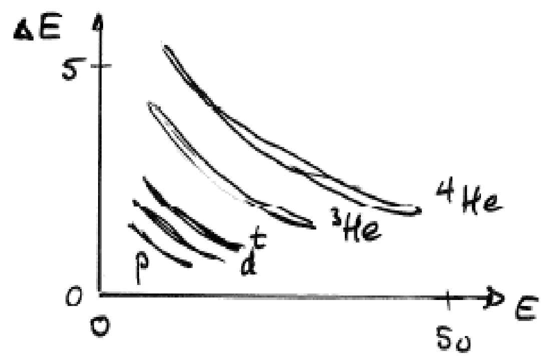

Magnetic spectrometer

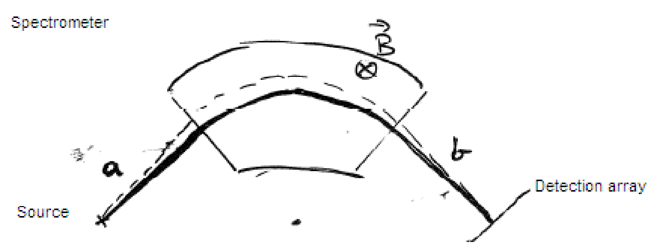

Force acting on particle: $F = qvB = m\frac{v^2}{r} \Rightarrow r = \frac{mv}{qB}$

If $a \cdot b = r^2$, there will be focusing in the horizontal plane. Focusing in the vertical direction takes place when angle of approach $\neq \frac{\pi}{2}$

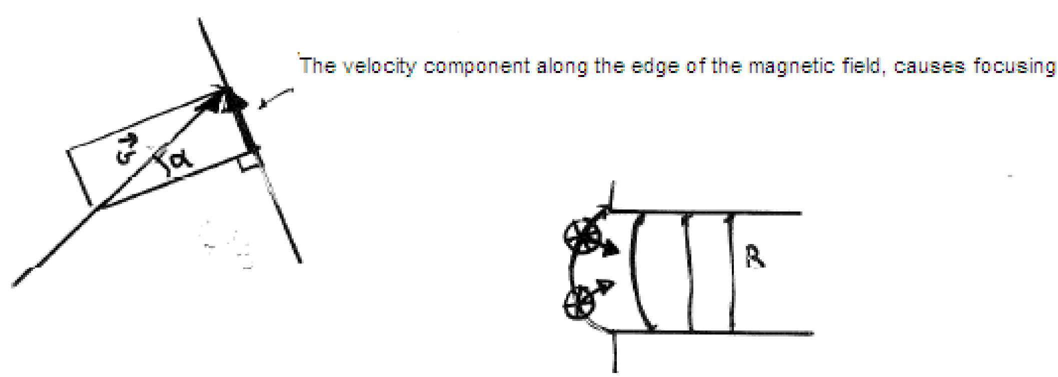

Accelerators

Dual Van de Graaf accelerator

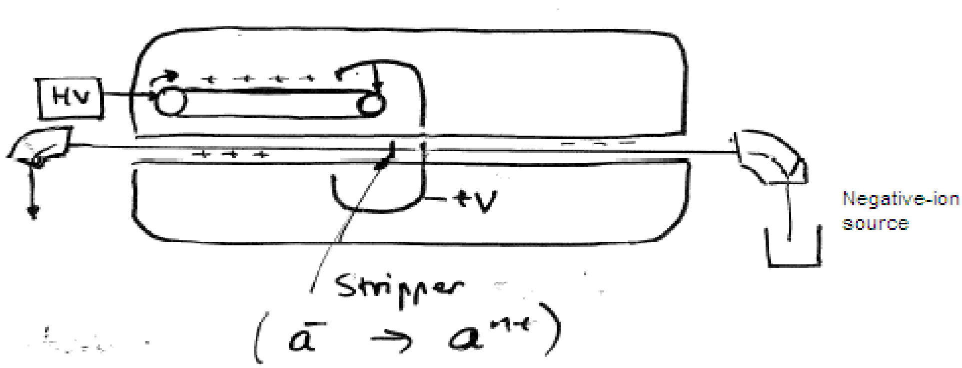

Terminal potential:	$HV = 20$ MV
Particle energy:	$E = (1 + n)eHV$

The advantage is that you get a DC beam with very high intensity.

Linear accelerator

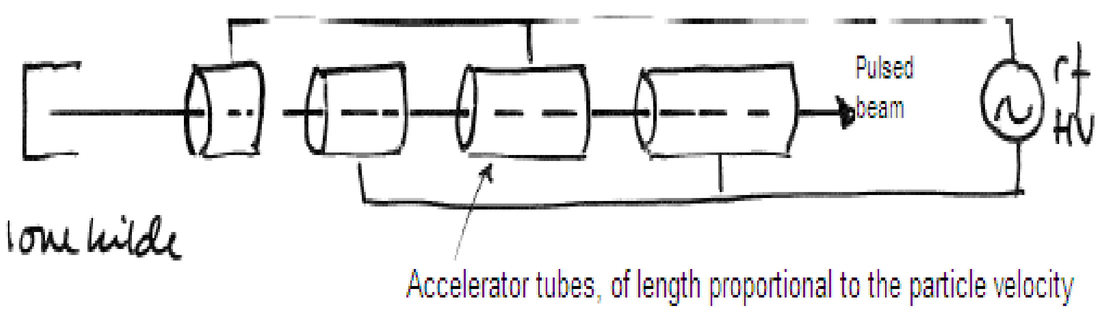

A phase stabilization is possible to achieve, if the particles are crossing the accelerator gap between two tubes when the field is increasing. Delayed particles will then feel a stronger acceleration. The phase stabilization gives a certain lateral defocusing, because the field is strongest at the end of the particle track between the tubes. The lateral defocusing described above, must be compensated for by adding several focusing rings inside the accelerator tubes.

SLAC: (Stanford Linear Accelerator) 20GeV electrons. It is about 3km long.

Linear accelerators are being used as radiation-therapy machines.

Cyclotron

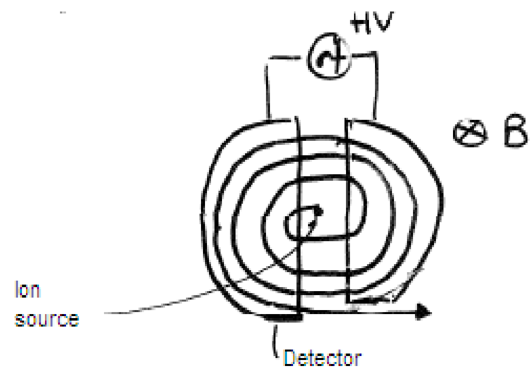

Force acting on particle	$F = qvB = m\frac{v^2}{r} \rightarrow v = \frac{qBr}{m}$
Period:	$T = \frac{2\pi r}{v} = \frac{2\pi m}{qB} \equiv \frac{1}{f}$
Max energy for r=R:	$E_{max} = \frac{q^2B^2R^2}{2m}$

To keep the period constant as E approaches E_{max}, the magnetic field B has to increase with r when $r \rightarrow R$. This results in a defocusing of the particle beam in the vertical plane. This has to be compensated for by splitting up the cyclotron in different sectors with higher and lower magnetic-field magnitudes, and using the focusing effect which is achieved at incoming angles $\neq \frac{\pi}{2}$

4.)

Nuclear structure (Lilley Chap. 2)

Models

Nuclear force

This is a short range attractive force, but repulsive for even shorter distances$\Rightarrow$ There is a certain optimal distance between nuclear particles.

Liquid drop model

The nucleus is considered as a spherical liquid drop with constant internal density.

Evidence for the existence of the liquid drop model:

The internal charge distribution:

a.) Electron scattering experiments imply the charge density function below:

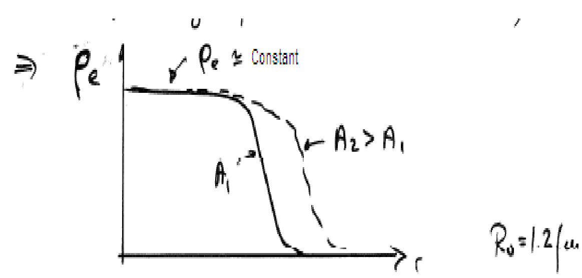

Number of nucleons per unit volume is approximately constant $\Rightarrow$ $\rho = \frac{A}{\frac{4}{3}\pi R^3}$

b.) The nuclear charge distribution affects the energy levels of the S-orbital electrons.

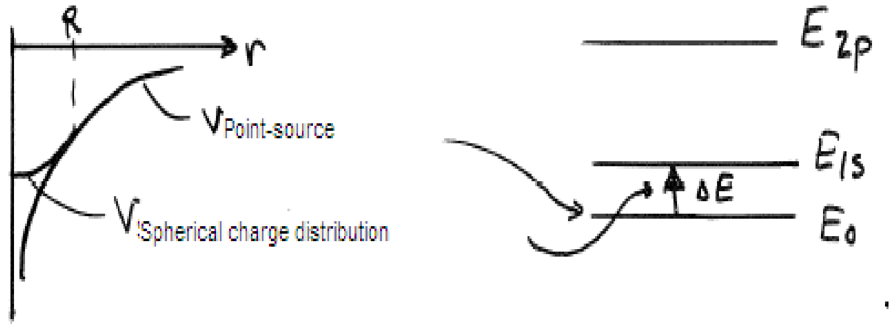

c.) The potential energy difference between mirror nuclei:

<u>Example:</u>

${}^{13}_{7}N_6 \xrightarrow{\beta^+} {}^{13}_{6}C_7$, Measure E_{max} for β^+

$$\Delta E_C = \frac{3}{5}\frac{e^2}{4\pi\varepsilon_0}\frac{1}{R}\underbrace{\left[Z^2-(Z-1)^2\right]}_{(2Z-1)=A} \Rightarrow \Delta E_c = \frac{3}{5}\frac{e^2}{4\pi\varepsilon_0}\frac{1}{R_0}A^{\frac{2}{3}}$$

<u>The internal mass distribution</u>:

a.) Neutron scattering (elastic)

This is the same calculation as used for electron scattering, remembering to exchange the electron's electro-magnetic potential with the neutron's potential

$\Rightarrow$ Scattering data give the Fourier transform of the mass distribution.

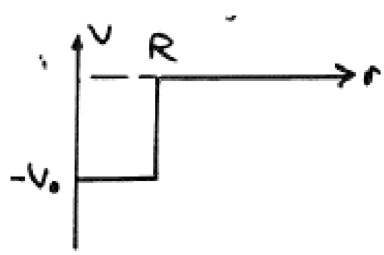

b.) Deviation from the expected angular dependency of Rutherford scattering for $r > R$.

c.) Calculating the tunneling probability for α-disintegration.

d.) Measuring the difference between E_k-energies for atoms

with $\underbrace{\pi - mesons}_{Strong\ force+Coulomb}$ and $\underbrace{muons}_{Coulomb\ only}$ instead of electrons.

These four points, from a.) through d.), result in a conclusion: $\rho_m \simeq \rho_e$, $R = R_0 A^{\frac{1}{3}}$, $R_0 = 1.2\text{fm}$

Measuring atomic masses

Mass excess, $\Delta = m - A$ is $\begin{cases} \geq 0, & \text{if } A < 12 \\ \leq 0, & \text{if } A > 12 \end{cases}$

Binding energy

Binding energy: $B = \left[Zm(^1H) + Nm_n - m(^A_ZX) \right] c^2$, where $c^2 = 931.5 \frac{MeV}{u}$

Neutron separation energy: $S_n = \left[m_n + m(^{A-1}_{Z}X_{N-1}) - m(^A_ZX_N) \right] c^2$

Proton separation energy: $S_p = \left[m_p + m(^{A-1}_{Z-1}X_N) - m(^A_ZX_N) \right] c^2$

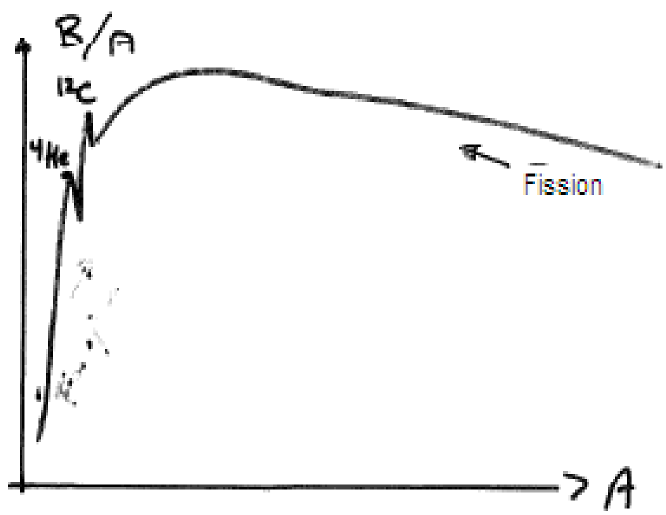

Binding energy: $B = a_v \cdot A - a_s A^{\frac{2}{3}} - a_c \cdot Z(Z-1)A^{-\frac{1}{3}}$ (Liquid drop model)

$-a_{sym} \cdot \frac{(A-2Z)^2}{A} + \delta_{pair}$ (Shell effects)

Where $\delta = \begin{cases} +a_p A^{-\frac{3}{4}}, & \text{if Z \& N are even numbers} \\ 0, & \text{if A is an odd number} \\ -a_p A^{-\frac{3}{4}}, & \text{if Z \& N are odd numbers} \end{cases}$

Semi-empirical mass formula: $M(Z, A) = Zm(^1H) + Nm_n - \frac{B(Z,A)}{c^2}$

M(A,Z) is sketched below for fixed values of A:

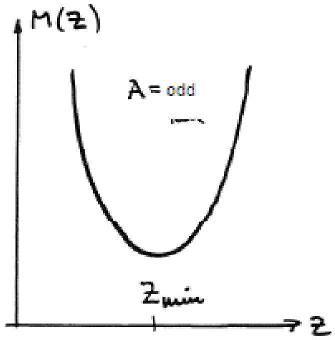

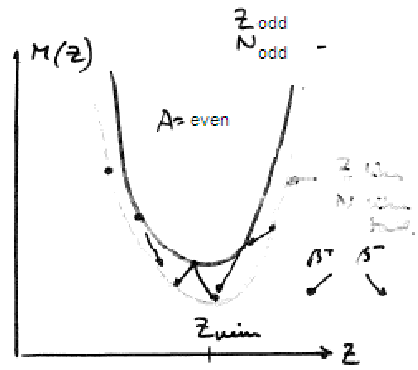

Minimum mass: $\frac{\partial M}{\partial Z} = 0 \Rightarrow Z = Z_{min} = \frac{[m_n - m(^1H)] + a_c A^{-\frac{1}{3}} + 4a_{sym}}{2a_c A^{-\frac{1}{3}} + 8a_{sym}A^{-1}}$

The nuclear shell model

This model is the nuclear analogy to the electron shell model.
Experimental data show that the ionisation energy decreases and the atomic radius increases rapidly for the first electron outside a full shell. I.e for Li, Na, K etc. The same occurs for nucleons in the nucleus.

Experimental data that justify the theory of a nuclear shell structure

a.) There is a rapid fall in 2-neutron and 2-proton separation energy when passing the magic nucleon numbers; 8, 20, 28, 50, 82, 126

b.) α-energy reaches maximum for radio-nuclei where the daughter nucleus has a structure corresponding to magic numbers.

c.) The neutron scattering cross-section for nuclei with N=magic numbers is extraordinarily small.

d.) There is a huge increase in the nuclear radius when the number of neutrons exceed magic numbers.

A realistic potential for the shell model (Woods-Saxon potential):

$$V = \frac{-V_0}{1 + e^{\frac{r-R}{a}}} \tag{1}$$

Where $V_0 \simeq 50MeV$, $R = R_0 A^{\frac{1}{3}}$, $R_0 = 1.2fm$

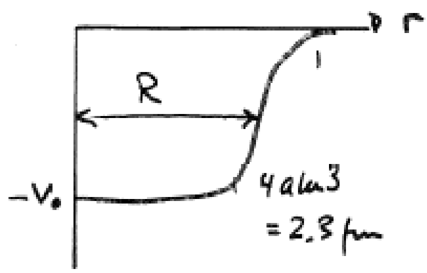

Spin-Orbit coupling

Energy difference:	$\Delta E = -(\vec{l} \cdot \vec{s})\ V_{so}, \quad V_{so} > 0$
Total angular momentum:	$\vec{j} = \vec{l} + \vec{s}$
From this, it follows that	$< \vec{l} \cdot \vec{s} >= \frac{1}{2} < [\vec{j}^2 - \vec{l}^2 - \vec{s}^2] >= \frac{1}{2}[j(j+1) - l(l+1) - s(s+1)]\hbar^2$
Energy splitting:	$\delta E = V_{so}[< \vec{l} \cdot \vec{s} >_{j=l-\frac{1}{2}} - < \vec{l} \cdot \vec{s} >_{j=l+\frac{1}{2}}] = \frac{\hbar^2}{2} V_{so}(2l+1)$

$j_l(k_{nl}R)=0$

$r=R$ gives n'th zero for $j_l(kr)$ $r\in(0,R)$

$\Rightarrow E_{nl}=\dfrac{\hbar^2k_{nl}^2}{2m}$

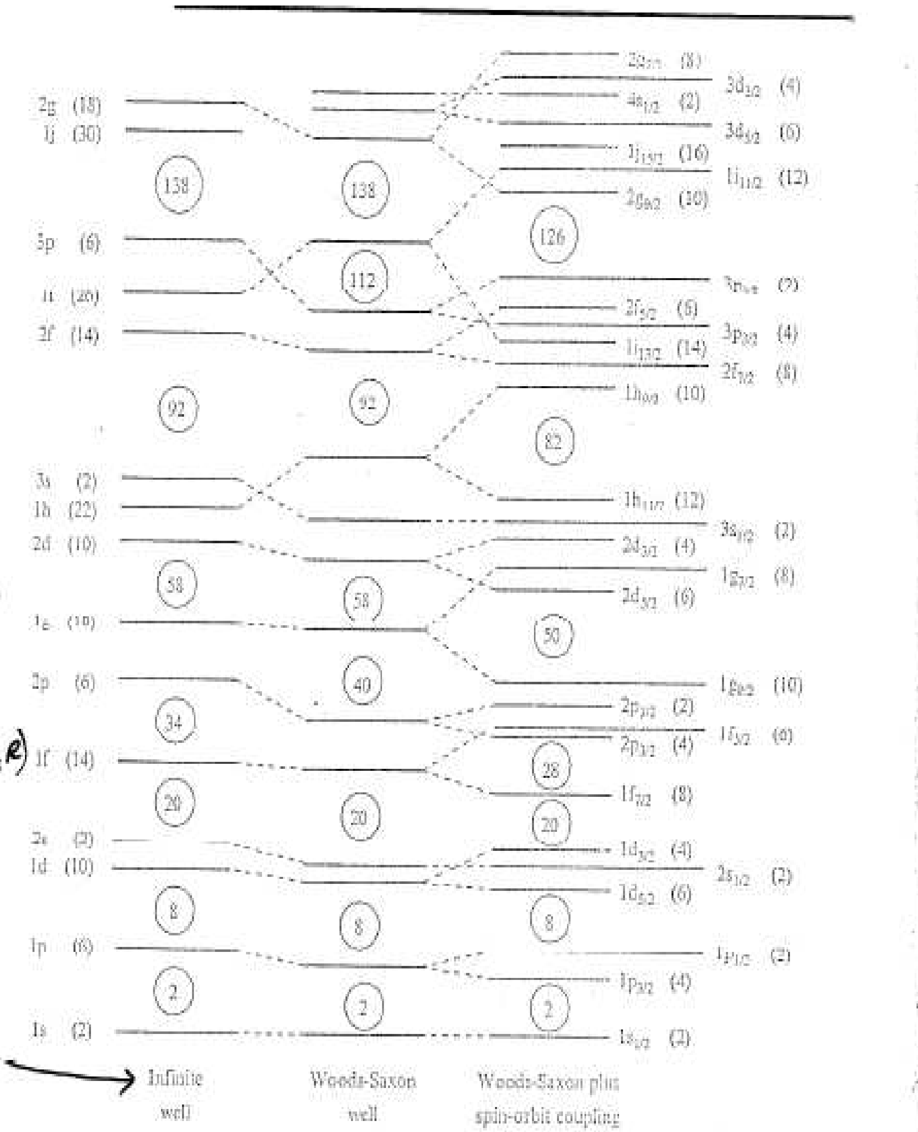

\# of identical nucleons per energy level: (2j+1)

Remember that the Pauli principle applies only for identical Fermions (protons and neutrons are counted independently).

$$\text{Parity:}\quad (-1)^l \Rightarrow \begin{cases} \pi^+ & \text{for s, d, g..} \\ \pi^- & \text{for p, f, h..} \end{cases}$$

This shell model with spin-orbit coupling gives the right spin and parity. Further on, it predicts reasonable energy levels, and introduces the magical numbers corresponding to filled shells.

Angular momentum and spin

For each nucleon:	$\vec{j} = \vec{l} + \vec{s}$
For the nucleus:	$\vec{I} = \sum \vec{j}_i$
	$\vec{I}^2 = \hbar^2 I(I+1)$
	$I_z = m\hbar$
For nuclei with one valence-nucleon:	$\vec{I} = \vec{j}_{vn}$
For nuclei with two valence-nucleons:	$\vec{I} = \vec{j}_1 + \vec{j}_2$
For nuclei with even numbers of A:	$I \in$ integer
For nuclei with odd numbers of A:	$I \in$ half integer
For even-even nuclei(Z&A even):	I=0 in the ground state

Valence nucleons

Excited states: The valence nucleon jumps to a higher energy state in the shell model by absorbing excitation energy. This model agrees with experimental data for nuclei with one valence nucleon.

Experimental data which justify the orbital model for nucleons

Electron-scattering experiments to find the charge-distribution difference between $^{206}_{82}Pb_{124}$ and $^{205}_{81}Tl_{124}$. The difference, $\Delta\rho_e$, takes place because Pb has one extra proton in a $3S_{\frac{1}{2}}$-state.
$\Rightarrow \Delta\rho_e$ corresponds to a $3s_{\frac{1}{2}}$-orbital.

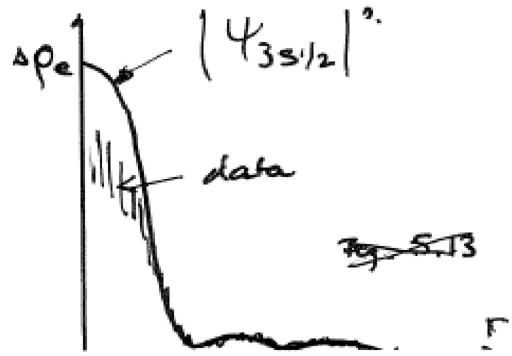

Protons and neutrons are found as proton- and neutron-pairs in the shell structure. To excite a nucleon, one has to break a pair bond (typically 2MeV binding energy). Energy and spin is then found from the two odd nucleons. Coupling of the two angular momenta $\vec{j}_1 + \vec{j}_2$ gives values from $|j_1 + j_2|$ to $|j_1 - j_2|$.

Collective structure contributions in even-even nuclei

Experimentally:

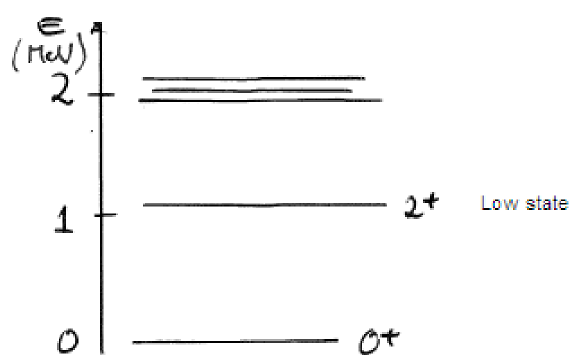

All even-even nuclei have a low 2^+ excited state with excitation energy around half the energy required to separate a pair of nucleons, indicating another type of excited state than single nucleon excitation.

Experimental data:

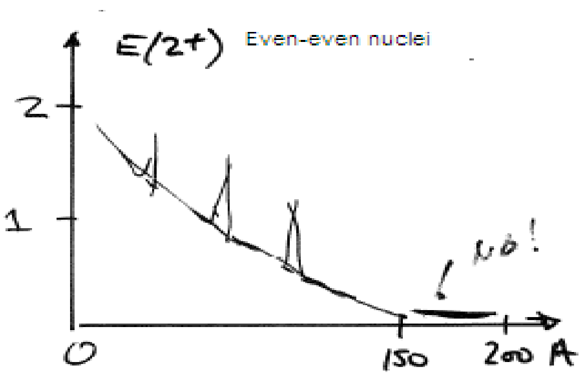

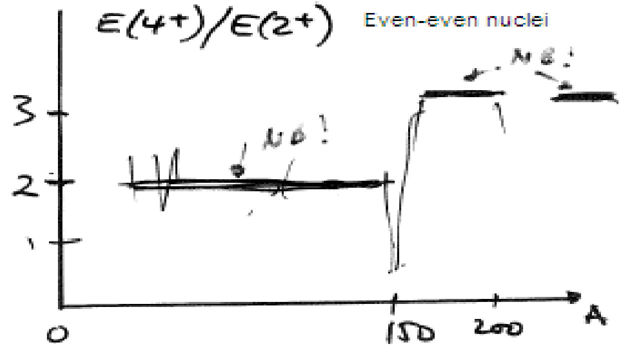

Nuclear vibrations(for $A < 150$)

The nuclear surface:

$$R(t) = R_{av} + \sum_{\lambda \geq 1} \sum_{\mu=-\lambda}^{\lambda} \alpha_{\lambda\mu}(t) Y_{\lambda\mu}(\theta, \phi) \tag{2}$$

A nuclear quadrupole-moment corresponds to $Y_{20}(l = 2)$

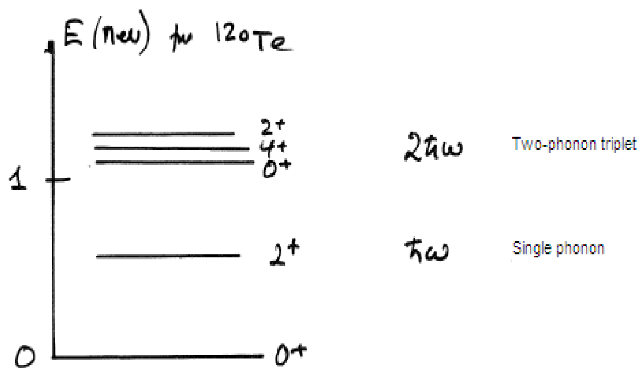

Exited phonon states with equidistant energy levels $\Rightarrow E = n \cdot \hbar\omega$

If the 4^+ state is due to a two-phonon excitation and 2^+ corresponds to a one-phonon excitation, one can easily draw the conclusion that $E(4^+)/E(2^+) = 2$. Experimental data for $A < 150$ confirms this model.

Rotating deformed nuclei $(150 < A < 190, A > 220)$

$$R(\theta,\phi) = R_0\big[1 + \beta Y_{20}(\theta,\phi)\big] \tag{3}$$

Deformation parameter: $\beta = \frac{4}{3}\sqrt{\frac{\pi}{5}}\frac{\Delta R}{R_{av}} \simeq \frac{\Delta R}{R_{av}}$

Intrinsic quadrupole moment, Q ,in the nucleus' rest frame: $Q_0 = \frac{3}{\sqrt{5\pi}} \cdot R_{av}^2 Z\beta(1 + 0.16\beta)$

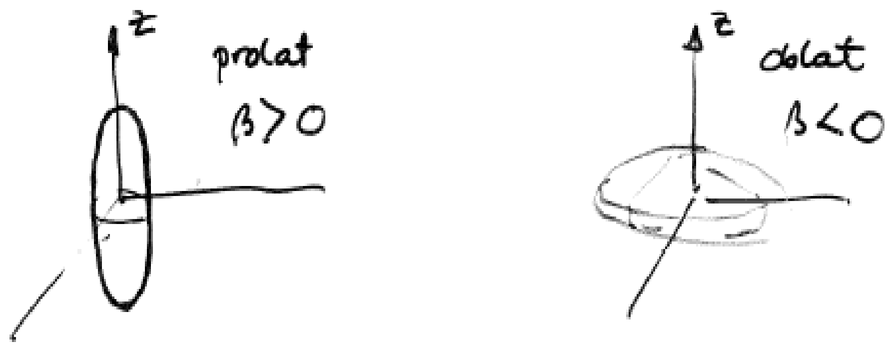

A rotating $\underbrace{\textit{prolate}}_{Q_0>0}$ ellipsoid rotates perpendicular to the symmetry-axis $\Rightarrow Q < 0$.

Rotational states

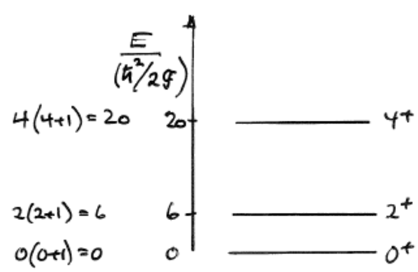

$$E = \frac{\hbar^2}{2\Upsilon} I(I+1) \tag{4}$$

The ground state for even-even nuclei has a total angular momentum I=0, and superimposed rotational states have even spin due to symmetry. Υ is the effective nuclear mass moment of inertia. Deformed nuclei are found where Z&N take values far from magic numbers.

Super-deformation

The Schrødinger equation for deformed nuclei gives a new set of states. When deforming a nucleus $\simeq$ 2:1 prolate ellipsoid, a new shell structure arises $\Rightarrow$ super-deformed states.

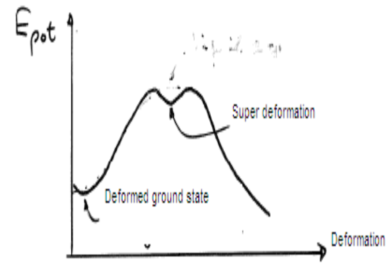

5.)

Nuclear instability (Lilley Chap 3)

γ-radioactivity

Transitions

Isomeric transition (leaves Z and N unchanged) from an exited nuclear state:	${}^{A}_{Z}X^{*} \rightarrow {}^{A}_{Z}X + \gamma$
Conservation of energy:	$E_i = E_f + E_\gamma + T_R$
Conservation of momentum:	$0 = \vec{P}_R + \vec{P}_\gamma \Rightarrow P_R = P_\gamma = \frac{1}{c}E_\gamma$
$\Rightarrow$	$E_\gamma = \frac{\Delta E}{1+\frac{\Delta E}{2M_x c^2}} \simeq \Delta E(1 - \frac{\Delta E}{2M_x c^2})$

Where, E_i and E_f represents the excitation energy in the initial and final states, $\Delta E = E_i - E_f$, and T_R is the recoil energy.

From the theory of classical electromagnetic radiation

Parity for multipole-field of order L:	$\pi(EL) = (-1)^L$, $\pi(ML) = (-1)^{L+1}$
Radiated power:	$P(\sigma L) = \frac{2(L+1)c}{\varepsilon_0 L[(2L+1)!!]^2}\left[\frac{\omega}{c}\right]^{2L+2}[m(\sigma L)]^2$

Where $(2L+1)!! \equiv (2L+1)(2L-1)(2L-3)....1$, $\sigma \in E, M$, and $m(\sigma L)$ is the time dependent multipole amplitude.

A quantum mechanical approach

Multipole moment: $M_{fi}(\sigma L) = \int \psi_f^* m(\sigma L) \psi_i d^3r$

Emitted power: $P(\sigma L) = T(\sigma L) \cdot \hbar\omega$

Emission rate: $T(\sigma L) = \frac{P(\sigma L)}{\hbar\omega} = \frac{2(L+1)}{\hbar\varepsilon_0 L[(2L+1)!!]^2} \left[\frac{\omega}{c}\right]^{2L+1} B(\sigma L)$

Reduced transition probability: $B(\sigma L) = \left| M_{fi} \right|^2$

Single nucleon (SP) model

Multipole operator: $m(EL) \propto e r^L Y_{LM}(\theta, \phi)$

$m(ML) \propto r^{L-1} Y_{LM}(\theta, \phi)$

Weisskopf sp-approximations: $B_{sp}(EL) = \frac{e^2}{4\pi}\left[\frac{3R^L}{L+3}\right]^2$

$B_{sp}(ML) = 10\left[\frac{\hbar}{m_p c R}\right]^2 B_{sp}(EL)$

These approximations lead to: $T(E1) = 10^{14} A^{\frac{2}{3}} E_\gamma^3$

$T(M1) = 3.1 \cdot 10^{13} E_\gamma^3$

If $L \to L+1$: $T(L+1) \to 6 \cdot 10^{-7} A^{\frac{2}{3}} E_\gamma^2 \cdot T(L)$

Note:

1.) The lowest multipole transition has the highest transition probability

2.) For a given order, $T(EL) \simeq 100 \cdot T(ML)$

Selection rules

The photon is a S=1 Boson. The direction of this spin is either parallel or antiparallel to $\vec{p}_\gamma$. This spin cannot be coupled to $\vec{l} = \vec{r} \times \vec{p}_\gamma$ because $\vec{S} \perp \vec{l}$.

Conservation of angular momentum: $\vec{I}_i = \vec{I}_f + \vec{L}$

$$|I_i - I_f| \leq L \leq |I_i + I_f|, \quad L \neq 0$$

Now, if:

$\Delta\pi = 0$:	Even EL, odd ML $\Rightarrow$	M1, E2, M3....
$\Delta\pi \neq 0$	Odd, EL, even ML $\Rightarrow$	E1, M2, E3....

If I_i or $I_f = 0 \Rightarrow$ A particular value of $L \Rightarrow$ Pure multipole transition.
If $I_i = I_f = 0$ Forbidden transition for γ-transition, but an electron conversion is possible.

Experimental determination of multipole contribution

Generally, $|I_i - I_f| \leq L \leq |I_f + I_i|$ give several possible L-values. This means that L has to be determined experimentally. The easiest way to approach this problem is to find the angular-correlation:

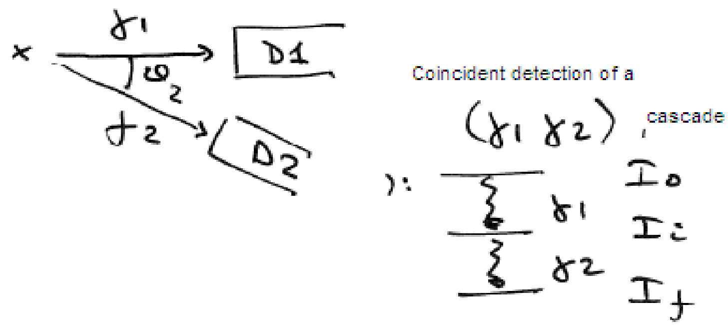

Conversion electrons

The nucleus de-excites by interaction with an atomic electron (mainly S-orbital electrons) $\Rightarrow$ electron emission.

Conservation of energy:	$T_e = \Delta E - E_B$
Binding energy:	$E_B(K) > E_B(L) > E_B(M)$....
Transition probability per unit time:	$\lambda_{tot} = \lambda_\gamma + \lambda_e$
Conversion coeff.:	$\alpha = \frac{\lambda_e}{\lambda_\gamma} \quad \Rightarrow \quad \lambda_t = \lambda_\gamma(1+\alpha)$
	$\alpha = \alpha_K + \alpha_{LI} + \alpha_{LII} + \alpha_{LIII} + \alpha_M$......

Maximum conversion: K-shell electron conversion (n=1) for low-energy, high-polarity transitions ($E \ll 2m_ec^2$) in heavy nuclei ($\propto Z^3$). The difference between $\alpha(EL)$ and $\alpha(ML)$ can be used to determine the change of parity. $\alpha = \infty$ for $0^+ \rightarrow 0^+$ because L=0 is a forbidden γ-emission transition. The competition between conversion electrons and γ-emission is analogous to the process where Auger electrons and characteristic X-ray emission compete when a de-exitation of electronic energy-states takes place. ($K - L_I$ transition is optically forbidden).

β-Disintegration

There are 3 different processes concerning this topic: $\beta^-, \beta^+, \varepsilon$

β^--disintegration

$$^A_ZX \rightarrow ^A_{Z+1}X' + e^- + \overline{\nu}_e$$

Energy released:

$$Q_{\beta^-} = (m_P - m_D)c^2$$

$$Q_{\beta^-} = (\Delta_P - \Delta_D)c^2$$

$$Q_{\beta^-} = T_{X'} + T_e + T_{\overline{\nu}_e}$$

Where $T_{X'}$, the recoil energy, is close to zero and $m_{\overline{\nu}_e} \simeq 0 \Rightarrow T_{\overline{\nu}_e} = E_{\overline{\nu}_e}$. This means that the energy released in the reaction can be written as below.

Energy released: $$Q_{\beta^-} = T_e + T_{\overline{\nu}_e} = T_{e,max} = T_{\overline{\nu}_e,max}$$

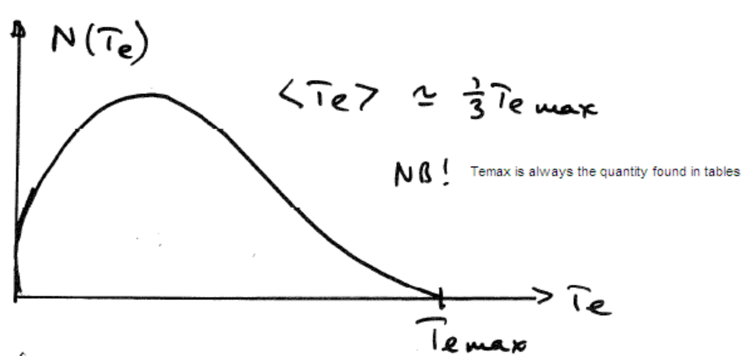

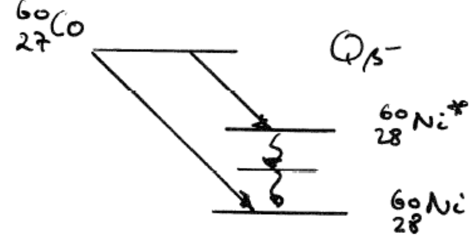

β^+-disintegration

$${}_Z^AX \rightarrow {}_{Z-1}^A X' + \beta^+ + \nu_e$$

Energy released: $Q_{\beta^+} = (m_P - m_D - 2m_e)c^2$

$$Q_{\beta^+} = (\Delta_P - \Delta_D - 2m_e)c^2$$

$$Q_{\beta^+} = \underbrace{T_{X'}}_{\simeq 0} + T_{\beta_+} + \underbrace{T_{\nu_e}}_{\simeq E_{\nu_e}} \text{ because } m_{\nu_e} \simeq 0$$

$$Q_{\beta^-} = T_{\beta^+,max} = T_{\nu_e,max}$$

Electron capture (ε or EC)

$${}_Z^AX + e^- \rightarrow {}_{Z-1}^A X' + \nu_e$$

Released energy: $Q_{EC} = c^2(m_P - m_D) - E_B$

$$Q_{EC} = T_X' + T_{\nu_e}$$

The recoil energy, T_X', is very small and can therefore in most cases be neglected. E_B is the binding energy for the captured electron's initial orbital. Since this is a two-body problem, the neutrino is emitted with well-defined energy and is therefore said to be mono-energetic.

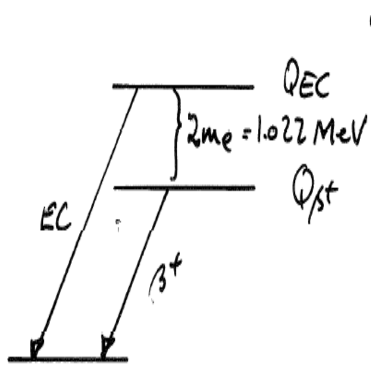

Possible Q_{EC} values if $m_P \simeq m_D$: $E_B(K) > E_B(L) \Rightarrow \begin{cases} Q_{EC(K)} < 0 & \text{No transition} \\ Q_{EC(L)} > 0 & \text{Transition possible} \end{cases}$

Fermi theory for β-disintegration

Distinctive traits (in comparison to α-disintegration):

1.) The potential barrier is of no relevance ($m_e \ll m_\alpha$, and therefore $P(tunneling) \simeq 1$).

2.) An electron and an anti neutrino has to be created.

3.) A relativistic approach is necessary.

4.) "3-body problem" for $\beta^\pm$.

Fermi's golden rule: $\lambda = \frac{2\pi}{\hbar}|V_{fi}|^2\rho(E_f)$

Matrix element: $V_{fi} = g\int \psi_f^* V \psi_i d^3r$

Initial state: $\psi_i = \psi_{iN}$

Final state: $\psi_f = \psi_{fN}\phi_e\phi_{\bar{\nu}_e}$

Where g is a constant which characterizes the strength of the weak interactions.

Number of states: $n = \frac{pL}{h}$, for $x \in [0, L]$ and $p \in [0, p]$

$\Rightarrow$ $d^2n = dn_e dn_{\nu_e} = \frac{(4\pi)^2 V^2 p^2 dpq^2 dq}{h^6}$

Where p is the linear momentum of the electron and q that of the neutrino. For the electron and neutrino states, we use zero order approximations which give allowed transitions.

Electron state: $\phi_e(\vec{r}) = \frac{1}{\sqrt{V}}e^{i\frac{\vec{p}\cdot\vec{r}}{\hbar}} \simeq \frac{1}{\sqrt{V}}\left[1 + i\frac{\vec{p}\cdot\vec{r}}{\hbar} + ...\right] \simeq \frac{1}{\sqrt{V}}$

Neutrino state: $\phi_{\overline{\nu}_e}(\vec{r}) = \frac{1}{\sqrt{V}}e^{i\frac{\vec{q}\cdot\vec{r}}{\hbar}} \simeq \frac{1}{\sqrt{V}}\left[1 + i\frac{\vec{q}\cdot\vec{r}}{\hbar} + ...\right] \simeq \frac{1}{\sqrt{V}}$

Now, by inserting this into Fermi's golden rule one obtains:

Transition probability rate: $d\lambda(p) = \frac{2\pi}{\hbar}\left| g \int \psi^*_{fN} \phi^*_e \phi^*_{\overline{\nu}_e} O_x \psi_i d^3r \right|^2 \frac{(4\pi)^2 V^2 p^2 dp q^2}{h^6} \frac{dq}{dE_f}$

Conservation of energy: $E_f = E_e + E_{\overline{\nu}_e} = E_e + qc$, assuming $M_{\overline{\nu}_e} \equiv 0$

$\Rightarrow$ $\frac{dE_f}{dq} = c$ for fixed E_e

Released energy: $Q = T_e + qc \Rightarrow q = \frac{Q - T_e}{c}$

Transition probability rate: $d\lambda(p) = \frac{2\pi}{\hbar} g^2 \left| M_{fi} \right|^2 (4\pi)^2 \frac{p^2 dp q^2}{h^6} \frac{1}{c}$

$d\lambda(p) \propto N(p)dp = Cp^2q^2dp$

Electron distribution: $N(p) = \frac{C}{c^2} p^2 (Q - T_e)^2 = \frac{C}{c^2} p^2 [Q - \sqrt{(pc)^2 + (mc^2)^2} + mc^2]^2$

$N(p)dp = N(T_e)dT_e \Rightarrow \frac{dp}{dT_e} = \frac{1}{c^2 p}(T_e + mc^2)$

$\Rightarrow$ $N(T_e) = \frac{C}{c^5} \sqrt{T_e^2 + 2T_e mc^2} (Q - T_e)^2 (T_e + mc^2)$

The Fermi factor $F_{\beta^\pm}(Z', T_e)$ represents the Coulomb interactions with the nucleus:

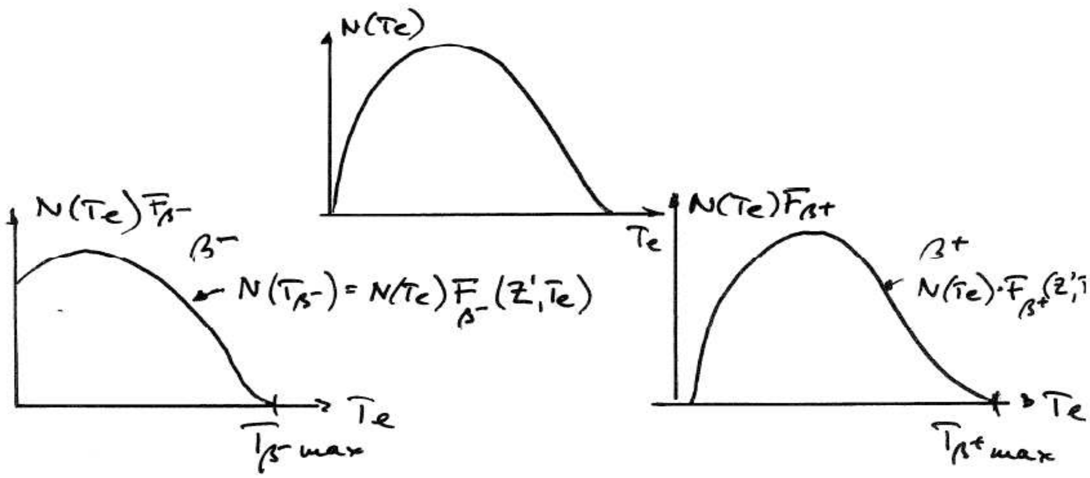

Electron distribution: $N(p) \propto p^2 (Q - T_e)^2 F(Z', p) \left| M_{fi} \right|^2 S(p, q)$

Where the form factor $S(p,q) = \begin{cases} 1, & \text{for allowed transitions} \\ \neq 1, & \text{for forbidden transitions} \end{cases}$

Fermi-Curie-plot

$$y = \sqrt{\frac{N(p)}{p^2 F(Z', p)}} \propto (Q - T_e), \quad M_{fi} = constant$$

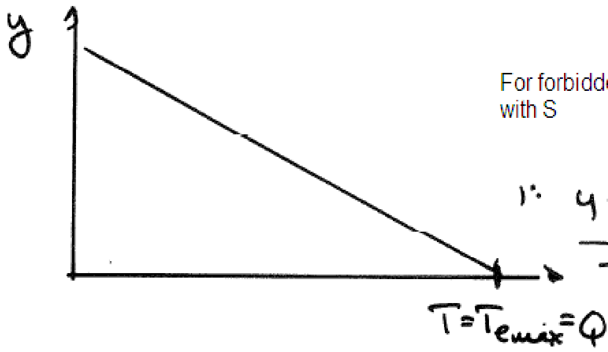

For forbidden transitions, the plot is linearized with S

1: $y = \sqrt{\frac{N}{p^2 \cdot F \cdot S}}$

T

Total transition probability rate: $\lambda = \int_{p=0}^{p,max} d\lambda(p)$

The Fermi integral: $f = \frac{1}{(mc)^3} \frac{1}{(mc^2)^2} \int_0^{p,max} F(Z', p) p^2 (E_0 - E_e)^2 dp$

Conservation of energy: $E_0 - E_e = Q + mc^2 - (T_e + mc^2) = Q - T_e$

Comparable half-life: $ft_{\frac{1}{2}} = f \frac{\ln 2}{\lambda}$

$$ft_{\frac{1}{2}} = 0.693 \cdot \frac{2\pi^3 \hbar^7}{g^2 m_e^5 c^4 |M_{fi}|^2} \simeq 10^3 - 10^{20} s$$

For "super-allowed transitions:

$$log ft_{\frac{1}{2}} \in (3 - 4)$$

For $0^+ - 0^+$, $M_{fi} = \sqrt{2} \Rightarrow ft_{\frac{1}{2}}$-values for these transitions should be of equal magnitude. This corresponds with experiments performed. $log ft_{\frac{1}{2}}$ increases for increasing order of forbiddenness.

Selection rules

Conservation of angular momentum:	$\vec{I}_i = \vec{I}_f + \vec{L}_\beta + \vec{S}_\beta$
Parity:	$\pi_P = \pi_D(-1)^{L_\beta}$
Allowed transitions:	$\vec{L}_\beta = \vec{0}$
First forbidden:	$\vec{L}_\beta = \vec{1}$
Second forbidden:	$\vec{L}_\beta = \vec{2}$
Fermi transitions	$\vec{S} = \vec{0}$
Gamow-Teller transitions	$\vec{S} = \vec{1}$

Where $\vec{L}_\beta$ and $\vec{S}_\beta$ refer to the (β, ν) particle system.

1.) Allowed transitions:($\vec{L}_\beta = 0$, $\pi_P = \pi_D$)

Fermi type: $(\vec{S} = \vec{0})$	Gamow-Teller type: $(\vec{S} = \vec{1})$
$\vec{I}_i = \vec{I}_f$	$\vec{I}_i = \vec{I}_f + \vec{1}$
$\Delta I = 0$	$\Delta I = 0, 1$; not $0^+ \to 0^+$
$0^+ \to 0^+$ Super-allowed.	$0^+ \to 1^+$ Pure Gamow-Teller.

2.) First forbidden transitions:($\vec{L}_\beta = \vec{1}, \pi_P = -\pi_D$)

Fermi type:$(\vec{S} = \vec{0})$	Gamow-Teller type:$(\vec{S} = \vec{1})$
$\vec{I}_i = \vec{I}_f + \vec{1}$	$\vec{I}_i = \vec{I}_f + \underbrace{\vec{1} + \vec{1}}_{\vec{0},\vec{1},\vec{2}}$
$\Delta I = 0, 1$	
	Three types:
	$\Delta I = 0$
	$\Delta I = 0, 1$
	$\Delta I = 0, 1, 2$

Violation of parity conservation during β-disintegration

When a physical law is invariant during a symmetry operation, there is a corresponding conserved quantity. Gravitation and electromagnetism are invariant during a spatial reflection (Parity operator P), charge (C) and time (T) $\Rightarrow$ Parity should be a conserved quantity.
$\Rightarrow < O_{PS} >= \int \Psi^* \hat{O}_{PS} \Psi d^3 r = 0$.
Where O_{PS} is an operator that is representing a pseudo-scalar quantity, for example $\vec{p} \cdot \vec{S}$, which is a product of a polar vector ($\vec{p}$) and an axial vector $\vec{S}$. $P(\vec{p}) = -\vec{p}$, $P(\vec{S}) = \vec{S}$. $< O_{PS} >= 0$ because the integrand is an odd function if parity is a conserved quantity.

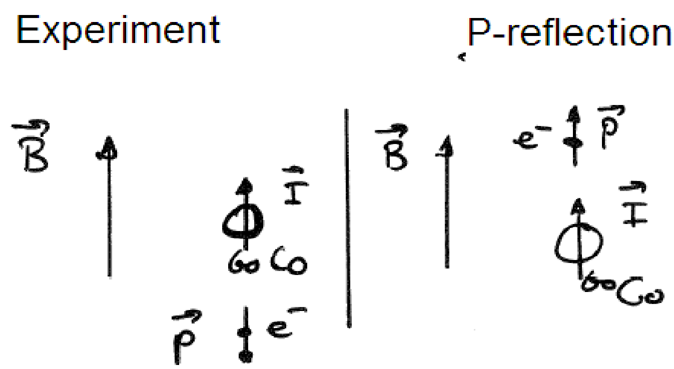

The P-reflection experiment emits in the "forward" direction, while the original experiment emits backwards relative to $\vec{I}$. Wu et al. showed in 1957 that $< \vec{p} \cdot \vec{I} > < 0$ in this experiment, i.e. parity is not necessarily conserved in $\beta-$disintegration.

α-disintegration

α-disintegration takes place in nuclei with low $\frac{N}{P}$-ratio.

$$^{A}_{Z}X \rightarrow ^{A-4}_{Z-2} X' + \alpha$$

Energy released:

$$Q_\alpha = (m_P - m_D - m_{He})c^2 \text{ (atomic masses)}$$

$$Q_\alpha = (\Delta_P - \Delta_D - \Delta_{He})c^2$$

$$Q_\alpha = T_{X'} + T_\alpha \text{(Assuming X is initially at rest)}$$

Conservation of momentum: $\vec{P}_{X'} + \vec{P}_\alpha = 0$

$\Rightarrow$ $T_\alpha = \frac{Q_\alpha}{1+\frac{M_\alpha}{M_{X'}}}$

These α-energies are well defined, i.e monoenergetic, because this is a two-body problem.

Ex:

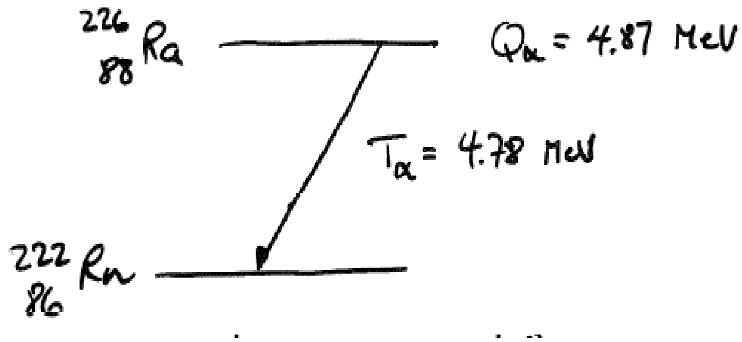

Disintegration constant: $\lambda = f \cdot P \cdot A_\alpha^2$

Where f is the number of collisions with the potential barrier per second, P is the tunneling probability and A is the spectroscopical factor expressed below.

Spectroscopical factor: $A_\alpha^2 = \left| < \Psi_f^*(A-4)\Psi_\alpha^*(4)|\Psi_i(A) > \right|^2$

The physical interpretation of this spectroscopical factor is that it is the probability for creating an α-particle inside the nucleus.

Gamow factor: $G = \int_a^b \sqrt{\frac{2m_\alpha}{\hbar^2}[V(r) - Q]}dr$

WKB-approximation solution: $G = \sqrt{\frac{2m_\alpha}{\hbar^2 Q}\frac{zZ'e^2}{4\pi\varepsilon_0}} \underbrace{\left[\arccos\sqrt{\frac{Q}{B}} - \sqrt{\frac{Q}{B}(1-\frac{Q}{B})}\right]}_{\simeq \frac{\pi}{2} - 2\sqrt{\frac{Q}{B}} \; for \; Q \ll B}$

Tunneling probability: $P = e^{-2G}$

Collision frequency: $f \simeq \frac{v}{a}$

Velocity : $v \simeq \sqrt{\frac{2(Q+V_0)}{m_\alpha c^2}} \cdot c$

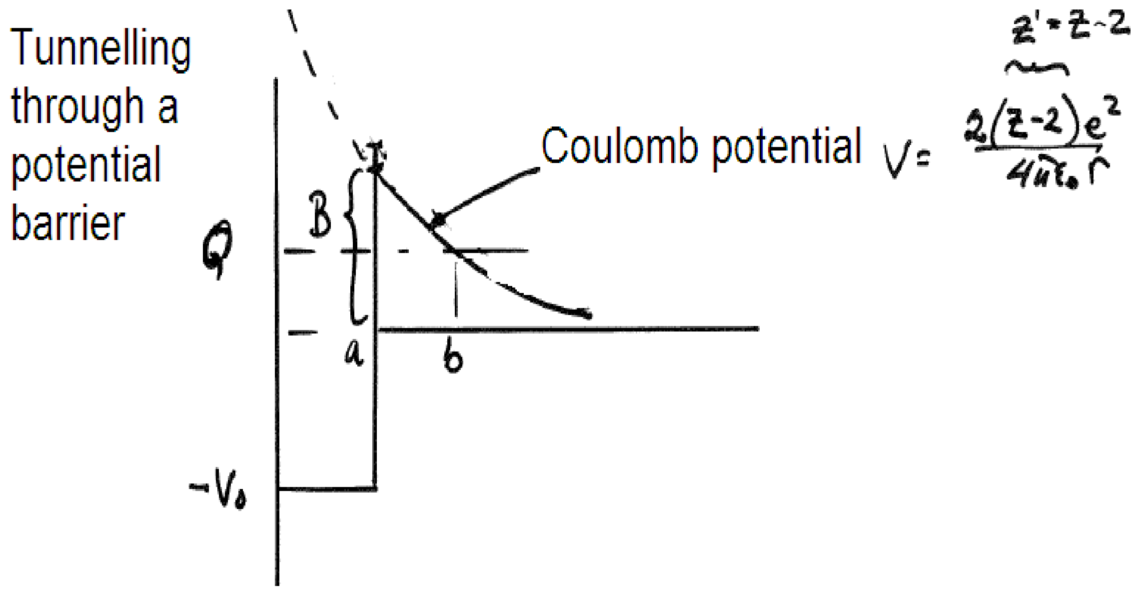

Where v is the α-particle's velocity inside its nucleus-orbital, and a is the nuclear radius R. A_α^2 is assumed to be 1.

Geiger-Nuttals rule: $$t_{\frac{1}{2}} = 0.693\frac{a}{c}\sqrt{\frac{mc^2}{2(V_0+Q)}}exp\Big[2\sqrt{\frac{2mc^2}{(\hbar c)^2 Q}}\cdot\frac{zZ'e^2}{4\pi\varepsilon_0}(\frac{\pi}{2}-2\sqrt{\frac{Q}{B}})\Big]$$

This can again be simplified by introducing a few assumptions. $V_0 + Q \simeq V_0, \quad 2\sqrt{\frac{Q}{B}} \ll \frac{\pi}{2} \Rightarrow \lg t_{\frac{1}{2}} = C_1 + \frac{C_2}{\sqrt{Q}}$. See Lilley Fig.3.9.

Effects due to angular momenta

The centrifugal potential makes the potential barrier increase.

Selection rule: $\vec{I_i} = \vec{I_f} + \vec{l_\alpha}$

$|I_i - I_f| \leq l_\alpha \leq |I_f + I_i|$

Parity rule: $\pi_P = \pi_D(-1)^{l_\alpha}$

A typical example is a transition to rotational energy-states in deformed nuclei. $l_\alpha \in$even numbers because of symmetry and parity.

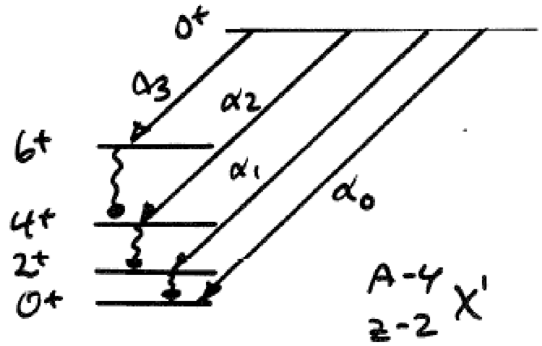

Deviation from Geiger-Nuttals rule:

1.) For deformed nuclei there is a higher probability for emitting through the poles,

because bigger $a(\equiv R) \Rightarrow$ lower potential barrier

2.) A_α^2 can be significantly ≤ 1, for example if the creation of an α-particle requires a break-up of nucleon bonds in filled shells.

7.)
Dosimetry (Lilley chap.7)

Including biological effects of radiation and radiation protection

Basic principles

Definition of dose: $D = \lim_{V \to 0} \frac{\bar{\varepsilon}}{\rho V}$ $\quad [Gy = \frac{J}{kg}]$

Charged particles(Directly ionizing radiation)

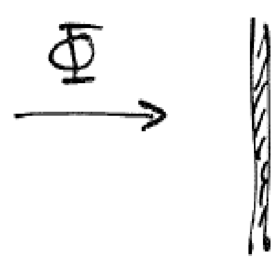

Dose: $D = \Phi(\frac{S_{col}}{\rho})$

Where S_{col} is the collision stopping power and Φ is the particle fluence.

For photons (Indirectly ionizing radiation)

Total linear attenuation coeff: $\mu = \tau + \sigma + \kappa$

Where τ represents the photo electric effect, σ the Compton effect and κ is pair production. These quantities are as already discussed, additive.

Mass energy transfer coeff.: $\frac{\mu_{tr}}{\rho} = \frac{\tau}{\rho}\left[1 - \frac{\delta}{h\nu}\right] + \frac{\sigma}{\rho}\left[1 - \frac{h\nu'}{h\nu}\right] + \frac{\kappa}{\rho}\left[1 - \frac{2mc^2}{h\nu}\right]$

Where the terms from left to right are corrections for X-ray radiation, compton scattering and radiation due to annihilation.

KERMA (Kinetic Energy Released per Mass)

Definition of KERMA: $K \equiv \Psi(\frac{\mu_{tr}}{\rho})$ $[\frac{J}{kg} = Gy]$

Mass energy absorption coeff.: $\frac{\mu_{en}}{\rho} = \left(\frac{\mu_{tr}}{\rho}\right)(1 - g)$

Where g is the correction factor for bremsstrahlung.

Collision KERMA: $D \stackrel{CPE}{=} K_c \equiv \Psi\left(\frac{\mu_{en}}{\rho}\right)$

CPE stands for Charged Particle Equilibrium (electron equilibrium).

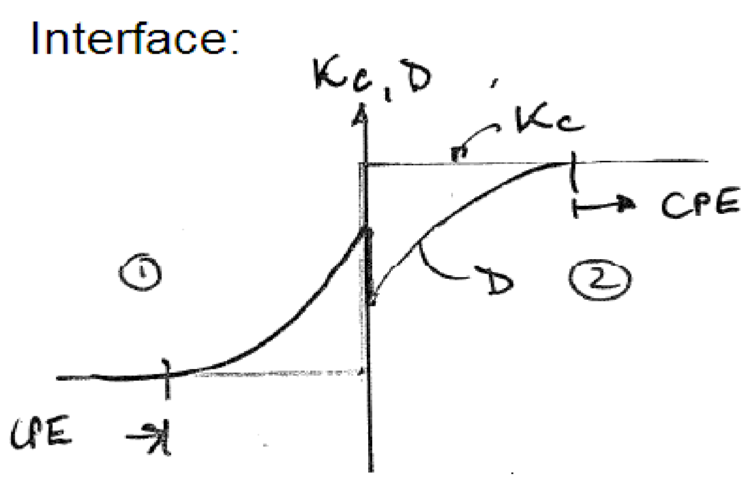

Illustrated cases: $\left(\frac{\mu_{en}}{\rho}\right)_1 < \left(\frac{\mu_{en}}{\rho}\right)_2$

$\left(\frac{S_c}{\rho}\right)_1 > \left(\frac{S_c}{\rho}\right)_2$

Continuous fluence of secondary electrons at the boundary: $\frac{D_2}{D_1} = \frac{(\frac{S_c}{\rho})_2}{(\frac{S_c}{\rho})_1}$

Bragg-Gray cavity theory

For a gas-filled dosimeter, which is constructed to measure the dose deposited in a medium:

Bragg-Gray cavity:

The cavity is so small compared to the range of the secondary electrons, that the ionisation that takes place in the dosimeter's gas is due to secondary electrons from the walls and the medium. If one assumes that the fluence of secondary electrons is approximately continuous over the boundary between the gas and the wall:

At the boundary: $\frac{D_{wall}}{D_{gas}} = \frac{(\frac{S_c}{\rho})_{wall}}{(\frac{S_c}{\rho})_{gas}}$

In this case, S_c represents the mean collision stopping power for the actual energy spectrum of the secondary electrons. Furtheron, if one assumes that the walls are so thick that CPE is reached inside the wall:

Inside the wall: $\frac{D_{medium}}{D_{wall}} = \frac{(\frac{\mu_{en}}{\rho})_{medium}}{(\frac{\mu_{en}}{\rho})_{wall}}$

$\Rightarrow$ $D_{medium} = \frac{(\frac{\mu_{en}}{\rho})_{medium}}{(\frac{\mu_{en}}{\rho})_{wall}} \cdot \frac{(\frac{S_c}{\rho})_{wall}}{(\frac{S_c}{\rho})_{gas}} \cdot \underbrace{D_{gas}}_{measured}$

Special case:

1.) Homogeneous dosimeter: $\left(\frac{S_c}{\rho}\right)_{wall} = \left(\frac{S_c}{\rho}\right)_{gas}$ (gas cavity does not need to be small)

2.) Tissue equivalent wall: $\left(\frac{\mu_{en}}{\rho}\right)_{medium} = \left(\frac{\mu_{en}}{\rho}\right)_{wall}$ (chamber walls do not need to be thick)

Micro dosimetry

Stochastic energy deposited in a small volume of gas, equivalent to the energy deposited in a microscopic tissue volume.

Specific energy: $z = \frac{\epsilon}{\rho \Delta V}$

This is a stochastic quantity for a fixed micro-volume.

Equivalent volumes:

Equivalent energy deposition along a particle-track through the two volumes:

$$\delta\epsilon = \left(-\frac{dE}{dx}\right)_{gas} \cdot l_{gas} = \left(-\frac{dE}{dx}_{medium}\right) \cdot l_{medium}$$

$$\Rightarrow l_{gas} = \frac{(\frac{S_c}{\rho})_{medium}}{(\frac{S_c}{\rho})_{gas}} \cdot \frac{\rho_{medium}}{\rho_{gas}} \cdot l_{medium}$$

If we choose l_{gas} of the order of 10mm, the detector will be equivalent to a cell diameter l_{medium} around 10 μm, since $\frac{(\frac{S_c}{\rho})_{medium}}{(\frac{S_c}{\rho})_{gas}}$ is about 1, and $\frac{\rho_{medium}}{\rho_{gas}}$ around 10^3.

Comparing the graphs of specific energy z versus dose D for gamma and neutron irradiation, we see that energy deposition by neutrons typically occurs in "packages" 100 times larger than by gamma.

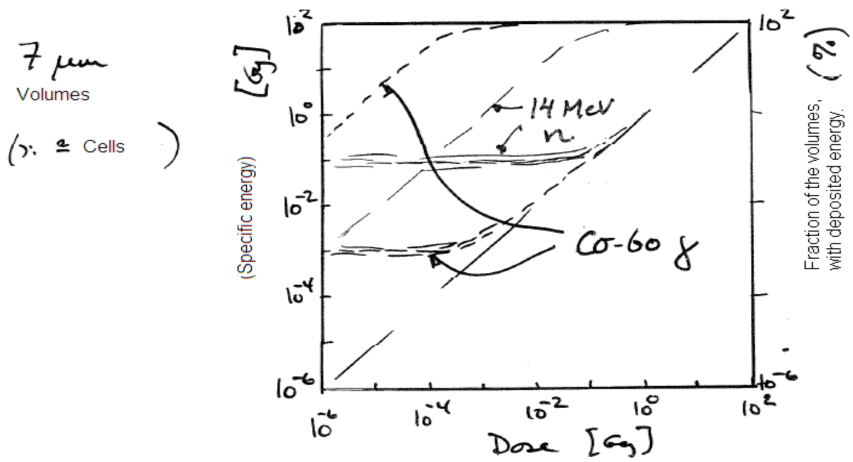

External dosimetry (γ-radiation)

From a point source of activity A:

Dose deposited in air, at distance r from the point source:

Dose rate: $\dot{D}_{air} \overset{CPE}{=} \dot{K}_{c,air} = \frac{A}{r^2}\Gamma_{air}$

Specific gamma radiation constant: $\Gamma = \frac{1}{4\pi}\sum_{\gamma i} k_i E_{\gamma i}\left(\frac{\mu_{en}}{\rho}\right)_{air,E_{\gamma i}}$ $\left[\frac{Gym^2}{sBq}\right]$

Sometimes, Γ is given relative to the exposition rate $[\frac{Coulomb}{kg \cdot s}]$

Specific gamma exposition constant: $\Gamma_{Exp} = \frac{\Gamma_{Dose}}{\frac{W}{e}}$

Where $\frac{W}{e}$ is the average amount of energy required to generate an ion pair in air ($34\ \frac{eV}{ip}$).

Internal dosimetry

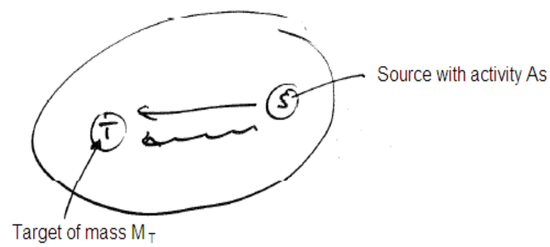

Dose rate in target organ: $\dot{D}_T = \sum_S A_S \cdot SEE(S \leftarrow T)$

Specific effective energy: $SEE(T \leftarrow S) = \frac{1}{M_T} \sum_i k_i E_i \phi_i (T \leftarrow S)$

Where M_T is the mass of the target organ, and the sum goes over the different types of radiation i, k_i is the yield of radiation of type i per disintegration, E_i is the mean quantum of energy of radiation type i, and ϕ_i is the fraction of this type of energy which is absorbed.

Absorbed fraction: $$\phi_i(T \leftarrow S) = \begin{cases} 1 & \text{if } S \equiv T, \text{ for } \alpha, \beta \\ 0 & \text{if } S \neq T, \text{ for } \alpha, \beta \\ \textit{Must be measured} & \text{for } \gamma \end{cases}$$

Dose: $$D = \sum_S \tilde{A} \cdot SEE(T \leftarrow S), \quad \tilde{A} = \int_0^t A(t)dt$$

A biokinetic model for $A(t)$ is required to calculate $\tilde{A}$.

$$\lambda_{tot} = \underbrace{\lambda_R}_{Radiological} + \underbrace{\lambda_B}_{Biological}$$

Biological effects of radiation

Indirect effects of ionising radiation

Radiation of water$\rightarrow$ Water radicals $\rightarrow$ Possible biological damage

$$H_2O\text{+ionising radiation} \rightarrow \begin{cases} H_2O^* \\ H_2O + e^- \rightarrow H_2O^- \\ H_2O^+ \end{cases}$$

$$H_2O^+ \rightarrow H^+ + OH'$$
$$H_2O^- \rightarrow H' + OH^-$$

Where OH' and H' are radicals. Effect of radicals on biomolecules:

$$RH + OH' \rightarrow R' + H_2O$$
$$RH + H' \rightarrow R' + H_2$$

Where R' represents a potentially lethal damage. Fixation of a possible damage in presence of oxygen:

$$R' + O_2 \rightarrow RO_2'$$

$$RO_2' + RH \rightarrow RO_2H + R'$$

Where RO_2H is a biomolecule with a fixed damage.

Radiative effects are combinations of direct and indirect effects, i.e. direct hits in biomolecules and generation of radicals through radiolysis of water).

Irradiation of biological cells decreases the colony forming ability of cells

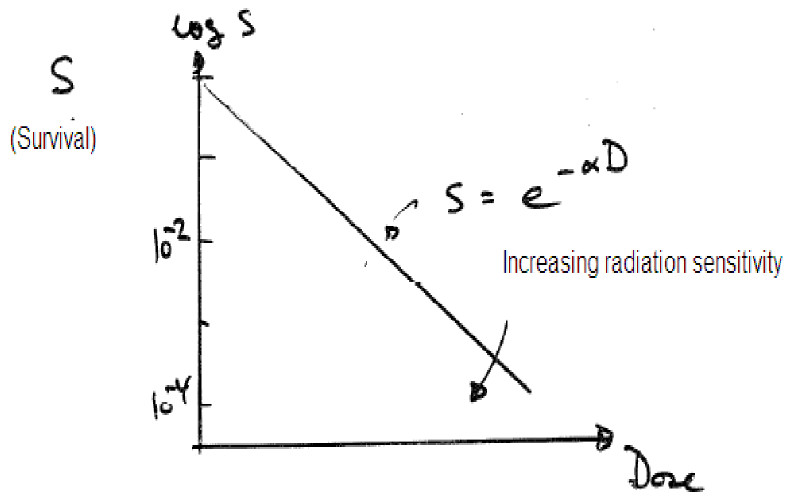

Single hit, single target theory:

Probability of survival: $P(survival) = P(no\ hits) = P(n=0) = \left(\frac{\mu^n e^{-\mu}}{n!}\right)_{n=0} = e^{-\mu} = e^{-\frac{D}{D_0}}$

Where n is the Poisson distributed variable for the number of hits, D_0 is the average dose corresponding to one lethal hit, and μ is the average number of hits at dose D, i.e. $\mu = D/D_0$.

Relative biological effect (RBE) for different types of radiation

RBE is per definition a comparison with Co-60 radiation.

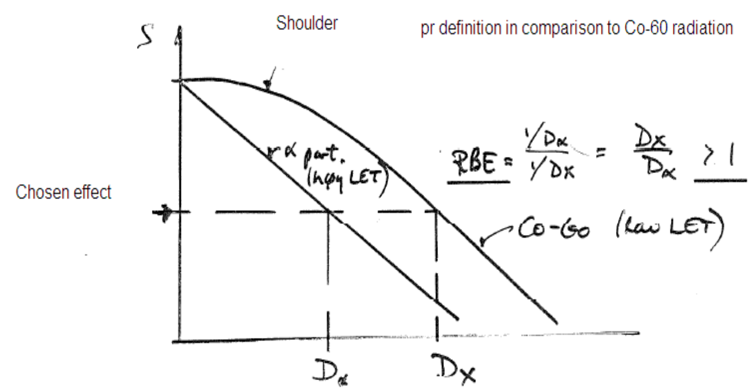

Chadwick and Leenhouts (1973)

$$S = e^{-(\alpha D + \beta D^2)}$$

For small doses: $P(damage) = 1 - S \simeq \underbrace{\alpha D}_{HighLET} + \underbrace{\beta D^2}_{LowLET}$

1.) The critical molecule is DNA.

2.) Double strand damage is the critical event.

3.) Single strand damage can be repaired.

4.) A high density of single strand damage($\propto \beta D^2$) can result in double strand damage.

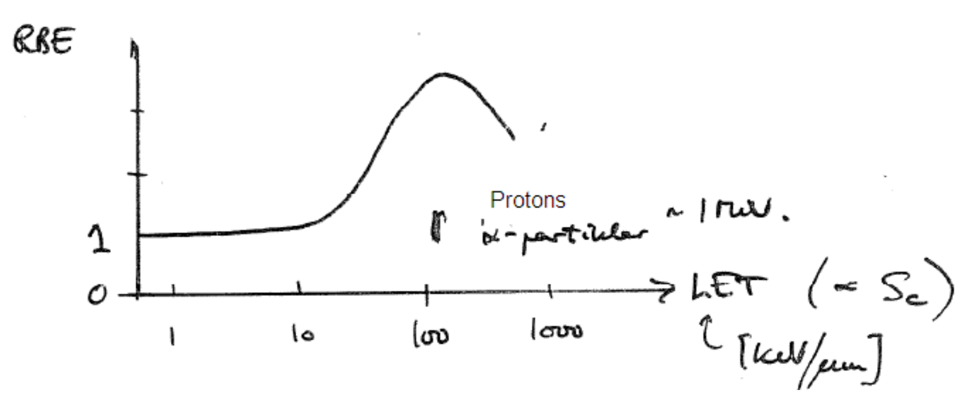

Modifying effects

Dose rate

Fractionation

Cell cycle

Oxygen

Radiation protection

This formalism is meant to be used to estimate low doses of ionizing radiation (up to 100 mGy) that may induce stochastic effects such as cancer development and/or genetic mutations.

Formalism

Equivalent dose (for organ T): $H_T = \sum_R \omega_R \cdot D_{T,R}, \quad [Sv]$

Radiation weighting factor : $\omega_R \; [\frac{Sv}{Gy}]$

Tissue weighting factors: $\sum_T \omega_T = 1$

$$\omega_R = \begin{cases} 1 & \text{for } \gamma,\ \beta \\ 2 & \text{for protons} \\ 20 & \text{for } \alpha\text{-particles, heavy ions, and fission fragments} \\ 2.5 & \text{for neutrons below 10 keV, increasing to} \\ 20 & \text{for neutrons around 1 MeV, decreasing to} \\ 2.5 & \text{for neutrons above 1000 MeV} \end{cases}$$

$$\omega_T = \begin{cases} 0.12 & \text{for bone marrow, colon, lung, stomach, breast, remainder tissue} \\ 0.08 & \text{for gonads} \\ 0.04 & \text{for bladder, oesophagus, liver, thyroid} \\ 0.01 & \text{for bone surface, brain, salivary glands, skin} \end{cases}$$

Effective dose for the entire body: $E = \sum_T \omega_T H_T = \sum_T \omega_T \sum_R \omega_R D_{T,R} \quad [Sv]$

The sums are over radiation doses to target tissue T from different types R of ionizing radiation that hit the target tissue (i.e. alpha, beta, gamma, or neutron irradiation). The radiation weighting factor ω_R indicates the biological effectiveness of each type of radiation, and the tissue weighting factors ω_T represent the health risk associated with irradiation of tissue or organ T. Notice that values for the radiation weighting factors and tissue weighting factors recently were revised (ICRP Publication 103, 2007), and therefore are different from previously published ones (ICRP 60, and Lilley 2001).

For internal radiation after inhalation or ingestion of radioactivity:

Committed effective dose: $E(50) = \underbrace{\int_0^{50} \dot{E(t)} dt}_{Bio-kinetic\ model}$

For radiation protection: $SEE(T \leftarrow S) = \sum_R \omega_R \cdot SEE_R(T \leftarrow S)$

i.e. SEE in $\left[\frac{Sv}{dis.}\right]$

Effective dose coefficients for inhalation and ingestion (ICRP 68, 1994): $e_{inh} = \frac{E(50)}{A_{inh}}$

$e_{ing} = \frac{E(50)}{A_{ing}}$

Annual limit on intake (inh. or ing.): $ALI = \frac{E_{lim}}{e_{50}} = \frac{E_{lim}}{\frac{E(50)}{A_{intake}}}$

Where E_{lim} represents a specific limit (20 mSv for workers).

The total sum:

$$\sum_{sources} \frac{A_{intake,inh}}{ALI_{inh}} + \sum_{sources} \frac{A_{intake,ing}}{ALI_{ing}} + \sum_{sources} \frac{E_{external}}{E_{lim}} \leq 1.0$$

Risk coefficients (ICRP 103, 2007):

Fatal cancer development	5.5% pr.Sv.
Heritable (genetic) damage	0.2% pr.Sv.
	5.7 % pr.Sv.

$$\text{Dose limits (for effective dose)}= \begin{cases} 20 \frac{mSv}{year} & \text{for worker in a radiation related profession} \\ 1 \frac{mSV}{year} & \text{for the public} \end{cases}$$

Radiation protection guide lines

1.) Every dose counts

2.) "Practice" is a will-fully chosen use of radiation.

Radiation protection principles that apply (only) for "practices":

- The reasons for use of radiation should be well-founded and properly stated.

- The dose should be ALARA (As Low As Reasonably Achievable)

- The usage of radiation ("practice") should not exceed any accepted dose limits. (20mSv/year for employees, 1mSv/year for the public)

3.) Intervention to reduce or eliminate radiation dose should have a net beneficial effect.

NB! Dose limits apply only to "practices", i.e dose contributions from natural background radiation do not count (around 3mSv/year in Norway).

6.)
Nuclear reactions (Lilley Chap.4)

$$a + X \to Y + b$$
$$X(a, b)Y$$

Scattering process:	The particles do not change their identity.
Elastic scattering:	The kinetic energy is conserved $\Rightarrow$ no excitations.
Radiative capture:	$b \equiv \gamma$
Nuclear photo effect	$a \equiv \gamma$
Direct reactions:	Only a few nucleons participate in the process, while the rest of the nucleons remain passive.
"Compound nucleus" reactions:	An excited intermediate state is formed, and the memory of formation of this intermediate state is lost before de-excitation.
Conservation laws:	Total energy
	Total momentum
	Total angular momentum
	Proton numbers and neutron numbers (Not conserved in weak interactions)
	Parity

Process:

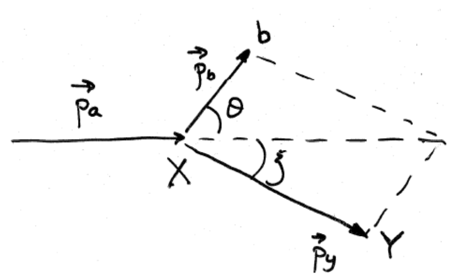

Conservation of energy:(relativistic) $\quad m_X c^2 + T_X + m_a c^2 + T_a = m_Y c^2 + T_Y + m_b c^2 + T_b$

$$(m_a + m_X - m_Y - m_b)c^2 \equiv Q = T_Y + T_b - T_X - T_a$$

$$Q \equiv (m_{initial} - m_{final})c^2 = T_{final} - T_{initial}$$

If $Q < 0$, the reaction is called an endoterm reaction (requires an input of energy)
If $Q > 0$, the reaction is called an exoterm reaction (releases energy)

Conservation of momentum in the lab system: $\quad p_a = p_b \cos\theta + p_Y \cos\xi$

$$0 = p_b \sin\theta - p_Y \sin\xi$$

Assuming $T_X = 0$. Furthermore, one defines the minimum energy required for the reaction to take place (Threshold energy), as the energy corresponding to a reaction where the final products are at rest in the CM system.

Threshold energy: $\quad T_{th} = T_{a,min} = -Q\frac{m_Y + m_b}{(m_Y + m_b) - m_a}$

Inelastic Coulomb scattering (Coulomb excitation)

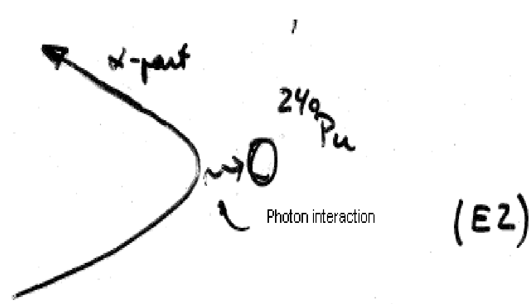

Inelastic Coulomb scattering:$Q_{ex} = (m_x + m_a - m_Y^* - m_b)c^2$ where $m_Y^* c^2 = m_Y c^2 + E_{ex}$ and $Q_{ex} = Q_0 - E_{ex}$.

Typical reaction:
Excitation of even-even nuclei from their ground state (0^+) to an excited state (2^+) via absorption/emission of virtual photons (E2).

$$Q_{ex} = Q_0 - E_{ex}$$

Nuclear force scattering(as opposed to Coulomb scattering)

$\Rightarrow$ Diffraction pattern in $\frac{d\sigma}{d\Omega}$ measured as a function of θ_{CM}

For neutron scattering:	An evident diffraction pattern arise at all scattering angles (All energies)
For charged particles (protons):	Diffraction pattern at high energies where the Coulomb potential is negligible, and for large scattering angles also at low energies.

Reaction cross section

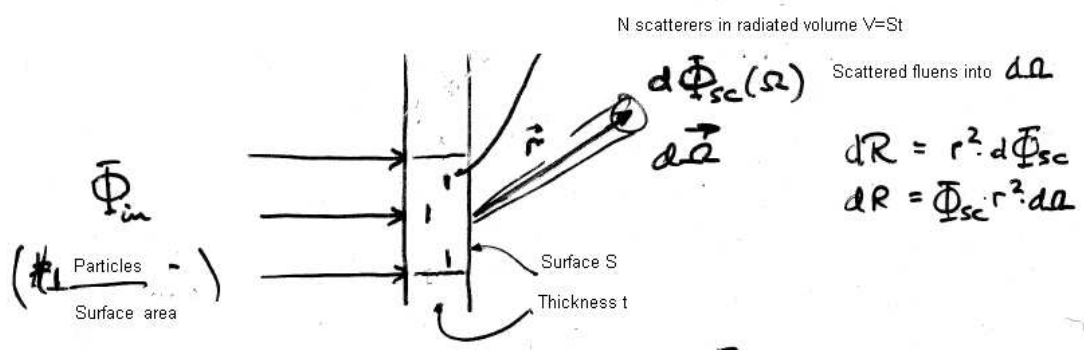

Cross section contribution per "scatterer":	$\sigma = \frac{1}{N}\frac{R_{sc}}{\Phi_{in}}$
Differential cross section:	$\frac{d\sigma}{d\Omega} = \frac{\frac{dR_{sc}}{d\Omega}}{N\Phi_{in}}, [\frac{barn}{st.rad}]$
Total cross section:	$\sigma = \int_\Omega \frac{d\sigma}{d\Omega}d\Omega = 2\pi\int_0^\pi \frac{d\sigma}{d\Omega}\sin\theta d\theta$
Several reactions:	$\sigma_{tot} = \sum_{b_i}\sigma_{b_i}$
Energy dependence:	
Double diff. cross section:	$\frac{d^2\sigma}{d\Omega dE_b}$
	$\frac{d\sigma}{dE_b}$

Where E_b represents the final energy of particle b.

Scattering and reaction cross sections

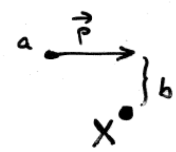

Semi-classical angular momentum: $l\hbar = pb$

$$b = \frac{l\hbar}{p} = \frac{l\hbar}{k\hbar} = l\frac{\lambda}{2\pi} = l\bar{\lambda}$$

For effective nuclear force scattering: $l_{max} = \frac{R}{\bar{\lambda}} = \frac{R_1+R_2}{\bar{\lambda}}$

Where $\bar{\lambda}$ represents the reduced de Broglie wavelength for particle a ($\lambda = h/p$).

Total semiclassical cross section:

$$\sigma = \sum_{l=0}^{\frac{R}{\bar{\lambda}}} (2l+1)\pi\bar{\lambda}^2 = \pi\left(R + \bar{\lambda}\right)^2$$

The particle's wave properties have a range $\bar{\lambda}$.

Quantum mechanically:

The wave function describing the incoming wave:

$$\Psi_{inc} = \frac{A}{2kr}\sum_{l=0}^{\infty} i^{l+1}\left(2l+1\right)\left[e^{-i\left(kr-\frac{l\pi}{2}\right)} - e^{i\left(kr-\frac{l\pi}{2}\right)}\right]P_l(\cos\theta)$$

Where the two exponential factors describe respectively an ingoing and an outgoing spherical wave.
A superposition of the two waves results in an incoming plane wave.

A scattered outgoing wave can have its phase and amplitude changed by the scattering process.

$$\Psi_{tot} = \Psi_{inc} + \Psi_{sc}$$

$$\Psi_{tot} = \frac{A}{2kr}\sum i^{l+1}\left(2l+1\right)\left[e^{-i\left[kr-\frac{l\pi}{2}\right]} - \eta e^{i\left[kr-\frac{l\pi}{2}\right]}\right]P_l(\cos\theta)$$

$$\Psi_{sc} = \frac{A}{2kr}\sum i^{i^{l+1}}\left(2l+1\right)\left(1-\eta_l\right)e^{i\left(kr-\frac{l\pi}{2}\right)}P_l(\cos\theta)$$

$$\Psi_{sc} = \frac{A}{2k}\frac{e^{ikr}}{r}\sum_{l=0}^{\infty}(2l+1)i(1-\eta_l)P_l(\cos\theta)$$

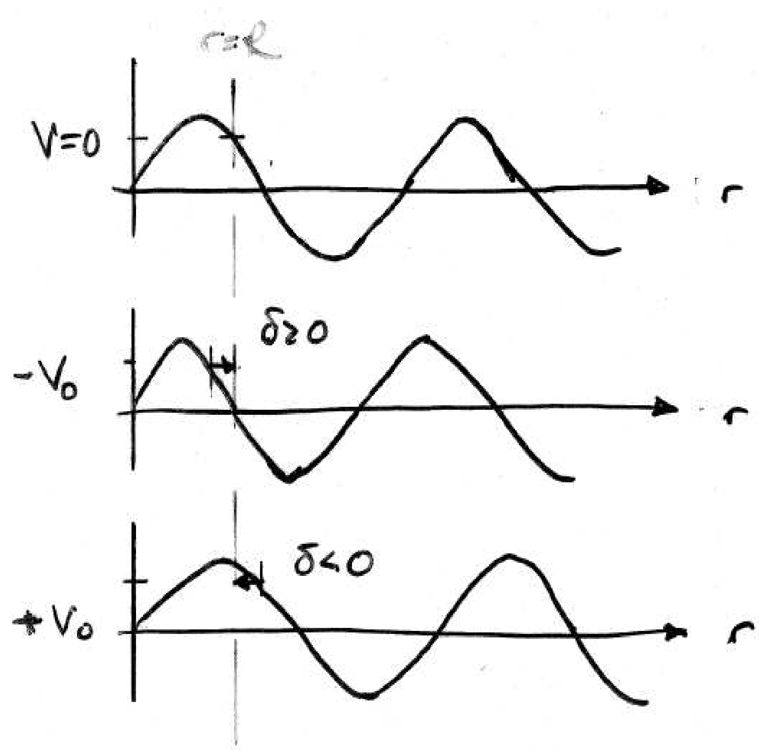

Scattered current density: $j_{sc} = \left(\Psi_{sc}^* \frac{\hbar}{im} \nabla \Psi_{sc}\right)$

$$= \frac{\hbar}{2im}\left(\Psi_{sc}^* \frac{\partial \Psi_{sc}}{\partial r} - \frac{\partial \Psi_{sc}^*}{\partial r}\Psi_{sc}\right)$$

$$j_{sc} = |A|^2 \frac{\hbar}{2mkr^2} \left|\sum_{l=0} (2l+1)\, i\,(1-\eta_l)\, P_l(\cos\theta)\right|^2$$

Incoming current density: $j_{inc} = \frac{\hbar k |A|^2}{m}$

Differential cross section: $\frac{j_{sc} r^2 d\Omega}{j_{inc}}$

$$\Rightarrow \frac{d\sigma_{sc}}{d\Omega} = \frac{1}{4k^2} \left|\sum_{l=0}^{\infty} (2l+1)\, i\,(1-\eta_l)\, P_l(\cos\theta)\right|^2$$

The total cross section is obtained by integrating over all possible angles.

Orthogonality requires: $\int P_l(\cos\theta) P_{l'}(\cos\theta) \sin\theta d\theta d\phi = \frac{4\pi}{2l+1}$ for $l = l'$

$$\int P_l(\cos\theta) P_{l'}(\cos\theta) \sin\theta d\theta d\phi = 0 \text{ for } l \neq l'$$

$$\Rightarrow \sigma_{sc} = \sum_{l=0}^{\infty} \pi ƛ^2 (2l+1) |1-\eta_l|^2, \quad ƛ = \frac{1}{k}$$

There is no scattering for $\eta_l = 1$. Only elastic scattering, i.e only a phase change and no reduction in amplitude is possible for $|\eta_l| = 1 \rightarrow \eta_l = e^{2i\delta_l}$

Total cross section: $\sigma_{sc} = \sum_{l=0}^{\infty} 4\pi ƛ^2 (2l+1) \sin^2\delta_l, \quad |1 - e^{2i\delta_l}| = 2\sin\delta_l$

Reaction cross section ($\equiv$ cross section concerning everything else than elastic interactions)

This is also denoted as the rate of loss of particles from energy channel k.

Rate of loss: $|j_{loss}| = |j_{in}| - |j_{out}|$

$$|j_{loss}| = \frac{|A|^2\hbar}{4mkr^2}\left[\left|\sum(2l+1)\,i^{l+1}e^{i\frac{l\pi}{2}}P_l\right|^2 - \left|\sum(2l+1)\,i^{l+1}e^{-i\frac{l\pi}{2}}\eta_l P_l\right|^2\right]$$

$$\Rightarrow \sigma_r = \sum_{l=0}^{\infty}\pi\lambdabar^2\,(2l+1)\left(1-|\eta_l|^2\right)$$

Total cross section: $\sigma_t = \sigma_{sc} + \sigma_r = \sum_{l=0}^{\infty} 2\pi\lambdabar^2\,(2l+1)\,(1-\Re\eta_l)$

Note that only inelastic scattering ($\sigma_r > 0, \sigma_{sc} = 0$) is impossible to achieve. To obtain inelastic scattering, $|\eta_l| < 1$. When this happens, $(1-\eta_l) \neq 0$, *i.e.* $\sigma_{sc} > 0$.

"Black disc" absorber:

$\eta_l = 0$ for $l \leq \frac{R}{\lambdabar}$ i.e no outgoing wave for $l \leq \frac{R}{\lambdabar}$

$\eta_l = 1$ for $l > \frac{R}{\lambdabar}$ i.e no scattering effect

Reaction cross section: $\sigma_r = \sum_{l=0}^{\frac{R}{\lambdabar}}\pi\lambdabar^2\,(2l+1) = \pi(R+\lambdabar)^2$

Scattering: $\sigma_{sc} = \sum_{l=0}^{\frac{R}{\lambdabar}}\pi\lambdabar^2\,(2l+1) = \pi(R+\lambdabar)^2$

Total: $\sigma_t = \sigma_r + \sigma_{sc} = 2\pi(R+\lambdabar)^2 = 2\cdot\sigma_{geometrical}$

$\sigma_{geometrical}$ is the semiclassical cross section.

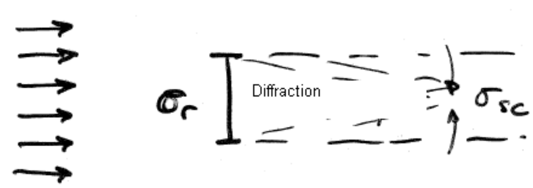

Calculation method

1.) Choose a form of the nuclear potential $V(r)$.

2.) Solve the Schr. equation for the two regions, inside ($r \leq R$) and outside ($r \geq R$) the region of interaction.

3.) Ψ and $\frac{\partial\Psi}{\partial r}$ must be continuous over the boundary $r = R \Rightarrow \eta_l$

4.) Calculate σ_r and σ_{sc} and compare with experimental results. This result tells us whether $V(r)$ was reasonably chosen.

This is hard for everything else than elastic scattering, because all inelastic channels are coupled together. Both *in* and *out* scattering relative to channel k, i.e from all k' into k and from k to all k''.

Optical model of nuclear scattering:

Choose a particular potential as a model for elastic scattering + absorption.

Potential: $U(r) = \underbrace{V(r)}_{Elastic\ scattering} + \underbrace{iW(r)}_{Absorption}$

$k = \frac{1}{\hbar}\sqrt{2m(E-U)}$

Choose for example: $U(r) = -V_0 - iW_0$ for $r < R$

$= 0$ for $r > R$

Outgoing wave: $\Psi = \frac{e^{ikr}}{r} = e^{ik_r \cdot r} \cdot \frac{e^{-k_i \cdot r}}{r}$ for $r < R$

$$k = k_r + ik_i = \frac{1}{\hbar}\sqrt{2m(E+V_0)} + i\frac{W_0}{2\hbar}\sqrt{\frac{2m}{E+V_0}}, \quad W_0 \ll V_0$$

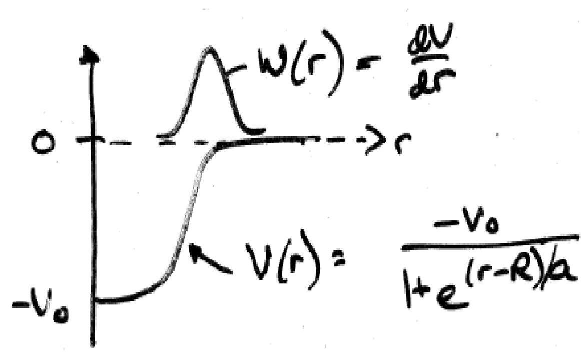

The only place where $W(r) \neq 0$ is close to the surface. This is because the internal nucleons cannot take part in absorption processes at moderate energies, because all the possible states are taken. This means that only the valence nucleons close to the surface can interact with incoming particles.

A realistic potential must also include spin-orbit coupling for valence nucleons, and Coulomb contribution if the incoming particle is charged. The optical model gives suprisingly good predictions (by calculating η_l) to experimental data, even though it only represents average nucleon properties. This model can only show that particles disappear from the elastic channel.

Direct reactions

An incoming particle interacts with single nucleons close to the surface of the nucleus. Typical incoming energies≥Coulomb barrier. Direct reactions show strong angular dependencies.

Selectivity:

Inelastic scattering reactions do not excite collective states. Transfer reactions result in excited states for single nucleons.

Ex.: Transfer of angular momentum by deuteron stripping reactions (d,n), (d,p)

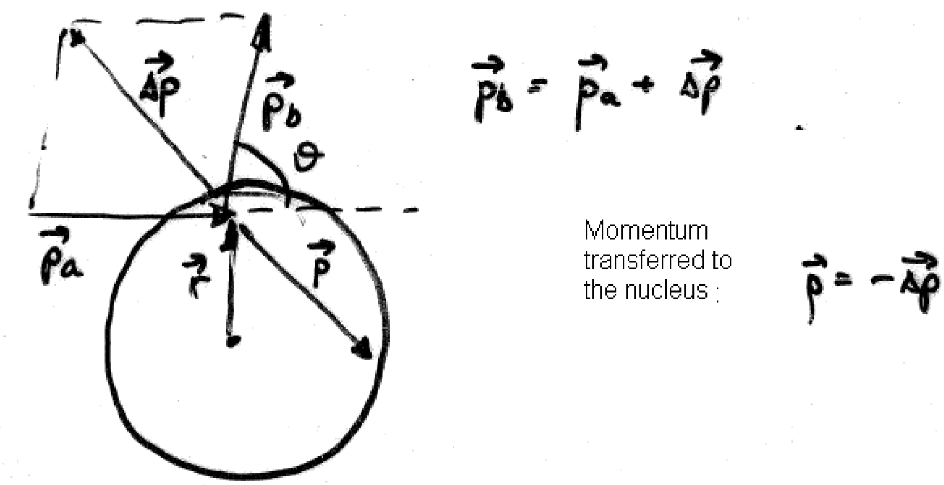

$$p^2 = p_a^2 + p_b^2 - 2p_a p_b \cos\theta$$

$$l \cdot \hbar \simeq R \cdot p \Rightarrow l = \left[\frac{2c^2 p_a p_b (2\sin^2 \frac{\theta}{2})}{\frac{(\hbar c)^2}{R^2}} \right]^{\frac{1}{2}}$$

Large scattering angles for outgoing particle = large transfer of angular momentum, $l \propto \sin\frac{\theta}{2}$.

$l = 1, 3, 5....$(odd numbers)$\Rightarrow$ parity change for the nucleus
$l = 0, 2, 4...$(even numbers)$\Rightarrow$ leaves the parity unchanged

Nuclear spin: $I_f = I_i + l \pm \underbrace{\frac{1}{2}}_{n\ or\ p}$

Compound reactions

$$a + x \rightarrow C^* \rightarrow Y + b$$

Well defined intermediate state (Compound nucleus) with a lifetime long enough that the final reaction, $C* \rightarrow Y + b$, has forgotten (i.e. is not influenced by) how C^* was created.

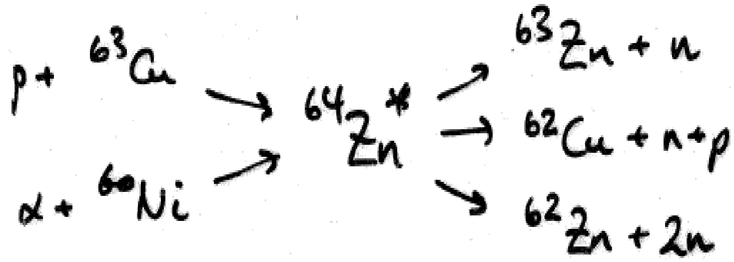

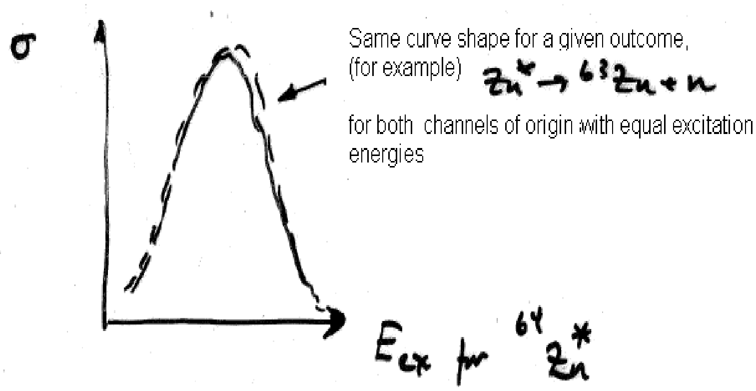

Resonance reactions

They appear at well defined excitation levels for C^*

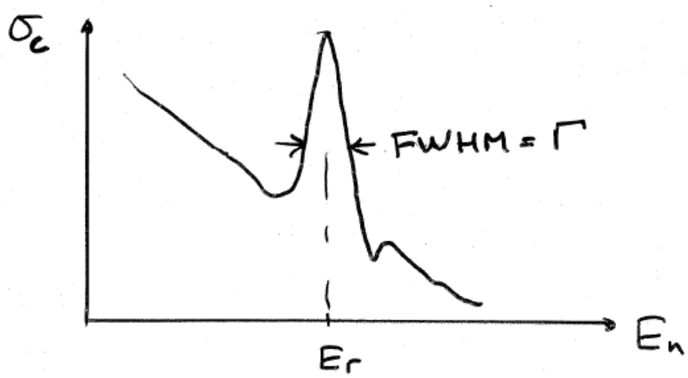

Example: Resonance peak in neutron capture cross section

Breit-Wigner formula:

$$\sigma_{\alpha,\beta} = g_\alpha(J)\frac{\pi}{k_\alpha^2}\frac{\Gamma_\alpha\Gamma_\beta}{(E-E_r)+(\frac{\Gamma}{2})^2}$$

$$\sigma_{\alpha\beta}(E = E_r \pm \frac{\Gamma}{2}) = \frac{1}{2}\sigma_{\alpha\beta}(E = E_r)$$

Spin factor: $g_\alpha(J) = \frac{2J+1}{(2i_a+1)(2i_A+1)}$

where i_a and i_A represent spin for the incoming particles.

$$g_\alpha = (2l+1) \text{ for } i_\alpha = i_A = 0$$

Generally: $\vec{I}_{C^*} = \vec{i_a} + \vec{l}_A + \vec{l}$

in this case, $\vec{l}$ represents the transferred angular momentum by (a, A).

Resonance level width: $\Gamma = \sum_{i\in\alpha,\beta}\Gamma_i = \hbar\sum\lambda_i = \hbar\lambda = \frac{\hbar}{\tau}$

τ is the mean lifetime of the intermediate state C^*.

Assuming $i_\alpha = i_A = 0$:

Maximum cross section for elastic scattering (At $E = E_r$): $\Gamma_\alpha \equiv \Gamma_\beta = \Gamma \Rightarrow \sigma_{\alpha\alpha}(max) = (2l+1)\frac{4\pi}{k_\alpha^2}$

Total absorption cross section: $\sigma_{abs} \propto \Gamma_\alpha \sum_{\beta\neq\alpha}\Gamma_\beta = \Gamma_\alpha(\Gamma - \Gamma_\alpha)$

$$\Rightarrow \sigma_{abs}(max) = (2l+1)\frac{\pi}{k_\alpha^2}$$

$$\Gamma_\alpha(1-\Gamma_\alpha)_{max} \text{ for } \Gamma_\alpha = \frac{\Gamma}{2}$$

Total capture cross section at $(E = E_\tau)$: $\sigma_C = (2l+1)\cdot\frac{4\pi}{k_\alpha^2}\frac{\Gamma_\alpha}{\Gamma}$

$$\sigma_{\alpha\beta} = \sigma_C \cdot \frac{\Gamma_\beta}{\Gamma} = \underbrace{(2l+1)\frac{4\pi}{k_\alpha^2}\frac{\Gamma_\alpha}{\Gamma}}_{\sigma_C} \cdot \underbrace{\frac{\Gamma_\beta}{\Gamma}}_{\textit{Exit channel } \beta}$$

Heavy ion reactions

Ex:

$$^{16}O +^{27} Al$$

Fusion

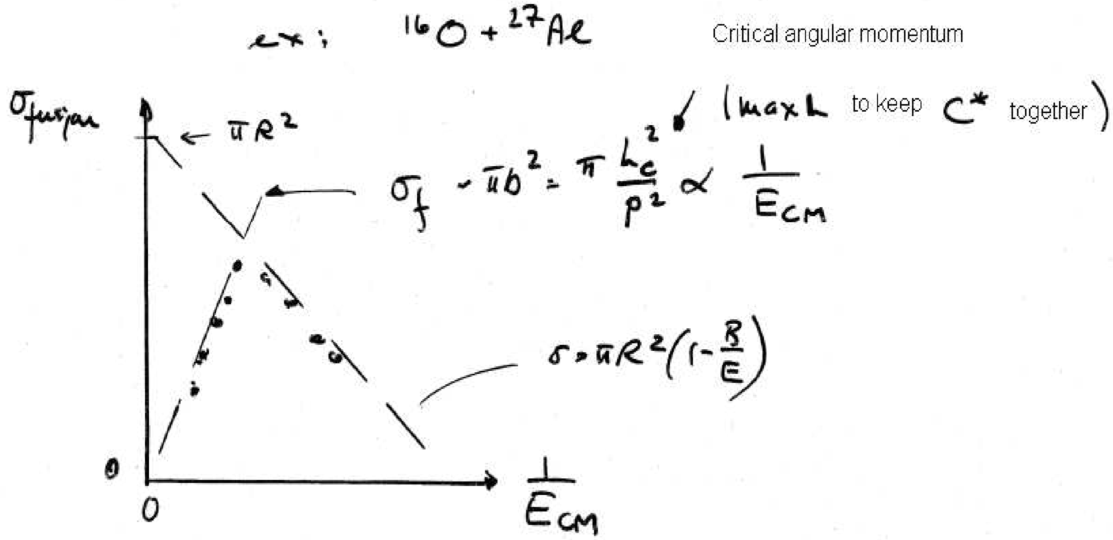
ex: $^{16}O + ^{27}Al$
Critical angular momentum
(max L to keep C* together)
σ_{fusion}
πR^2
$\sigma_f \sim \pi b^2 = \pi \frac{L_c^2}{p^2} \propto \frac{1}{E_{CM}}$
$\sigma = \pi R^2 (1 - \frac{B}{E})$
0
0
$\frac{1}{E_{CM}}$

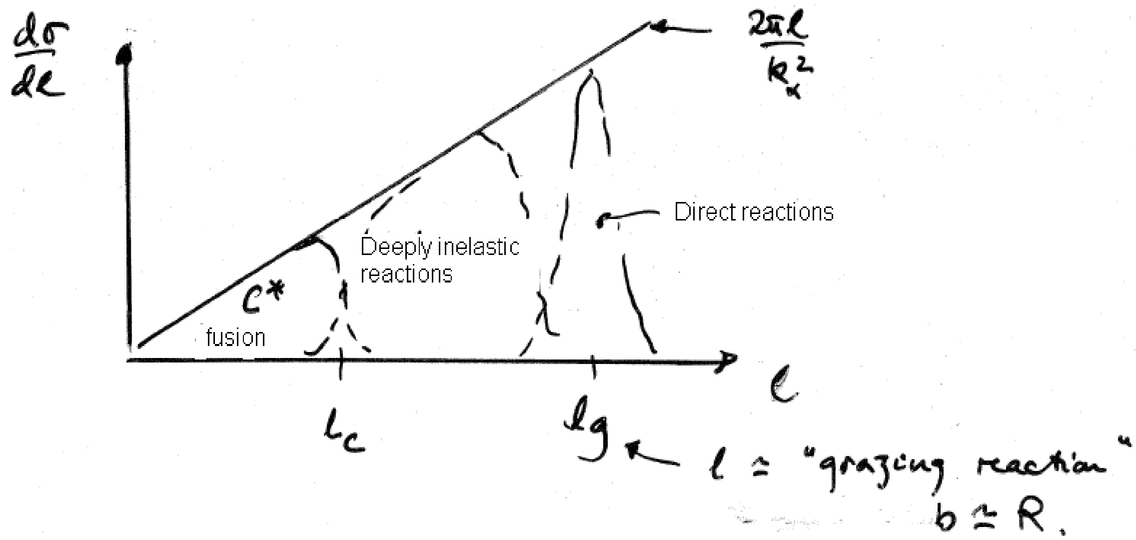
$\frac{d\sigma}{dl}$
$\frac{2\pi l}{k_\alpha^2}$
Direct reactions
Deeply inelastic reactions
C*
fusion
l
l_c
l_g
$l \simeq$ "grazing reaction"
$b \simeq R$.

8.)
Our radiological environment

The average effective annual dose

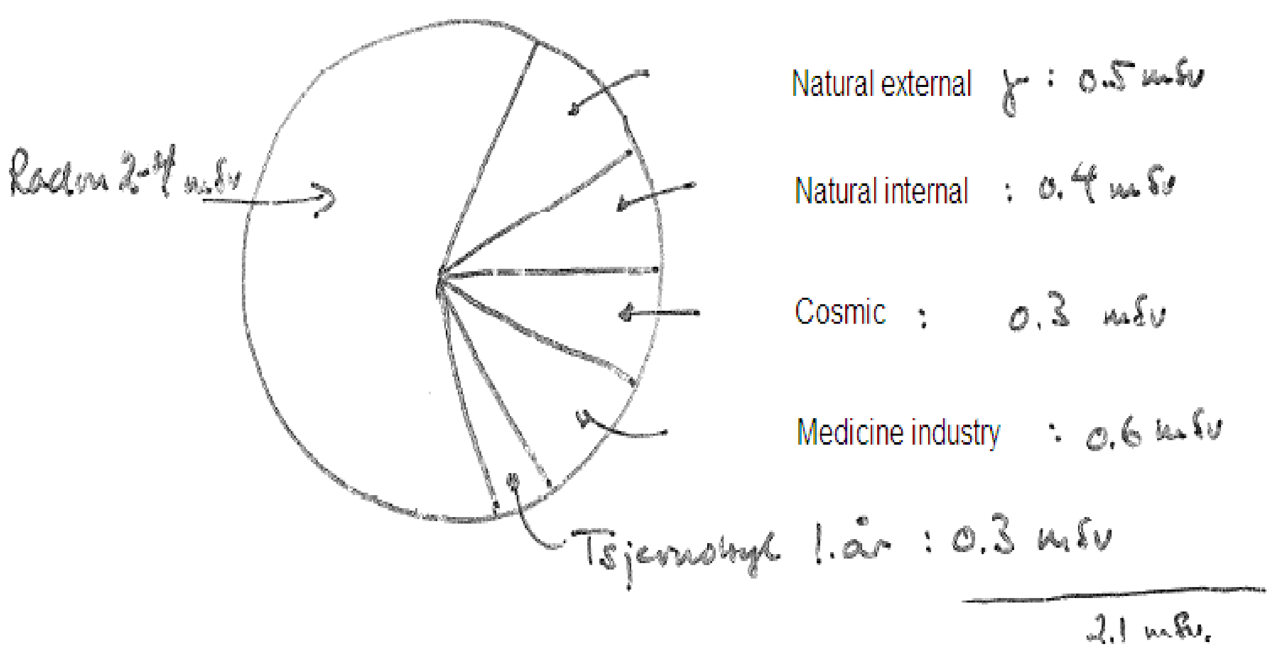

Indoor radon

Rn-222 is the biggest problem, because of a relatively large abundance of its element of origin, U-238, and a relatively long lifetime compared to other Rn-isotopes (Rn-220 and Rn-219).

Building sites with high concentrations of Ra $[\frac{Bq}{kg}]$ ($Ra - 226 \rightarrow Rn - 222$) and high gas permeability represent the biggest problem.

Indoor Rn-concentration

$$\frac{d\chi_{Rn}}{dt} = \dot{u}(t) - \chi_{Rn}\left(\lambda_{Rn} + \lambda_v\right)$$

- $\chi_{Rn,air}$= the concentration of Rn-222 activity in air. $\left[\frac{Bq}{m^3}\right]$
- $\dot{u}(t)$ =the rate of flow of Rn-222 into the building. $\left[\frac{Bq}{m^3 \cdot s}\right]$
- λ_{Rn}= the disintegration constant. $\left[\frac{1}{s}\right]$
- λ_v = the rate of flow out of the building. $\left[\frac{1}{s}\right]$

If $\dot{u}$ and λ_v are constant, the equilibrium concentration is:

$$\chi_{Rn,air} = \frac{\dot{u}}{\lambda_{Rn} + \lambda_v}$$

What contributes to $\dot{u}(t)$ is:

- Ground conditions
- Building materials
- Water (household water)
- Outdoor air (ventilation)

Rn and Rn-daughters get stuck to tiny particles of dust and surfaces (plate-out).

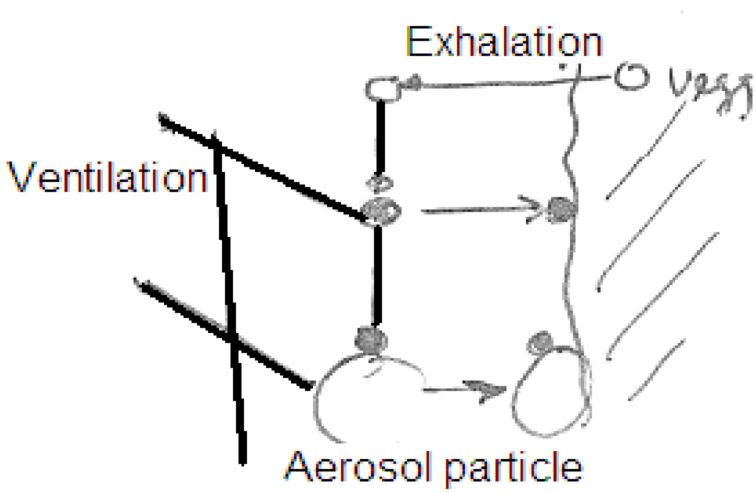

Rn-concentration in Norwegian houses

Most probable value:	$20 \frac{Bq}{m^3}$
Mean value:	$88 \frac{Bq}{m^3}$ in 2001
	3% of the houses had values $> 400 \frac{Bq}{m^3}$ in 2001
	9% of the houses had values $> 200 \frac{Bq}{m^3}$ in 2001

Rn dosimetry and risk limits (ICRP 50)

Contributions from Rn-222 (a gas) and its metal-like daughter nuclides have to be accounted for separately.

1.) Contributions from Rn:

Dose rate in soft tissue excluding the lungs (due to Rn dissolved in the tissue):

$$\dot{D}_{soft\ tissue} = S_{st} \cdot \chi_{Rn,air}, \qquad S_{st} = 0.005 \frac{\frac{nGy}{h}}{\frac{Bq}{m^3}}$$

For lung tissue, the contribution from Rn in the alveolar air comes in addition to the contribution from dissolved Rn:

Dose rate:	$\dot{D}_{lungs} = S_l \cdot \chi_{Rn,air}, \quad S_l = 0.04 \frac{\frac{nGy}{h}}{\frac{Bq}{m^3}}$
Equivalent dose rate:	$\dot{H}_T = \omega_R \dot{D}_{T,R}, \qquad \omega_R = 20$ for α
Effective dose rate:	$\dot{E} = \sum \omega_T \dot{H}_T = \omega_R(\omega_l \dot{D}_l + \omega_{st} \dot{D}_{st}), \qquad \omega_l = 0.12, \quad \omega_{st} = 0.88$
$\Rightarrow$	$\dot{E} = S_{tot,Rn} \cdot \chi_{Rn,air}, \qquad S_{tot,Rn} = 0.2 \frac{nSvh^{-1}}{Bqm^{-3}}$

2.) Contributions from short-lived Rn-daughter nuclei:

Chain of disintegrations:

No	Nuclide	$T_{\frac{1}{2}}$	E_α	ε_{pi}	$\frac{\varepsilon_{pi}}{\lambda_i}$
			$[MeV]$	$[MeV]$	$[\frac{MeV}{Bq}]$
0	^{222}Rn	3.82d	5.49		
1	^{218}Po	3.05m	6.00	13.7	3620
2	^{214}Pb	26.8m		7.69	17800
3	^{214}Bi	19.7m		7.69	13100
4	^{214}Po	164μ s	7.69	7.69	$2{\cdot}10^{-3}$
5	^{210}Pb	19.4yrs			

Where numbers 1 through 4 represent short-lived daughter nuclei.

Equilibrium activity concentration: $C_{act,eq} = \lambda_{Rn} \cdot C_{Rn} = \lambda_i \cdot C_i, \quad i = 1, ..4$

Where C_{Rn} is the number of Rn atoms per unit volume of air.
Now, in a real situation, the activity concentration of Rn-daughters will be lower than the equilibrium Rn activity concentration. This is because of ventilation and plate-out, which affect the daughters more than it affects Rn itself.
The potential α-energy per Rn-daughter atom ($\varepsilon_{pi}, \quad i = 1, ..4$) is the sum of α-disintegration energies for one atom of the nuclide and its short-lived daughter nuclei:

$$\varepsilon_{pi} = \sum_{j \geq i}^{4} E_{\alpha j}$$

Potential α-energy per unit activity: $\frac{\varepsilon_{pi}}{\lambda_i} = \frac{N_i \varepsilon_{pi}}{\lambda_i N_i} = \frac{\varepsilon_{pi} T_{\frac{1}{2},i}}{\ln 2}$

Potential α-energy concentration: $C_p = \sum_{i=1}^{4} C_{act,i} \cdot \frac{\varepsilon_{pi}}{\lambda_i} [\frac{J}{m^3}]$

Equivalent equilibrium Rn-concentration in air: $EEC_{Rn} \equiv \chi_{eq,Rn} = \frac{\sum_{i=1}^{4} C_{act,i} \cdot \frac{\varepsilon_{pi}}{\lambda_i}}{\sum_{i=1}^{4} \frac{\varepsilon_{pi}}{\lambda_i}}$

$$= \frac{C_p}{\sum_{i=1}^{4} \frac{\varepsilon_{pi}}{\lambda_i}} = K \cdot C_p$$

EEC_{Rn} is the concentration of activity of Rn in equilibrium with its short-lived daughter nuclei, which would have the same potential α-energy per unit volume air as the mixture of interest:

$$\chi_{eq,Rn} = 0.10 \cdot C_{act,Po-218} + 0.51 \cdot C_{act,Pb-214} + 0.38 \cdot C_{act,Bi-214}$$

Note! Contribution from $C_{act,Po-214}$ is extremely small because $\frac{\varepsilon_{pi}}{\lambda_i} \ll 1$ for Po-214.

Empirical value of the equilibrium factor: $F = \frac{EEC_{Rn}}{\chi_{Rn,air}} \simeq 0.5$

Heavy duty ventilation results in a smaller F-value.

Intake of potential α-energy during a time interval T:

$$I_{pot} = \frac{E}{A}\dot{V}_{in}T \cdot \chi_{eq,Rn}, \qquad \frac{E}{A} = \sum_{i=1}^{4} \frac{\varepsilon_{pi}}{\lambda_i} = 55.5 \cdot 10^{-10} \quad J/Bq$$

Assume the inhalation rate to be: $\dot{V}_{in} = 0.8\frac{m^3}{h}$ during the time interval T.

The trachea-bronchial region: $\frac{D_{T-B}}{I_{pot}} = 1.5\frac{Gy}{J} \equiv K_{T-B}$

Pulmonal region: $\frac{D_P}{I_{pot}} = 0.2\frac{Gy}{J} \equiv K_P$

T-B dose rate: $\dot{D}_{T-B} = \frac{D_{T-B}}{T} = S_{T-B} \cdot \chi_{eq,Rn} = F \cdot S_{T-B} \cdot \chi_{Rn,air}$

where $S_{T-B} = K_{T-B}\frac{E}{A}\dot{V}_{in} = 7\frac{nGyh^{-1}}{Bqm^{-3}}$

P dose rate: $\dot{D}_P = \frac{D_P}{T} = S_P \cdot \chi_{eq,Rn} = F \cdot S_P \cdot \chi_{Rn,air}$

where $S_P = K_P \cdot \frac{E}{A} \cdot \dot{V}_{in} = 0.9\frac{nGyh^{-1}}{Bqm^{-3}}$

Equivalent dose rate: $\dot{H}_T = \omega_R \dot{D}_{T,R}$, for α $\omega_R = 20$

Effective dose rate: $\dot{E} = \sum \omega_T \dot{H}_T = \omega_R[\omega_{T-B}\dot{D}_{T-B} + \omega_p \dot{D}_p]$

When taking into account the tissue weighting factors, it is assumed that T-B and P contribute equally to the total lung tissue weighting factor.

$$\Rightarrow \qquad \omega_{T-B} = \omega_P = \omega_{\frac{L}{2}} = 0.06$$

$$\Rightarrow \qquad \dot{E} = S_{tot,Rn-daughters} \cdot \chi_{eq,Rn} = F \cdot S_{tot,Rn-daugthers} \cdot \chi_{Rn,air}$$

$$S_{tot,Rn-daughters} = 9.5\frac{nSvh^{-1}}{Bqm^{-3}}$$

Finally, the total contribution from both Rn and its daughters becomes:

$$\dot{E}_{tot} = [S_{tot,Rn} + F \cdot S_{tot,Rn-daughters}]\chi_{Rn,air}$$
$$\dot{E}_{tot} = \overline{S} \cdot \chi_{Rn,air}$$

If one assumes that F=0.5 $\Rightarrow \overline{S} = [0.2 + 0.5 \cdot 9.5]\frac{nSvh^{-1}}{Bqm^{-3}} = 5\frac{nSvh^{-1}}{Bqm^{-3}}$

Yearly, one can assume that an average person stays indoors about 80% of the time. This becomes about 7000 hours per year. Further on, assuming that the Rn exposure outdoors can be neglected:

$$\Rightarrow \qquad \overline{S}_{yr} = 5\frac{nSvh^{-1}}{Bqm^{-3}} \cdot 7000\frac{h}{yr} = 35\frac{\frac{\mu Sv}{yr}}{Bqm^{-3}}$$

The mean Rn-concentration in Norwegian houses was $\chi_{Rn,air} = 88\frac{Bq}{m^3}$ in 2001. From this, it follows that the effective dose rate becomes:

$$\Rightarrow \qquad \dot{E}_{tot} = 35 \cdot 88 \frac{\mu Sv}{yr} = 3.0 \frac{mSv}{yr}$$

Cancer risk due to Rn exposure

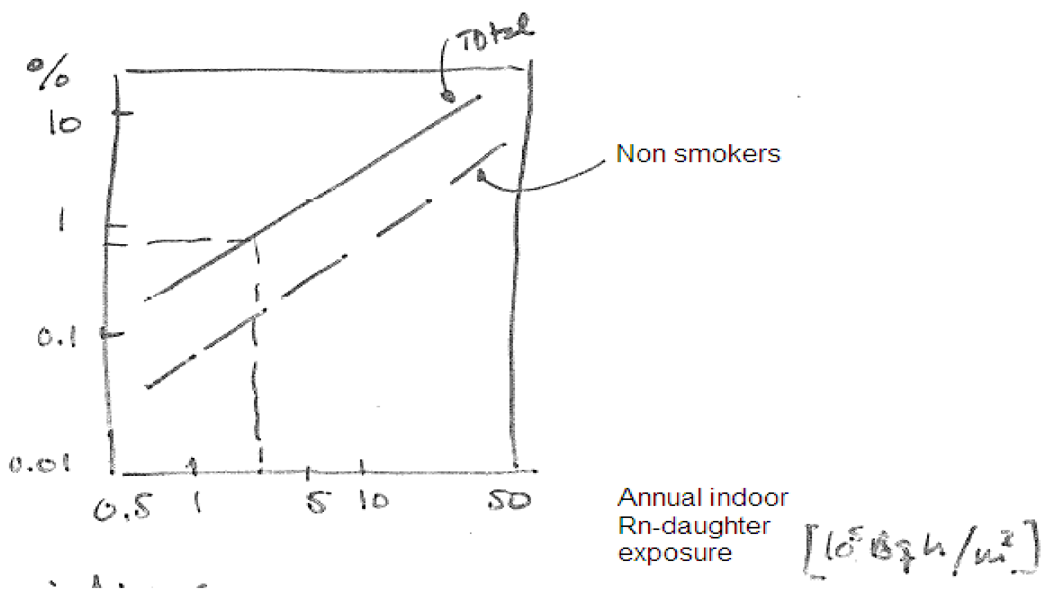

Concentration limits in Norway

`Limits have been revised: If radon concentration is above 100 Bq/m3, actions should be taken. Maximum limit is 200 Bq/m3.`

~~$\chi_{Rn,air} < 200$: It is not necessary to take action.~~

~~$200 < \chi_{Rn,air} < 400$: Simple actions required.~~

~~$\chi_{Rn,air} > 400$: Expensive actions required~~

Measuring the amount of Rn and Rn-daughters

Important conditions to take into account

1.) The measuring device must not be affected by deposited Rn-daughters. For example on the surface of the detector.

2.) It must be known to which degree it measures Rn, and to which degree it measures Rn-daughters.

3.) Integration over long time is necessary to obtain good accuracy.

Measuring methods for air-borne *Rn*

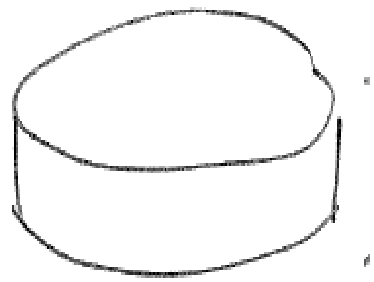

1.) The CB (Coal Box)-method, consists of a box containing active coal, which absorbs *Rn*-gas. The box is open only during exposure when *Rn* gas is adsorbed to the active coal. Measuring the activity of *Rn*-daughters, originating from the absorbed *Rn*-gas, is done using a NaI scintillation crystal via γ spectroscopy. A problem here is that the coal adsorbs air humidity more efficiently than *Rn*-gas. This means that the measuring results are more accurate in dry places. Another inaccuracy of this method is that it does not integrate over very long time.

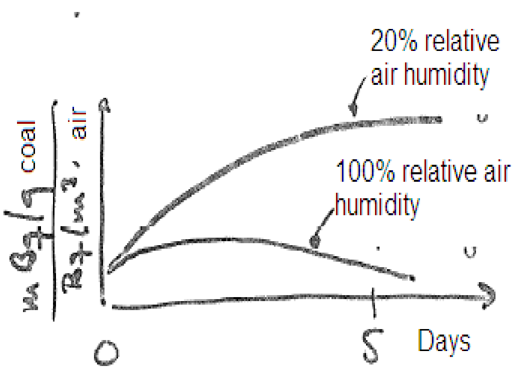

Other sources of radiation

Cosmic radiation

Particle radiation (85% protons, 15% α-particles) from space, and particle radiation as well as γ-radiation from the sun. These primary particles are transformed into secondary cosmic radiation consisting of various particle types and some γ-radiation, due to interactions and reactions in the atmosphere. Cosmic radiation increases with altitude above sea level.

Ground-level: $0.35\frac{mSv}{yr}$ i.e. $0.04\ \frac{\mu Sv}{h}$

Air-traffic altitude: (10.000m) $5\frac{\mu Sv}{h}$

External γ-radiation

External γ-radiation is mostly due to the existence of radioactive minerals in the ground. The following nuclides constitute the main contributions to dose:

^{40}K 40%

^{232}Th 40%

^{226}Ra 20%

The average effective dose from external γ is around $0.55\frac{mSv}{yr}$

Naturally occuring internal radiation

Natural internal radiation is mainly due to radiation from ^{40}K (β-emitter, $T_{\frac{1}{2}}$=10^9yrs). Natural K consists of about a fraction of 10^{-4} ^{40}K. The amount of K inside our bodies is regulated by the metabolism. This again implies that the dose contribution is kept at a constant level.
Average effective dose from internal radiation is about $0.37\frac{mSv}{yr}$.

The Tsjernobyl accident

The outburst resulted in a release of about 3.5% of the total amount of activity contained in the reactor. All the gaseous nuclei (^{85}Kr and ^{133}Xe) were released. The fall-out consisted mainly of ^{137}Cs and ^{134}Cs. The mean ^{137}Cs fall-out in Norway was $7\frac{kBq}{m^2}$, but some places had more than $80\frac{kBq}{m^2}$.

Dosimetry

Total transfer factor for effective dose due to all the nuclides, based on ^{137}Cs ground deposition. For northern areas, in units of $\frac{\mu Sv}{kBqm^{-2}}$:

	Year 1	Total
External	10	86
Internal	27	59
Sum	$\simeq 40$	$\simeq 150$

Internal dosimetry is based on averaged transfer coefficients, assumptions concerning diet-composition and biokinetical models for up-take of radioactive substances.

Average dose based on Norwegian conditions:

Year 1 $\quad 40\frac{\mu Sv}{kBqm^{-2}} \cdot 7\frac{kBq}{m^2} = 0.28mSv$

Total $\quad 150\frac{\mu Sv}{kBqm^{-2}} \cdot 7\frac{kBq}{m^2} = 1.0mSv$

Dose-reducing measures

Use of Cs-binders (as feed-admixture and tablets) reduces the up-take of Cs in domestic animals by up to 50-80%.

9.)
Industrial, analytical, and medical applications. (Lilley Chap.8 and 9)

Industrial use

1.) Tracer-based measurements (incorporation in biological systems, measuring abration and leaks)

2.) Thickness measurements, level measurements.

3.) Material modifications (hardening and shrinking)

4.) Food sterilization (spice)

5.) Industrial radiography (welding inspection)

Neutron activation analysis

1.) This is an alternative solution to the regular tracer techniques. Only the samples collected are made radioactive.

2.) Deciding the amount of unknown elements in a sample.

Induced activity: $A(t) = \lambda n(t) = \dot{\Phi}\sigma \cdot N_{target}[1 - e^{-\lambda t}]$ for $\dot{\Phi}\sigma \ll \lambda$

$$\frac{dN_{target}}{dt} = -\dot{\Phi}\sigma N_{target}$$

$$\frac{dn}{dt} = \dot{\Phi}\sigma N_{target} - \lambda \cdot n$$

$$\Rightarrow \quad n(t) = \frac{\dot{\Phi}\sigma \cdot N_{target}}{\lambda - \dot{\Phi}\sigma}[e^{-\dot{\Phi}\sigma t} - e^{-\lambda t}]$$

Rutherford backscattering

Rutherford scattering cross-section in the lab system for $M < \infty$ ($M \to \infty$ makes the lab and CM systems equivalent):

Rutherford cross-section: $\frac{d\sigma_R}{d\Omega} = 1.296\left[\frac{zZ}{E_0}\right]^2\left[\frac{1}{sin^4\frac{\psi}{2}} - \left(\frac{m}{M}\right)^2 + ...\right]\frac{mb}{sr}$

Where ψ is the scattering angle in the lab system. The energy of the particle (m) backscattered from the target (M):

Particle energy: $E(\pi) = \left[\frac{M-m}{M+m}\right]^2 E_0$

E_0 is the particle energy immediately before interacting with the target (energy loss along particle track).

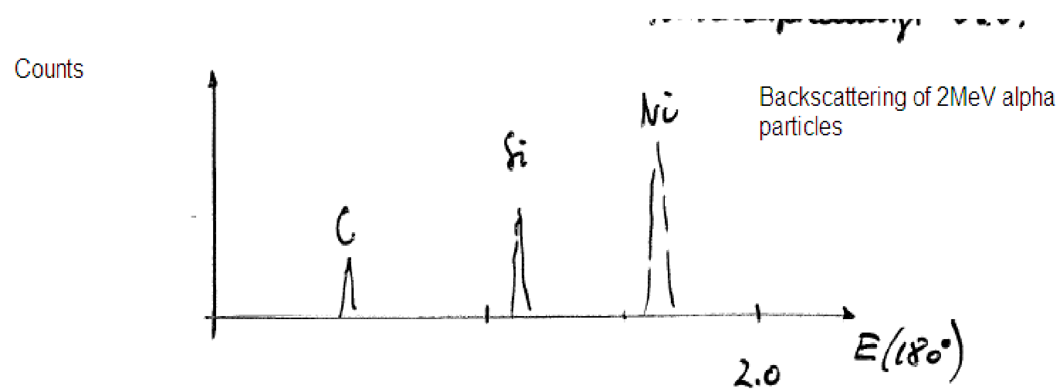

In "thick" samples, the particle energy is degraded both before and after backscattering. The method is ideal to detect occurance of heavy elements in a material consisting of light elements.

Particle-induced X-ray emission (PIXE)

This method is particularly sensitive when it comes to finding elements. The sensitivity is 0.1ppm, i.e. 1000 times better than the usual method of X-ray microanalysis by electron microscopy. Both identification and quantification based on excitation of characteristic X-ray radiation.

X-ray production rate: $R_X = \dot{\Phi} \cdot \sigma_x \cdot \underbrace{n_T}_{\frac{\#_T}{V_T}} \cdot \underbrace{Adx}_{V_{Target}}$

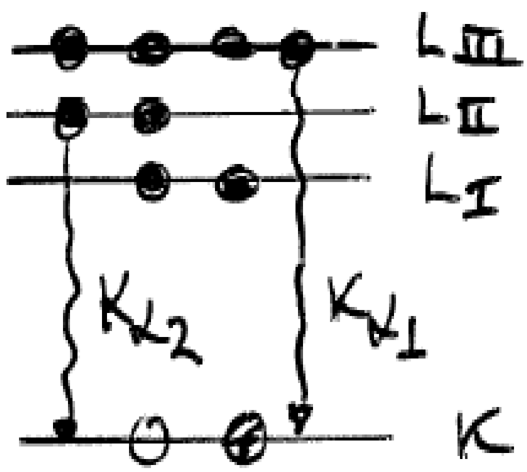

$L_I \rightarrow K$ is optically forbidden.

Accelerator-based mass spectroscopy

This is a sensitive method for counting ^{14}C. This makes it ideal for carbon dating of biological materials. What makes this method so effective is that it counts all the ^{14}C atoms in the sample, while radioactivity-based counting only counts a fraction $\lambda \cdot T \ll 1$ during the time interval T.($\lambda = \frac{\ln 2}{5730 yrs}$ for ^{14}C)

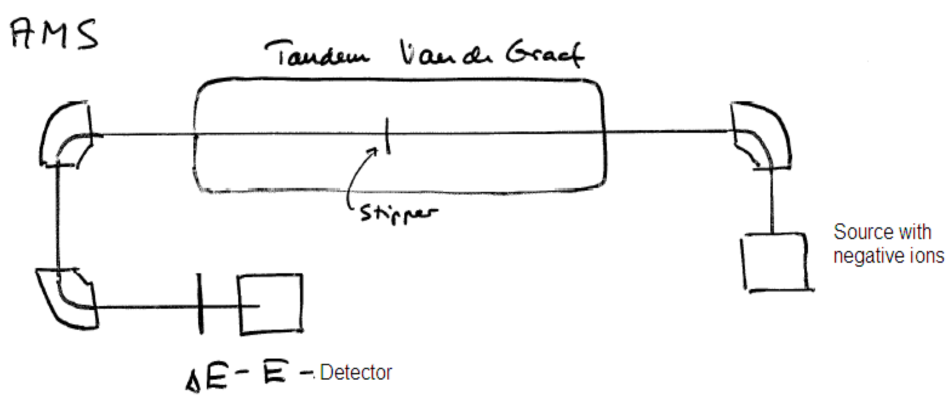

Deflector magnets : $\vec{F} = q(\vec{v} \times \vec{B}) = m\vec{a} \Rightarrow r = \frac{mv}{qB}$.

Deflector magnets: $\vec{F} = q(\vec{v} \times \vec{B}) = m \cdot \vec{a} \Rightarrow r = \frac{mv}{qB}$

Low-activity counting

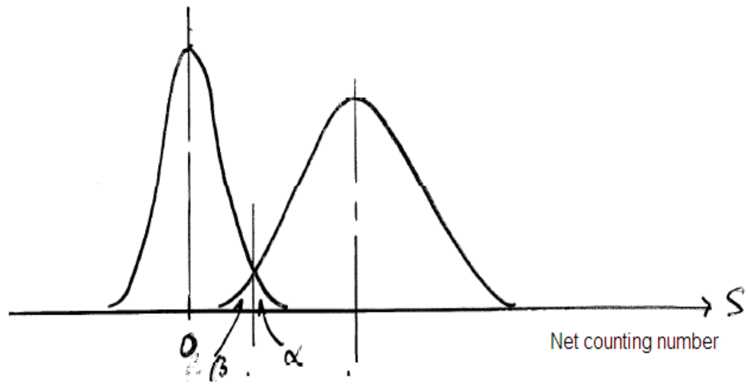

Radioactivity is modelled as a Bernoulli process which is represented by a binomial distribution.

For $N \gg 1$, $p = \lambda t \ll 1$, the Binomial distribution≃Poisson distribution≃Gaussian distribution.
To keep it simple, one uses a Gaussian distribution as a statistical model, combined with the result from the Poisson distribution:

Standard deviation: $\sqrt{\lambda t} = \sqrt{n}$

Net number of counts: $S = n_g - n_b$

Where n_g is the gross counts and n_b is the number of counts due to background radiation. Both these numbers are counted during the same time interval t.

Standard deviation: $\sigma_S = \sqrt{\sigma_{ng}^2 + \sigma_{nb}^2} = \sqrt{n_g + n_b} = \sqrt{S + 2n_b}$

Minimum significant activity

P(Type I error)=P(false positive)$\leq \alpha$ for $S \leq L_C$

The sample has 0 activity $\Rightarrow \sigma_S = \sigma_0 = \sqrt{2n_b}, \quad (S \simeq 0)$

$$P_0(S) = \frac{1}{\sqrt{2\pi}\sigma_0} \cdot e^{-\frac{S^2}{2\sigma_0^2}}$$

$$L_c = k_\alpha \cdot \sigma_0$$

Where α represents an α-fractile in the Gaussian distribution. For example $\alpha = 0.05 \Rightarrow k_\alpha = 1.645$

Minimum detectable true activity

P(Type II error)=P(false negative)$\leq \beta$ for $S \geq L_d$

$$L_d = L_C + k_\beta \sigma_d = k_\alpha \sigma_0 + k_\beta \sigma_d$$

In this case, S is $N(L_d, \sigma_d)$.

Variance: $\sigma_d^2 = S_d + 2n_b = L_d + \sigma_0^2$

$\Rightarrow$ $[L_d - k_\alpha \sigma_0]^2 = k_\beta^2 \sigma_d^2 = k_\beta^2 [L_d + \sigma_0^2]$

$\Rightarrow$ $L_d = \frac{k_\beta^2 + 2k_\alpha \sigma_0}{2} + \sqrt{\left[\frac{k_\beta^2 + 2k_\alpha \sigma_0}{2}\right]^2 + [k_\beta^2 - k_\alpha^2]\sigma_0^2}$

1.) $k_\alpha = k_\beta = k \Rightarrow L_d = k^2 + 2k\sigma_0$

2.) $k_\alpha \sigma_0 \gg k_\beta^2 \Rightarrow L_d = (k_\alpha + k_\beta)\sigma_0$

I	II	III
$S < L_c$	$L_c < S < L_d$	$S > L_d$
No significant activity	Significant activity, but P(false negative)$> \beta$	Significant, true activity

Detection limits: $A_c = \frac{L_c}{\varepsilon \cdot T}$, $A_d = \frac{L_d}{\varepsilon \cdot T}$

During the time interval T, with an assumed counting efficiency ε.

If the accurate background counting rate, r_b is known, the standard deviation: $\sigma_0 = \sqrt{n_b} = \sqrt{B}$
I.e, $\sigma_{nb} = 0$, $B = r_b \cdot T$

Nuclear imaging (Lilley chap 9)

Projection imaging (external source, conventional X-ray)

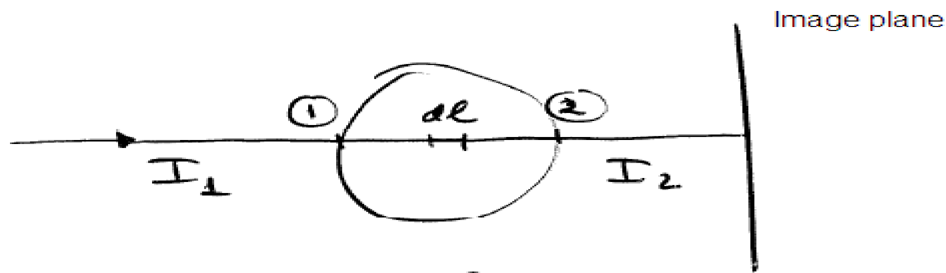

$$\ln\left(\frac{I_1}{I_2}\right) = \int_1^2 \mu \, dl$$

Internal source distribution imaged by a gamma camera

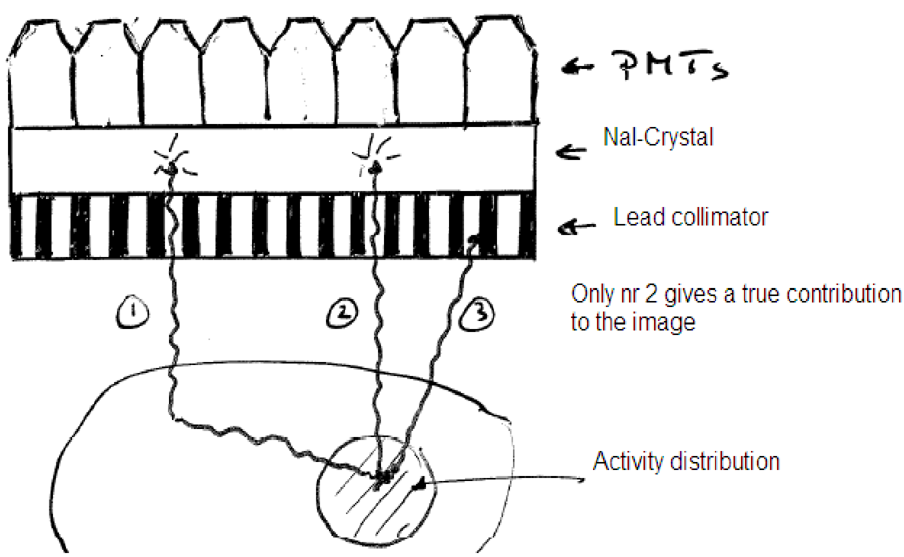

Projection imaging: $X = \frac{\sum s_i x_i}{\sum s_i}$, $Y = \frac{\sum s_i Y_i}{\sum s_i}$, where s_i is the signal in PMT i.

Energy discrimination: $E = \sum s_i$ inside the full-energy peak.

X-ray CT (Computed Tomography)

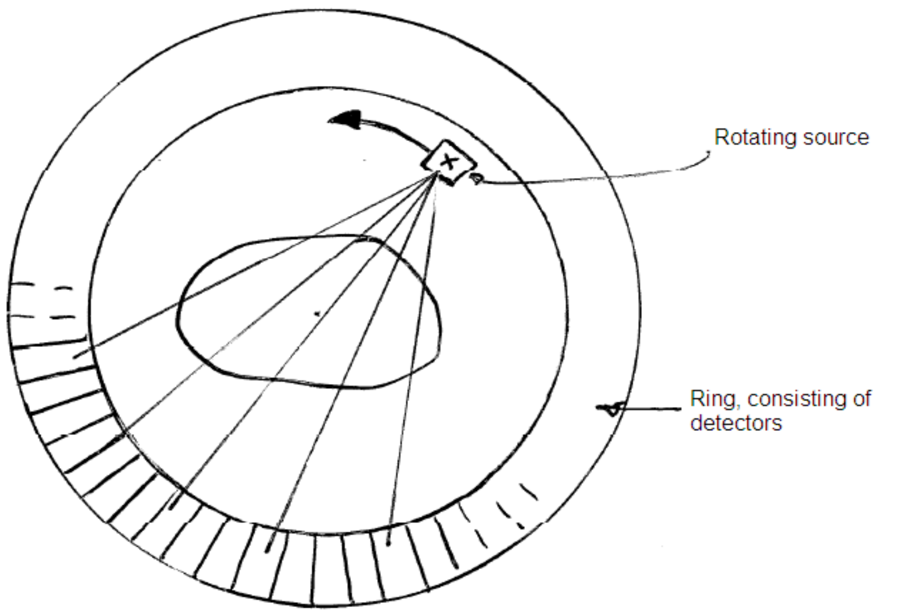

Positron Emission Tomography (PET)

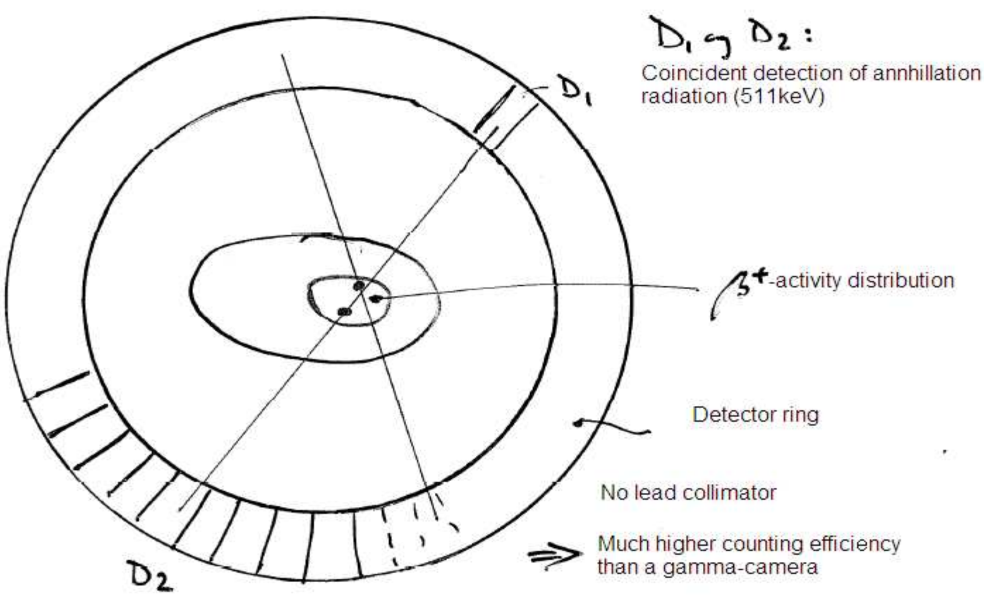

Filtered back-projection for reconstruction of images registered as a set of projection profiles

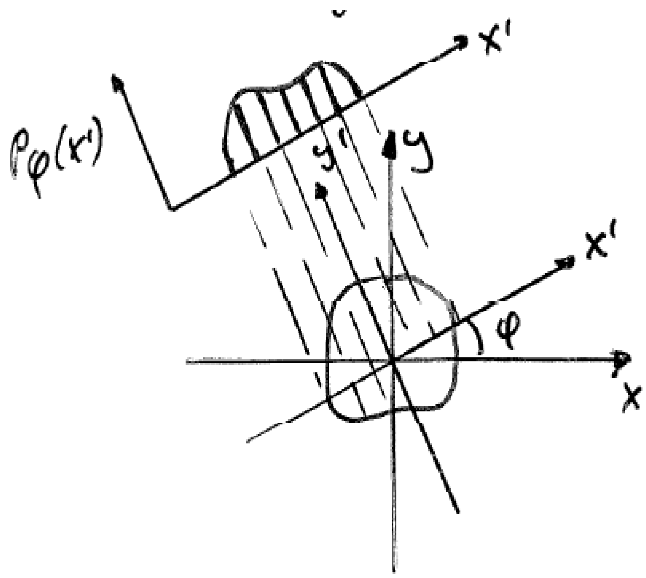

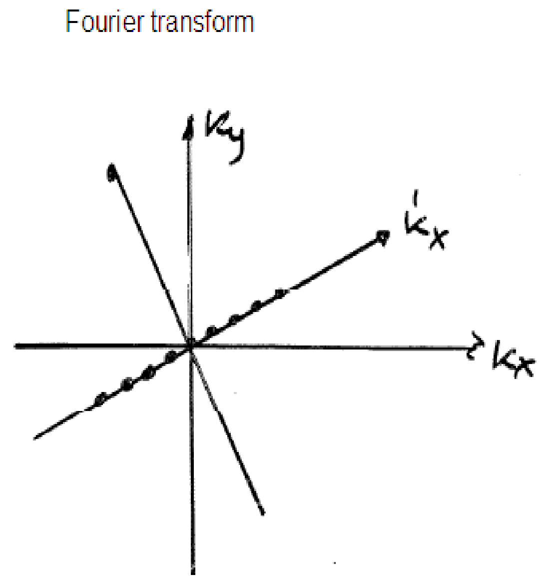

Central section theorem: The one-dimensional Fourier transform of the object's projection profile in the ϕ direction, is equal to the central section of the two-dimensional Fourier transform of the object through the origin in the ϕ-direction. $\rightarrow M(k'_x, k'_y = 0) = M(k, \phi) = P_\phi(k'_x)$, where M is the Fourier transform of the object and P_ϕ is the Fourier transform of the profile in direction ϕ.

Filtered profile: $p^\dagger_\phi(x') = \mathcal{F}^{-1}[P_\phi(k) \cdot H(k)]$

Filter function: $H(k) = |k|$

$\Rightarrow$ $p^\dagger_\phi(x') = \int_{-\infty}^{\infty} p_\phi(u) \cdot h(x' - u) du$

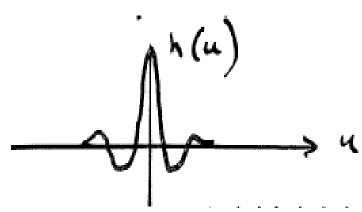

Filtered back-projection: $\mu(x, y) = \mathcal{F}^{-1}[M^P(k, \phi)] = \int_0^\phi p^\dagger_\phi(x') \mid_{x'=xcos\phi+ysin\phi} d\phi$

Projection imaging results in averaging, which again leads to loss of high frequency information. Filtering with high frequency enhancement before image reconstruction by back-projection. Filtered back-projection can be used for SPECT, PET, X-ray CT, MR, etc.

MR imaging

For all nuclei with spin $I \neq 0$.
Mostly used for ^1H-mapping.

Net magnetization: $\vec{M} = \gamma \vec{L}, \quad \gamma = \frac{2\mu_p}{\hbar}$

$$M = \Delta N \cdot \mu_p$$

$$L = \Delta N \cdot S_Z = \Delta N \cdot \frac{1}{2}\hbar$$

$$\Delta N = N_+ - N_- = N_+[1 - e^{-\frac{\Delta E}{kT}}] \simeq \frac{N}{2} \cdot \frac{2\mu_p B}{kT}, \qquad \Delta E = 2\mu_p B$$

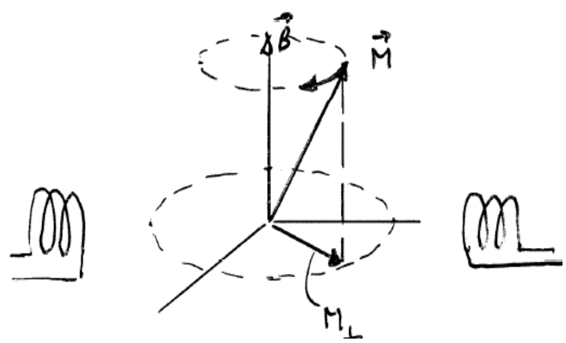

Precession of $\vec{M}$ around the direction of the $\vec{B}$-field at the Larmor frequency ω_L.

Torque: $\frac{d\vec{L}}{dt} = \vec{M} \times \vec{B}$

$\Rightarrow \quad \omega_L = \frac{2\mu_p \cdot B}{\hbar} = \gamma B$

Excitation field at Larmor frequency ω_L: B_{ex} in the horizontal plane. $\frac{B_{ex}}{2}$ is found to be a constant field in a rotating co-ordinate system, rotating at the Larmor frequency: $\Rightarrow$ Precession around the x'-axis at the frequency $\omega' = \frac{2\mu_p}{h} \cdot \frac{B_{ex}}{2}$

90^o excitation pulse: $\omega' \cdot T = \frac{\pi}{2}$

180^o excitation pulse: $\omega' \cdot T = \pi$

After excitation, $\vec{M}$ will go through a relaxation process and turn back to it's former direction along the $\vec{B}$-direction, during the time interval T_1 (Spin-lattice relaxation period). Loss of phase coherence in the $x'y'$ plane occurs due to spin-spin interaction with the time constant $T_2^*(< T_1)$.

Spin echo (measured by the observer in the rotating co-ordinate system, rotating at the Larmor frequency).

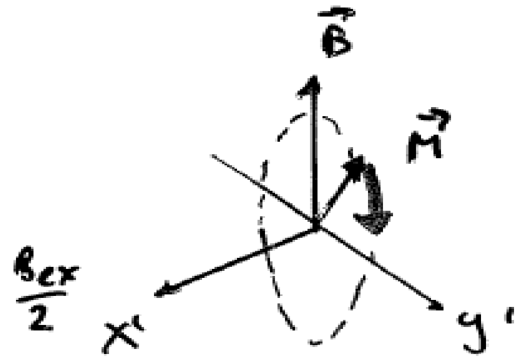

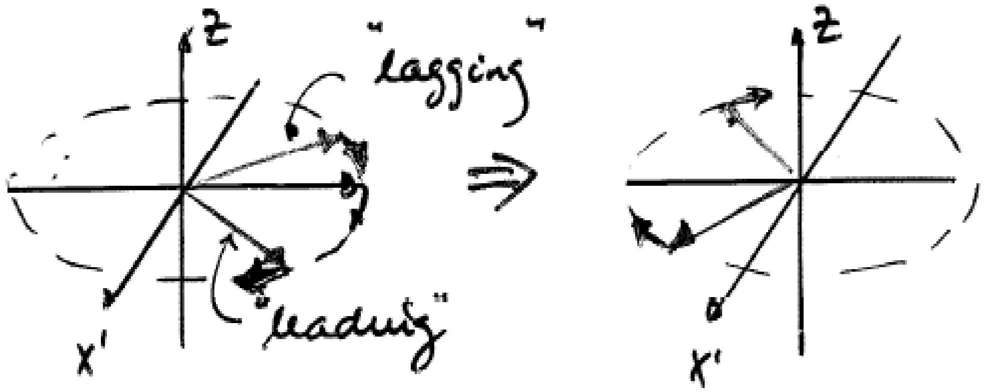

180^0 precession around x' due to the excitation field $\frac{B_{ex}}{2}$.

Pulse sequence:

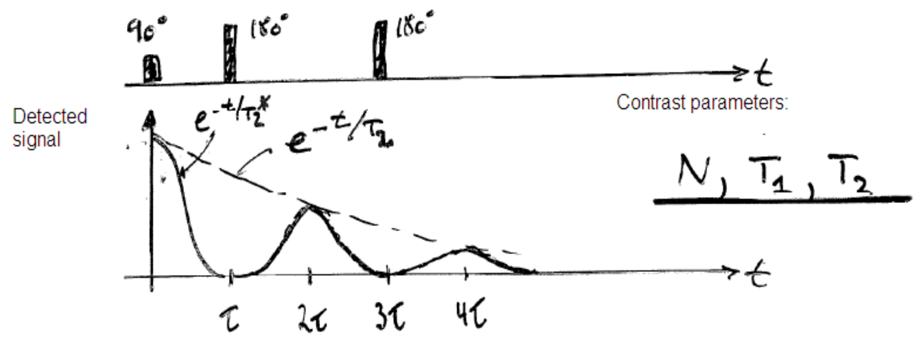

MR tomography (cross-sectional imaging)

Selective excitation of a section by a field gradient (B_z) in the z-direction.

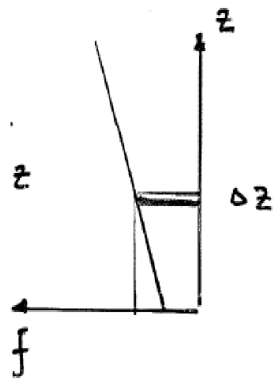

Field: $\vec{B} = \vec{B}_0 + z\vec{B}_z$

$\Rightarrow$ $f_{ex} = f_{Larmor}$ for a section of thickness Δz

Read-out gradient in the ϕ-direction in the cross-sectional plane (x, y)
$\Rightarrow$ The signal represents the sum of the signal for all y' at each value of x' in the ϕ-direction.
$\Rightarrow$ Projection imaging and image reconstruction by filtered back-projection.

10.)
Fission and fusion

Fission (Lilley Chap.10)

Average binding energy per nucleon:

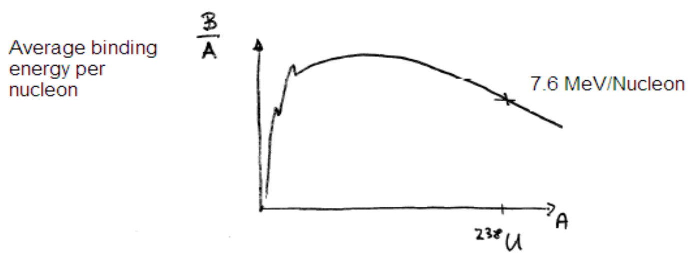

Nuclear fission: $A \to A_1 + A_2$

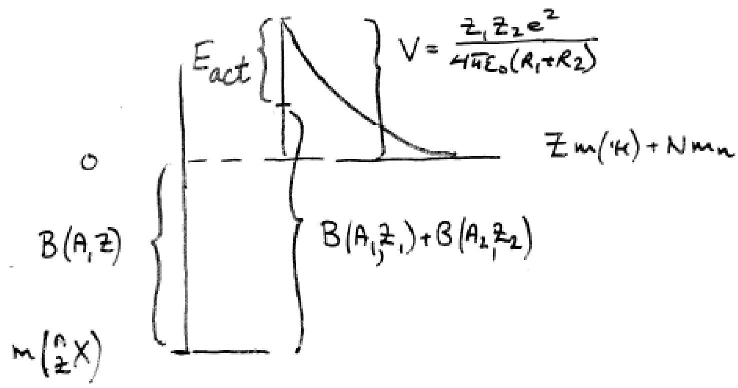

Fission barrier≡ activation energy

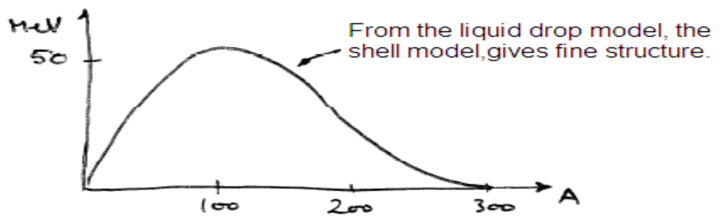

Example (Fission by capture of thermal neutrons)

$$^{235}U + n \rightarrow^{93}_{37} Rb +^{141}_{55} Cs + 2n$$

Where the last term, 2n, represents prompt, fast neutrons. Yield, $\nu = 2.5 \frac{n}{fission}$.

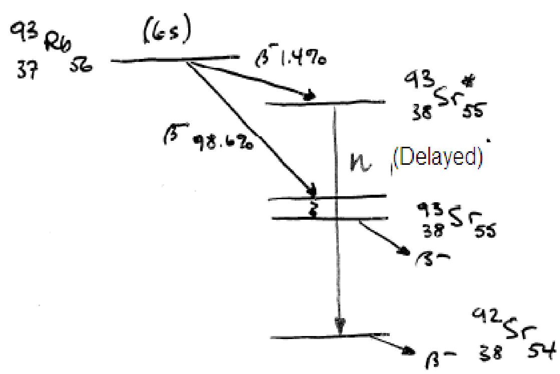

Fission cross-section

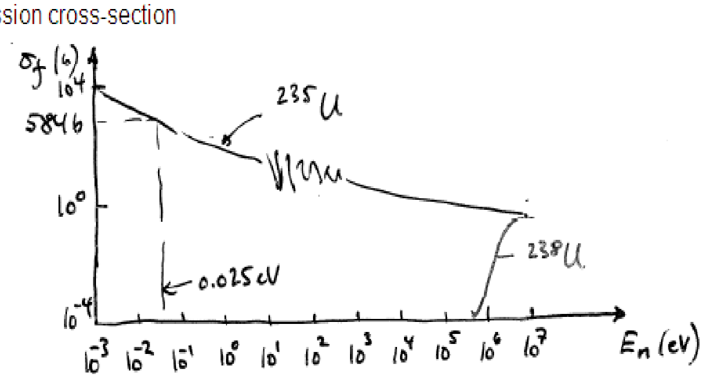

Thermal neutrons against ^{235}U:

$$\sigma_{fission} = 584b$$

$$\sigma_{rc} = 97b \text{ (radiative capture)}$$

$$\sigma_{sc} = 9b \text{ (elastic scattering)}$$

Neutron capture results in a compound nucleus with an excitation energy E_{ex}.

Reaction:	$^{235}U + n \rightarrow ^{236} U^*$
Excitation energy:	$E_{ex} = \left[m(^{236}U^*) - m(^{236}U) \right] c^2$
For low-energy neutrons (Kinetic energy negligible):	$m(^{236}U^*) = m(^{235}U) + m_n$
$\Rightarrow$	$E_{ex} = 6.5 MeV = B_n$

Where B_n represents the binding energy of the captured neutron. Neutron capture in nuclei with odd neutron numbers gives a larger value for E_{ex} than neutron capture in nuclei with even neutron numbers. This is because of pair-contributions to the binding energy. This all results in a large fission cross-section for neutron-induced fission in nuclei with an odd number of neutrons.

Energy distribution

$$^{235}U + n \rightarrow ^{236} U^* \rightarrow ^{93} Rb + ^{141} Cs + 2n, \qquad Q = 181 MeV$$
$$\overline{Q} = 200 MeV \textit{ (all possible outcomes)}$$

Distribution:

$T_{m_1} + T_{m_2}$	80%	168MeV
T_{2n}		5MeV
Prompt γ		7MeV
Gamma from radiative neutron capture		5MeV
β-disint. of fragments		20MeV
γ-fragments		7MeV
Sum:		212MeV

12 MeV of the β disintegration energy is in the form of neutrino energy, which is not recoverable. Net result is therefore 200 MeV.

Fission and nuclear structure

Deformed nuclei can reach intermediate states (fission isomeric states) with increased deformation which results in a lower fission barrier.

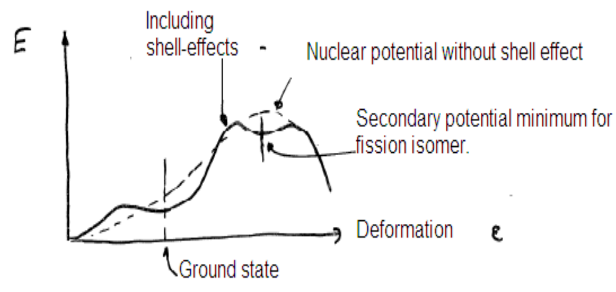

Fission resonance: Transition from one of the ground state's excited levels to one of the fission-isomeric exited states, where energy, spin, and parity coincide with the former state.

Controlled fission reaction

Neutron reproduction factor for an infinite medium: $k_\infty = \eta \cdot \varepsilon \cdot p \cdot f$

Where η represents the yield of fast neutrons for each thermal neutron absorbed in the fission fuel.

$\eta = \nu \frac{\sigma_f}{\sigma_f + \sigma_c}$, $\quad \nu = 2.42 \frac{neutrons}{fission}$ for ^{235}U

$\eta = 1.33$ for $(\underbrace{^{235}U}_{0.72\%} \,\&\, \underbrace{^{238}U}_{99.28\%})$ in naturally occuring U.

ε: Fast fission factor (fast neutron capture→ fission.

p: Resonance escape probability (i.e. moderation probability)

f: Thermal utilization factor (fraction of thermal neutrons absorbed in the fuel in contrast to the ones absorbed in the moderator or other non-fuel absorbers).

η is determined by the fuel composition. Moreover, ε, p and f are all dependent on both the geometry and the moderator material.

Loss of fast and thermal neutrons l_f and l_t(fractions).

For a finite geometry: $k = k_\infty \cdot (1 - l_f) \cdot (1 - l_t)$

The chain reaction is easier to control due to delayed neutrons after β-disintegration of fission fragments ("Delayed critical").

Nuclear reactor

Fuel:	1.)	Naturally occuring ^{235}U (0.72%) or enriched ^{235}U.
	2.)	^{239}Pu or ^{233}U from breeder reactors.
Moderator:	1.)	Low mass number (effective moderation).
	2.)	Minimal neutron capture.
	3.)	Chemical stability
	4.)	Cheap and accessible.
Moderator materials used:		Carbon is ok, but violates 1.), D_2O is good, but violates 4.), H_2O is good, but violates 2.)
Control rods:		Cd (Large capture cross section for thermal neutrons)
Reactor types:	1.)	Boiling water reactor (has negative power feedback through void fraction)
	2.)	Pressurized water reactor
	3.)	Heavy-water reactor
	4.)	Gas-cooled reactor
	5.)	Natrium-cooled fast breeder reactor

Breeder reactor

This reactor burns ^{239}Pu. Moreover, it converts ^{238}U to ^{239}Pu and ^{232}Th to ^{233}U:

Conversion of ^{238}U: $\quad {}^{238}U + n \rightarrow^{239} U(23m) \rightarrow^{239} Np + \beta^- + \overline{\nu}$

Furthermore, ^{239}Np has a half-life $t_{\frac{1}{2}} = 2.3d$ and decays into $^{239}Pu + \beta^- + \overline{\nu}$.

Conversion of ^{232}Th: $\quad {}^{232}Th + n \rightarrow^{233} Th(22m) \rightarrow^{233} Pa + \beta^- + \overline{\nu}$

Furthermore, ^{233}Pa has a half-life $t_{\frac{1}{2}} = 27d$ and decays into $^{233}U + \beta^- + \overline{\nu}$.

Fission products

1.) Can disturb the chain reaction ("reactor poison" due to high neutron capture cross section) for example ^{135}Xe.

2.) Can contain nuclei which are valuable for medical purposes.

3.) Are highly active radioactive waste. (Radioactive waste problems)

Thorium power?

^{232}Th is an abundant, *fertile* nuclide that through conversion to ^{233}U can be used as a component in nuclear reactor fuels, for existing reactors and for new designs (advanced CANDU reactor, molten salt reactor, accelerator-driven systems)

Fusion (Lilley Chap.11)

Advantages relative to a fission reactor for power production:

1.) Easily accessible fuel material (hydrogen, deuterium, tritium).

2.) The reaction products are light and stable nuclei, i.e no problems with highly radioactive waste.

Main problem: To get a reliable reaction going, because the Coulomb-barrier has to be overcome.

Relevant processes:

1.) D-D reaction: $D(d,n)^3He$

$^2H +^2 H \rightarrow^3 He + n$, Q=3.3MeV

$D(d,p)T$

$^2H +^2 H \rightarrow^3 H + p$, Q=4.0MeV

2.) D-T reaction: $D(t,n)^4He$

$^3H +^2 H \rightarrow^4 He + n$, Q=17.6MeV

The D-T reaction is the reaction chosen for further fusion reactor development because:

1.) There is a large output of energy.

2.) The Coulomb barrier is the same as for the D-D reaction.

Coulomb barrier: $V_c = \frac{e^2}{4\pi\varepsilon_0} \cdot \frac{Z_a \cdot Z_x}{R_a + R_x}$

D-T reaction: $V_c = 200keV$

Energy: $T_a \simeq 1 - 10keV \ll V_c$ which corresponds to a temperature $10^7 - 10^8 K$

This means that tunneling is required to overcome the barrier.

Fusion cross-section: $\sigma_{fu} \propto \frac{1}{v^2} e^{-2G}$

Reaction rate: $\sigma_{fu} \cdot v$

$p(v) \propto v^2 e^{-\frac{mv^2}{2kT}}$

$\langle \sigma v \rangle = \int \frac{1}{v^2} e^{-2G} \cdot v \cdot e^{-\frac{mv^2}{2kT}} v^2 dv$

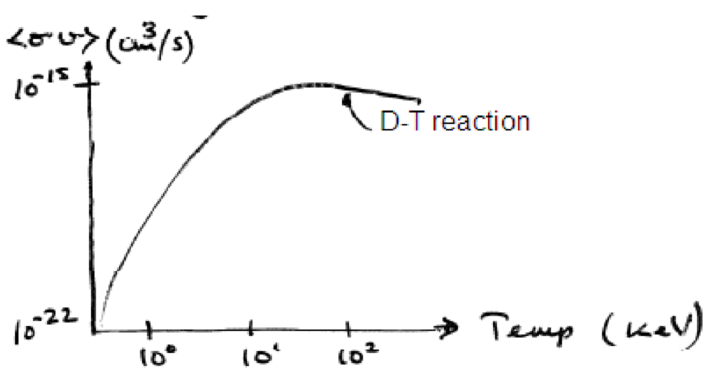

Controlled thermal fusion reactor?

Heating the reactor up to about $10^8 K$ (10keV).
Loss due to bremsstrahlung $\ll$ fusion power output at T >4keV.

Fusion energy released per unit volume: $E_f = \frac{1}{4} n^2 < \sigma v > Q\tau$
There are equal densities of D and T, $\frac{n}{2}$. In addition there are free electrons in the plasma, i.e $n_e = n$. Q is the released energy per fusion reaction and is equal to 17.6MeV for D-T. τ is the confinement time, i.e the time the reaction can be maintained by magnetic confinement of plasma. Thermal energy required per unit volume to reach temperature T:

Energy required: $E_{th} = \frac{3}{2} nkT + \frac{3}{2} n_e kT = 3nkT$

Net energy output if $E_f > E_{th}$

$\Rightarrow$ Lawson criterion: $n\tau > \frac{12kT}{<\sigma v> Q} \simeq 10^{20} \frac{s}{m^3}$ for D-T

Fusion reactions in the sun

The sun is a very successful fusion reactor, which maintains nearly constant output power.
Step 1(rate limiting): $^1H +^1 H \rightarrow {}^2H + e^+ + \nu, \quad Q = 1.44 MeV$
Low reaction rate due to weak interaction ($p \rightarrow n + e^+ + \nu$) which must take place within the time interval of the collision of the two protons.

Solar temperature: $15 \cdot 10^6 K \simeq 1 keV$

Reaction rate: $5 \cdot 10^{-18} s^{-1} \frac{1}{proton} \cdot 10^{56} protons \simeq 10^{38} \frac{reactions}{sec}$

$\Rightarrow$ constant "low" rate.

Further reactions follow quickly:

1.) $^2H + {}^1H \rightarrow {}^3He + \gamma$, Q=5.49MeV

2.) $^3He + {}^3He \rightarrow^4 He + 2^1H + \gamma$, Q=12.86MeV

Total result: $4^1H \rightarrow^4 He + 2e^+ + 2\nu$, Q=26.7MeV

The CNO-cycle (in second generation stars)

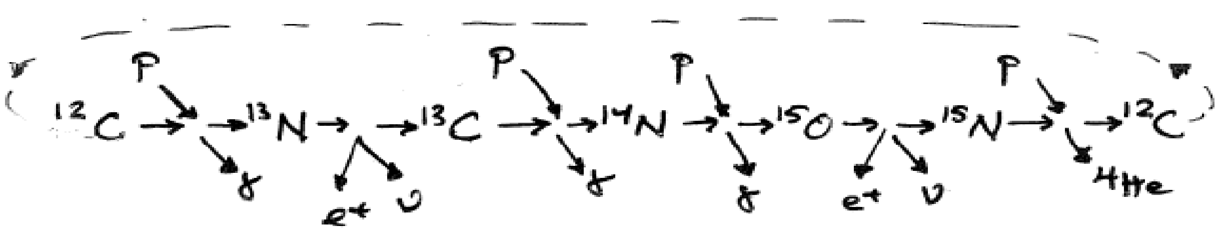

Same net result: $4^1H \rightarrow^4 He + 2e^+ + 2\nu, \quad Q = 26.7 MeV$

Helium burning

Reaction 1: $\alpha + \alpha + \alpha \rightleftharpoons {}^8Be + \alpha \rightleftharpoons^{12} C^* \overset{0.04\%}{\rightarrow} {}^{12}C + \gamma$

Reaction 2: $\alpha +^{12} C \rightarrow^{16} O + \gamma$ etc $\rightarrow {}^{20}Ne,^{24} Mg$

Further burning:

For example: $^{12}C + {}^{12}C \rightarrow \begin{cases} ^{20}Ne + \alpha \\ ^{23}Na + p \\ ^{23}Mg + n \end{cases}$

$$^{16}O + ^{16}O \rightarrow ^{28}Si + \alpha$$

$\Rightarrow$ Formation of ^{56}Fe, is the last nucleus in this process. Further nucleon synthesis is mainly due to neutron capture and β-disintegration.